

# Dynamical principles in neuroscience

Mikhail I. Rabinovich\*

*Institute for Nonlinear Science, University of California, San Diego,  
9500 Gilman Drive 0402, La Jolla, California 92093-0402, USA*

Pablo Varona

*GNB, Departamento de Ingeniería Informática, Universidad Autónoma de Madrid,  
28049 Madrid, Spain and Institute for Nonlinear Science, University of California,  
San Diego, 9500 Gilman Drive 0402, La Jolla, California 92093-0402, USA*

Allen I. Selverston

*Institute for Nonlinear Science, University of California, San Diego,  
9500 Gilman Drive 0402, La Jolla, California 92093-0402, USA*

Henry D. I. Abarbanel

*Department of Physics and Marine Physical Laboratory (Scripps Institution of  
Oceanography) and Institute for Nonlinear Science, University of California,  
San Diego, 9500 Gilman Drive 0402, La Jolla, California 92093-0402, USA*

(Published 14 November 2006)

Dynamical modeling of neural systems and brain functions has a history of success over the last half century. This includes, for example, the explanation and prediction of some features of neural rhythmic behaviors. Many interesting dynamical models of learning and memory based on physiological experiments have been suggested over the last two decades. Dynamical models even of consciousness now exist. Usually these models and results are based on traditional approaches and paradigms of nonlinear dynamics including dynamical chaos. Neural systems are, however, an unusual subject for nonlinear dynamics for several reasons: (i) Even the simplest neural network, with only a few neurons and synaptic connections, has an enormous number of variables and control parameters. These make neural systems adaptive and flexible, and are critical to their biological function. (ii) In contrast to traditional physical systems described by well-known basic principles, first principles governing the dynamics of neural systems are unknown. (iii) Many different neural systems exhibit similar dynamics despite having different architectures and different levels of complexity. (iv) The network architecture and connection strengths are usually not known in detail and therefore the dynamical analysis must, in some sense, be probabilistic. (v) Since nervous systems are able to organize behavior based on sensory inputs, the dynamical modeling of these systems has to explain the transformation of temporal information into combinatorial or combinatorial-temporal codes, and vice versa, for memory and recognition. In this review these problems are discussed in the context of addressing the stimulating questions: What can neuroscience learn from nonlinear dynamics, and what can nonlinear dynamics learn from neuroscience?

DOI: [10.1103/RevModPhys.78.1213](https://doi.org/10.1103/RevModPhys.78.1213)

PACS number(s): 87.19.La, 05.45.-a, 84.35.+i, 87.18.Sn

## CONTENTS

I. What are the Principles?	1214	3. Synaptic plasticity	1222
A. Introduction	1214	4. Examples of the cooperative dynamics of individual neurons and synapses	1223
B. Classical nonlinear dynamics approach for neural systems	1215	B. Robustness and adaptability in small microcircuits	1224
C. New paradigms for contradictory issues	1217	C. Intercircuit coordination	1228
II. Dynamical Features of Microcircuits: Adaptability and Robustness	1218	D. Chaos and adaptability	1229
A. Dynamical properties of individual neurons and synapses	1218	III. Informational Neurodynamics	1231
1. Neuron models	1218	A. Time and neural codes	1231
2. Neuron adaptability and multistability	1219	1. Temporal codes	1231
		2. Spatiotemporal codes	1232
		3. Coexistence of codes	1233
		4. Temporal-to-temporal information transformation: Working memory	1234
		B. Information production and chaos	1237
		1. Stimulus-dependent motor dynamics	1237
		2. Chaos and information transmission	1239
		C. Synaptic dynamics and information processing	1240

\*Electronic address: mrabinovich@ucsd.edu

D. Binding and synchronization	1242
IV. Transient Dynamics: Generation and Processing of Sequences	1244
A. Why sequences?	1244
B. Spatially ordered networks	1244
1. Stimulus-dependent modes	1244
2. Localized synfire waves	1247
C. Winnerless competition principle	1248
1. Stimulus-dependent competition	1248
2. Self-organized WLC networks	1249
3. Stable heteroclinic sequence	1250
4. Relation to experiments	1251
D. Sequence learning	1252
E. Sequences in complex systems with random connections	1254
F. Coordination of sequential activity	1256
V. Conclusion	1258
Acknowledgments	1259
Glossary	1259
References	1260

*“Will it ever happen that mathematicians will know enough about the physiology of the brain, and neurophysiologists enough of mathematical discovery, for efficient cooperation to be possible?”*

—Jacques Hadamard

## I. WHAT ARE THE PRINCIPLES?

### A. Introduction

Building dynamical models to study the neural basis of behavior has a long tradition (Ashby, 1960; Block, 1962; Rosenblatt, 1962; Freeman, 1972, 2000). The underlying idea governing neural control of behavior is the three-step structure of nervous systems that have evolved over billions of years, which can be stated in its simplest form as follows: Specialized neurons transform environmental stimuli into a neural code. This encoded information travels along specific pathways to the brain or central nervous system composed of billions of nerve cells, where it is combined with other information. A decision to act on the incoming information then requires the generation of a different motor instruction set to produce the properly timed muscle activity we recognize as behavior. Success in these steps is the essence of survival.

Given the present state of knowledge about the brain, it is impossible to apply a rigorous mathematical analysis to its functions such as one can apply to other physical systems like electronic circuits, for example. We can, however, construct mathematical models of the phenomena in which we are interested, taking account of what is known about the nervous system and using this information to inform and constrain the model. Current knowledge allows us to make many assumptions and put them into a mathematical form. A large part of this review will discuss nonlinear dynamical modeling as a particularly appropriate and useful mathematical framework that can be applied to these assumptions in order to

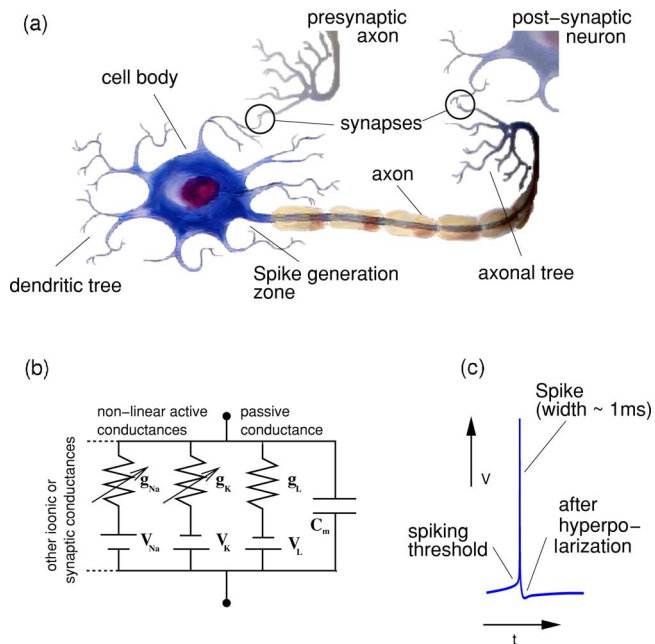


FIG. 1. (Color online) Illustration of the functional parts and electrical properties of neurons. (a) The neuron receives inputs through synapses on its dendritic tree. These inputs may or may not lead to the generation of a spike at the spike generation zone of the cell body that travels down the axon and triggers chemical transmitter release in the synapses of the axonal tree. If there is a spike, it leads to transmitter release and activates the synapses of a postsynaptic neuron and the process is repeated. (b) Simplified electrical circuit for a membrane patch of a neuron. The nonlinear ionic conductances are voltage dependent and correspond to different ion channels. This type of electrical circuit can be used to model isopotential single neurons. Detailed models that describe the morphology of the cells use several isopotential compartments implemented by these circuits coupled by a longitudinal resistance; these are called compartmental models. (c) A typical spike event is of the order of 100 mV in amplitude and 1–2 ms in duration, and is followed by a longer after-hyperpolarization period during which the neuron is less likely to generate another spike; this is called a refractory period.

simulate the functioning of the different components of the nervous system, to compare simulations with experimental results, and to show how they can be used for predictive purposes.

Generally there are two main modeling approaches taken in neuroscience: *bottom-up* and *top-down models*.

- Bottom-up dynamical models start from a description of individual neurons and their synaptic connections, that is, from acknowledged facts about the details resulting from experimental data that are essentially reductionistic (Fig. 1). Using these anatomical and physiological data, the particular pattern of connectivity in a circuit is reconstructed, taking into account the strength and polarity (excitatory or inhibitory) of the synaptic action. Using the wiring diagram thus obtained along with the dynamical features of the neurons and synapses, bottom-up models have been able to predict functional properties of

neural circuits and their role in animal behavior.

- Top-down dynamical models start with the analysis of those aspects of an animal's behavior that are robust, reproducible, and important for survival. The top-down approach is a more speculative big-picture view that has historically led to different levels of analysis in brain research. While this hierarchical division has put the different levels on an equal footing, the uncertainty implicit in the top-down approach should not be minimized. The first step in building such large-scale models is to determine the type of stimuli that elicit specific behaviors; this knowledge is then used to construct hypotheses about the dynamical principles that might be responsible for their organization. The model should predict how the behavior evolves with a changing environment represented by changing stimuli.

It is possible to build a sufficiently realistic neural circuit model that expresses dynamical principles even without knowledge of the details of the neuroanatomy and neurophysiology of the corresponding neural system. The success of such models depends on the universality of the underlying dynamical principles. Fortunately, there is a surprisingly large amount of similarity in the basic dynamical mechanisms used by neural systems, from sensory to central and motor processing.

Neural systems utilize phenomena such as synchronization, competition, intermittency, and resonance in quite nontraditional ways with regard to classical nonlinear dynamics theory. One reason is that the nonlinear dynamics of neural modules or microcircuits is usually not autonomous. These circuits are continuously or sporadically forced by different kinds of signals, such as sensory inputs from the changing environment or signals from other parts of the brain. This means that when we deal with neural systems we have to consider stimulus-dependent synchronization, stimulus-dependent competition, etc. This is a departure from the considerations of classical nonlinear dynamics. Another very important feature of neuronal dynamics is the coordination of neural activities with very different time scales, for example, theta rhythms (4–8 Hz) and gamma rhythms (40–80 Hz) in the brain.

One of our goals in this review is to understand why neural systems are very specific from the nonlinear dynamics point of view and to discuss the importance of such specificities for the functionality of neural circuits. We will talk about the relationship between neuroscience and nonlinear dynamics using specific subjects as examples. We do not intend to review here the methods or the nonlinear dynamical tools that are important for the analysis of neural systems as they have been discussed extensively in many reviews and books (e.g., Guckenheimer and Holmes, 1986; Crawford, 1991; Abarbanel et al., 1993; Ott, 1993; Kaplan and Glass, 1995; Abarbanel, 1997; Kuznetsov, 1998; Arnold et al., 1999; Strogatz, 2001; Izhikevich, 2006).

## B. Classical nonlinear dynamics approach for neural systems

Let us say a few words about the role of *classical dynamical theory*. It might seem at first sight that the apparently infinite diversity of neural activity makes its dynamical description a hopeless, even meaningless, task. However, here one can exploit the knowledge accumulated in classical dynamical theory, in particular, the ideas put forth by Andronov in 1931 concerning the structural stability of dynamical models and the investigation of their bifurcations (Andronov, 1933; Andronov and Pontryagin, 1937; Andronov et al., 1949). The essential points of these ideas can be traced back to Poincaré (Poincaré, 1892; Goroff, 1992). In his book *La Valeur de la Science*, Poincaré (1905) wrote that "the main thing for us to do with the equations of mathematical physics is to investigate what may and should be changed in them." Andronov's remarkable approach toward understanding dynamical systems contained three key points:

- Only models exhibiting activity that does not vary with small changes of parameters can be regarded as really suitable to describe experiments. He referred to them as models or dynamical systems that are structurally stable.
- To obtain insight into the dynamics of a system it is necessary to characterize all its principal types of behavior under all possible initial conditions. This led to Andronov's fondness for the methods of phase-space (state-space) analysis.
- Considering the behavior of the system as a whole allows one to introduce the concept of topological equivalence of dynamical systems and requires an understanding of local and global changes of the dynamics, for example, bifurcations, as control parameters are varied.

Conserving the topology of a phase portrait for a dynamical system corresponds to a stable motion of the system with small variation of the governing parameters. Partitioning parameter space for the dynamical system into regions with different phase-space behavior, i.e., finding the bifurcation boundaries, then furnishes a complete picture of the potential behaviors of a dynamical model. Is it possible to apply such a beautiful approach to biological neural network analysis? The answer is yes, at least for small, autonomous neural systems. However, even in these simple cases we face some important restrictions.

Neural dynamics is strongly dissipative. Energy derived from biochemical sources is used to drive neural activity with substantial energy loss in action-potential generation and propagation. Nearly all trajectories in the phase space of a dissipative system are attracted by some trajectories or sets of trajectories called attractors. These can be fixed points (corresponding to steady-state activity), limit cycles (periodic activity), or strange attractors (chaotic dynamics). The behavior of dynamical systems with attractors is usually structurally stable. Strictly speaking a strange attractor is itself structurally

	Type of bifurcation	Notes	Examples and references
Local bifurcations	Period-doubling	Below the period doubling bifurcation, a stable periodic orbit exists. As the control parameter $\mu$ is increased, the original periodic orbit becomes unstable, and the orbit with double period appears.	Cerebellar Purkinje cells (Mandelblat <i>et al.</i> 2001) Pacemaker neurons (Maeda <i>et al.</i> 1998)
	Saddle-node	A pair of periodic orbits is created out of nothing. One of the orbits is unstable (the saddle $L^+$ ), while the other is stable (the node $L^-$ ). The saddle-node bifurcation is fundamental to the study of neural systems since it is one of the most basic processes by which periodic rhythms are created.	AB neuron from the crustacean pyloric CPG (Guckenheimer <i>et al.</i> 1993)
	Period-adding cascade	This bifurcation consists of several saddle-node bifurcations in which a $(n+1)$ -spike bursting behavior is born and the $n$ -spike bursting behavior disappears.	Burst flexibility in coupled chaotic neurons (Huerta <i>et al.</i> 1997) Neural relaxation oscillators (Coombs and Osbaldestin, 2000) Chay neuron model (Chay 1985; Gu <i>et al.</i> 2003) Bursting electronic neuron (Maeda and Makino, 2000)
Global bifurcations	Period-doubling cascade	This diagram shows not one, but rather an infinite number of period doubling bifurcations. As $\mu$ is increased a period two orbit becomes a period four orbit, etc. This process converges at a finite value of $\mu$ , beyond which a chaotic motion and an infinite number of unstable periodic orbits appear to exist.	Thermosensitive neurons (Feudel <i>et al.</i> 2000) Aplysia R15 neuron (Canavier <i>et al.</i> 1990) Salamander visual system (Crevier and Meister 1998)
	Saddle-node homoclinic	This bifurcation is characterized by the transition from the synchronization regime (stable limit cycle $L^+$ on an invariant torus) to the quasiperiodic regime (beating). The stable and unstable $L^-$ limit cycles collide and disappear.	Periodic modulation of tonic spiking activity VLSI neuron model (Bondarenko <i>et al.</i> 2003)
	Blue-sky catastrophe	At control parameter values smaller than the critical one, the system has two periodic orbits: a stable orbit $L^+$ and a saddle orbit $L^-$ . The orbits, which do not lie in the stable manifold of $L^-$ , tend to $L^+$ as time increases. This is one of the basic processes by which periodic bursts are created.	Leach heart interneuron model (Shilnikov and Cymbalyuk 2005) (Gavrilov and Shilnikov 2000) Pacemaker neuron model (Soto-Trevino <i>et al.</i> 2005)

FIG. 2. Six examples of limit cycle bifurcations observed in living and model neural systems [see Chay (1985); Canavier *et al.* (1990); Guckenheimer *et al.* (1993); Huerta *et al.* (1997); Crevier and Meister (1998); Maeda *et al.* (1998); Coombes and Osbaldestin (2000); Feudel *et al.* (2000); Gavrilov and Shilnikov (2000); Maeda and Makino (2000); Mandelblat *et al.* (2001); Bondarenko *et al.* (2003); Gu *et al.* (2003); Shilnikov and Cymbalyuk (2005); Soto-Trevino *et al.* (2005)].

unstable, but its existence in the system state space is a structurally stable phenomenon. This is a very important point for the implementation of Andronov's ideas.

The study of bifurcations in neural models and in *in vitro* experiments is a keystone for understanding the dynamical origin of many single-neuron and circuit phenomena involved in neural information processing and the organization of behavior. Figure 2 illustrates some typical local bifurcations [their support consists of an equilibrium point or a periodic trajectory—see the detailed definition by Arnold *et al.* (1999)] and some global bifurcations (their support contains an infinite set of orbits) of periodic regimes observed in neural systems. Many of these bifurcations are observed both in experiments and in models, in particular in the conductance-based Hodgkin-Huxley-type equations (Hodgkin and Huxley, 1952), considered the traditional framework for modeling neurons, and in the analysis of network stability and plasticity.

The most striking results in neuroscience based on classical dynamical system theory have come from bottom-up models. These results include the description

of the diversity of dynamics in single neurons and synapses (Koch, 1999; Vogels *et al.*, 2005), the spatiotemporal cooperative dynamics of small groups of neurons with different types of connections (Selverston *et al.*, 2000; Selverston, 2005), and the principles of synchronization in networks with dynamical synapses (Loebel and Tsodyks, 2002; Elhilali *et al.*, 2004; Persi *et al.*, 2004).

Some top-down models also have attempted a classical nonlinear dynamics approach. Many of these models are related to the understanding and description of cognitive functions. Nearly half a century ago, Ashby hypothesized that cognition could be modeled as a dynamical process (Ashby, 1960). Neuroscientists have spent considerable effort implementing the dynamical approach in a practical way. The most widely studied examples of cognitive-type dynamical models are multi-attractor networks: models of associative memory that are based on the concept of an energy function or Lyapunov function for a dynamical system with many attractors (Hopfield, 1982) [see also Cohen and Grossberg (1983); Waugh *et al.* (1990); Doboli *et al.* (2000)]. The dynamical process in such networks is often called

“computation with attractors.” The idea is to design during the learning stage, in a memory network phase space, a set of attractors, each of which corresponds to a specific output. Neural computation with attractors involves the transformation of a given input stimulus, which defines an initial state inside the basin of attraction of one attractor, leading to a fixed desired output.

The idea that computation or information processing in neural systems is a dynamical process is broadly accepted today. Many dynamical models of both bottom-up and top-down type that address the encoding and decoding of neural information as the input-dependent dynamics of a nonautonomous network have been published in the last few years. However, there are still huge gaps in our knowledge of the actual biological processes underlying learning and memory, making accurate modeling of these mechanisms a distant goal. For reviews see [Arbib et al. \(1997\)](#) and [Wilson \(1999\)](#).

Classical nonlinear dynamics has provided some basis for the analysis of neural ensembles even with large numbers of neurons in networks organized as layers of nearly identical neurons. One of the elements of this formulation is the discovery of stable low-dimensional manifolds in a very high-dimensional phase space. These manifolds are mathematical images of cooperative modes of activity, for example, propagating waves in nonequilibrium media ([Rinzel et al., 1998](#)). Models of this sort are also interesting for the analysis of spiral waves in cortical activity as experimentally observed *in vivo* and *in vitro* ([Huang et al., 2004](#)). Many interesting questions have been approached by using the phase portrait and bifurcation analysis of models and by considering attractors and other asymptotic solutions. Nevertheless, new directions may be required to address the important complexity of nervous system functions.

### C. New paradigms for contradictory issues

The human brain contains approximately  $10^{11}$  neurons and a typical neuron connects with  $\approx 10^4$  other neurons. Neurons show a wide diversity in terms of their morphology and physiology (see Fig. 3). A wide variety of intracellular and network mechanisms influence the activity of living neural circuits. If we take into account that even a single neuron often behaves chaotically, we might argue that such a complex system most likely behaves as if it were a turbulent hydrodynamic flow. However, this is not what is observed. Brain dynamics are more or less regular and stable despite the presence of intrinsic and external noise. What principles does nature use to organize such behavior, and what mathematical approaches can be utilized for their description? These are the very difficult questions we need to address.

Several important features differentiate the nervous system from traditional dynamical systems:

- The architecture of the system, the individual neural units, the details of the dynamics of specific neurons, as well as the connections among neurons are not

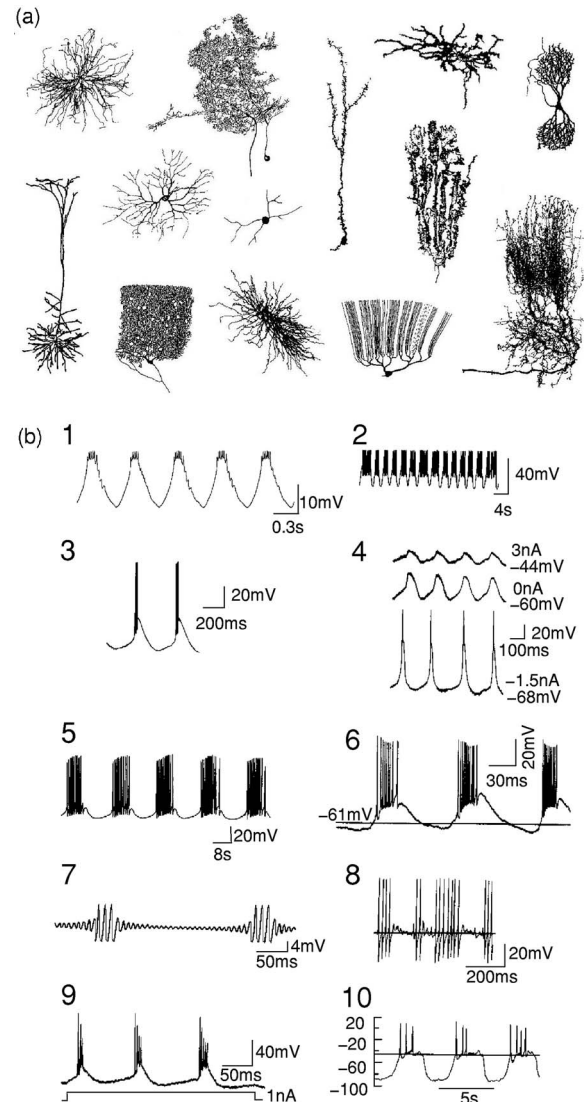


FIG. 3. Examples of (a) the anatomical diversity of neurons, and (b) the single-neuron membrane voltage activity associated with them. (1) Lobster pyloric neuron; (2) neuron in rat midbrain; (3) cat thalamocortical relay neuron; (4) guinea pig inferior olfactory neuron; (5) aplysia R15 neuron; (6) cat thalamic reticular neuron; (7) sepiia giant axon; (8) rat thalamic reticular neuron; (9) mouse neocortical pyramidal neuron; (10) rat pituitary gonadotropin-releasing cell. In many cases, the behavior depends on the level of current injected into the cell as shown in (b). Modified from [Wang and Rinzel, 1995](#).

usually known in detail, so we can describe them only in a probabilistic manner.

- Despite the fact that many units within a complex neural system work in parallel, many of them have different time scales and react differently to the same nonstationary events from outside. However, for the whole system, time is unified and coherent. This means that the neural system is organized hierarchically, not only in space (architecture) but also in time: each behavioral event is the initial condition for the next window of time. The most interesting phenomenon for a neural system is the presence not of at-

tractor dynamics but of nonstationary behavior. Attractor dynamics assumes long-time evolution from initial conditions; we must consider transient responses instead.

- The structure of neural circuits is—in principle—genetically determined; however, it is nevertheless not fixed and can change with experience (learning) and through neuromodulation.

We could expand this list, but the facts mentioned already make the point that the nervous system is a very special field for the application of classical nonlinear dynamics, and it is clear now why neurodynamics needs new approaches and a fresh view.

We use the following arguments to support an optimistic view about finding dynamical principles in neuroscience:

- Complex neural systems are the result of evolution, and thus their complexity is not arbitrary but follows some universal rules. One such rule is that the organization of the central nervous system (CNS) is hierarchical and based on neural modules.
- It is important to note that many modules are organized in a very similar way across different species. Such units can be small, like central pattern generators (CPGs), or much more complex, like sensory systems. In particular, the structure of one of the oldest sensory systems, the olfactory system, is more or less the same in invertebrates and vertebrates and can be described by similar dynamical models.
- The possibility of considering the nervous system as an ensemble of interconnected units is a result of the high level of autonomy of its subsystems. The level of autonomy depends on the degree of self-regulation. Self-regulation of neural units on each level of the nervous system, including individual neurons, is a key principle determining hierarchical neural network dynamics.
- The following conjecture seems reasonable: Each specific dynamical behavior of the network (e.g., traveling waves) is controlled by only a few of the many parameters of a system (like neuromodulators, for example), and these relevant parameters influence the specific cell or network dynamics independently—at least in a first approximation. This idea can be useful for the mathematical analysis of network dynamics and can help to build an approximate bifurcation theory. The goal of this theory is to predict the transformation of specific dynamics based on bifurcation analysis in a low-dimensional control subspace of parameters.
- For the understanding of the main principles of neurodynamics, phenomenological top-down models are very useful because even different neural systems with different architectures and different levels of complexity demonstrate similar dynamics if they execute similar functions.

In the main part of this review we discuss two critical functional properties of neural systems that at first glance appear incompatible: *robustness* and *sensitivity*. Finding solutions to such apparent contradictions will help us formulate some general dynamical principles of biological neural network organization. We note two examples.

Many neural systems, especially sensory systems, must be robust against noise and at the same time must be very sensitive to incoming inputs. A new paradigm that can deal with the existence of this fundamental contradiction is the winnerless competition (WLC) principle (Rabinovich *et al.*, 2001). According to this principle, a neural network with nonsymmetric inhibitory connections is able to exhibit structurally stable dynamics if the stimulus is fixed, and qualitatively change its dynamics if the stimulus is changed. This ability is based on different features of the signal and the noise, and the different ways they influence the dynamics of the system.

Another example is the remarkable reproducibility of transient behavior. Because transient behavior, in contrast to the long-term stable stationary activity of attractors, depends on initial conditions, it is difficult to imagine how such behavior can be reproducible from experiment to experiment. The solution to this paradox is related to the special role of global and local inhibition, which sets up the initial conditions.

The logic of this review is related to the specificity of neural systems from the dynamical point of view. In Sec. II we consider the possible dynamical origin of robustness and sensitivity in neural microcircuits. The dynamics of information processing in neural systems is considered in Sec. III. In Sec. IV, together with other dynamical concepts, we focus on a new paradigm of neurodynamics: the winnerless competition principle in the context of sequence generation, sensory coding, and learning.

## II. DYNAMICAL FEATURES OF MICROCIRCUITS: ADAPTABILITY AND ROBUSTNESS

### A. Dynamical properties of individual neurons and synapses

#### 1. Neuron models

Neurons receive patterned synaptic input and compute and communicate by transforming these synaptic input patterns into an output sequence of spikes. Why spikes? As spike wave forms are similar, information encoded in spike trains mainly relies on the interspike intervals. Relying on timing rather than on the details of action-potential wave forms increases the reliability and reproducibility in interneuronal communication. Dispersion and attenuation in transmission of neural signals from one neuron to others changes the wave form of the action potentials but preserves their timing information, again allowing for reliability when depending on interspike intervals.

The nature of spike train generation and transformation depends crucially on the properties of many voltage-gated ionic channels in neuron cell membranes.

The cell body (or soma) of the neuron gives rise to two kinds of processes: short dendrites and one or more long, tubular axons. Dendrites branch out like trees and receive incoming signals from other neurons. In some cases the synaptic input sites are on dendritic spines, thousands of which can cover the dendritic arbor. The output process, the axon, transmits the signals generated by the neuron to other neurons in the network or to an effector organ. The spikes are rapid, transient, all-or-none (binary) impulses, with a duration of about 1 ms (see Fig. 1). In most cases, they are initiated at a specialized region at the origin of the axon and propagate along the axon without distortion. Near its end, the tubular axon divides into branches that connect to other neurons through synapses.

When the spike emitted by a presynaptic neuron reaches the terminal of its axon, it triggers the emission of chemical transmitters in the synaptic cleft (the small gap, of order a few tens of nanometers, separating the two neurons at a synapse). These transmitters bind to receptors in the postsynaptic neuron, causing a depolarization or hyperpolarization in its membrane, exciting or inhibiting the postsynaptic neuron, respectively. These changes in the polarization of the membrane relative to the extracellular space spread passively from the synapses on the dendrites across the cell body. Their effects are integrated, and, when there is a large enough depolarization, a new action potential is generated (Kandel et al., 2000). Other types of synapses called gap junctions function as Ohmic electrical connections between the membranes of two cells. A spike is typically followed by a brief refractory period, during which no further spikes can be fired by the same neuron.

Neurons are quite complex biophysical and biochemical entities. In order to understand the dynamics of neurons and neural networks, phenomenological models have to be developed. The Hodgkin-Huxley model is foremost among such phenomenological descriptions of neural activity. There are several classes of neural models possessing various degrees of sophistication. We summarize the neural models most often considered in biological network development in Table I. For a more detailed description of these models see, for example, Koch (1999), Gerstner and Kistler (2002), and Izhikevich (2004).

Detailed conductance-based neuron models take into account ionic currents flowing across the membrane (Koch, 1994). The neural membrane may contain several types of voltage-dependent sodium, potassium, and calcium channels. The dynamics of these channels can also depend on the concentration of specific ions. In addition, there is a leakage current of chloride ions. The flow of these currents results in changes in the voltage across the membrane. The probability that a type of ionic channel is open depends nonlinearly on the membrane voltage and the current state of the channel. These dependencies result in a set of several coupled nonlinear differential equations describing the electrical activity of the cell. The intrinsic membrane conductances can enable neurons to generate different spike patterns, in-

cluding high-frequency bursts of different durations which are commonly observed in a variety of motor neural circuits and brain regions [see Fig. 3(b2)]. The biophysical mechanisms of spike generation enable individual neurons to encode different stimulus features into distinct spike patterns. Spikes, and bursts of spikes of different durations, code for different stimulus features, which can be quantified without *a priori* assumptions about those features (Kepecs and Lisman, 2003).

How detailed does the description of neurons or synapses have to be to make a model of neural dynamics biologically realistic while still remaining computationally tractable? It is reasonable to separate neuron models into two classes depending on the general goal of the modeling. If we wish to understand, for example, how the ratio of inhibitory to excitatory synapses in a neural ensemble with random connections influences the activity of the whole network, it is reasonable to use a simple model that keeps only the main features of neuron behavior. The existence of a spike threshold and the increase of the output spike rate with an increase in the input may be sufficient. On the other hand, if our goal is to explain the flexibility and adaptability of a small network like a CPG to a changing environment, the details of the ionic channel dynamics can be of critical importance (Prinz et al., 2004b). In many cases neural models built on simplified paradigms lead to more detailed conductance-based models based on the same dynamical principles but implemented with more biophysically realistic mechanisms. A good indication that the level of the description was chosen wisely comes if the model can reproduce with the same parameters the main bifurcations observed in the experiments.

## 2. Neuron adaptability and multistability

Multistability in a dynamical system means the coexistence of multiple attractors separated in phase space at the same value of the system's parameters. In such a system qualitative changes in dynamics can result from changes in the initial conditions. A well-studied case is the bistability associated with a subcritical Andronov-Hopf bifurcation (Kuznetsov, 1998). Multistable modes of oscillation can arise in delayed-feedback systems when the delay is larger than the response time of the system. In neural systems multistability could be a mechanism for memory storage and temporal pattern recognition in both artificial (Sompolinsky and Kanter, 1986) and living (Canavier et al., 1993) neural circuits. In a biological nervous system recurrent loops involving two or more neurons are found quite often and are particularly prevalent in cortical regions important for memory (Traub and Miles, 1991). Multistability emerges easily in these loops. For example, the conditions under which time-delayed recurrent loops of spiking neurons exhibit multistability were derived by Foss et al. (1996). The study used both a simple integrate-and-fire neuron and a Hodgkin-Huxley (HH) neuron whose recurrent inputs are delayed versions of their output spike trains. The authors showed that two kinds of multistability with

TABLE I. Summary of many frequently used neuronal models.

Model	Example	Variables	Remarks	References
Integrate-and-fire neurons	$\frac{dv(t)}{dt}$ $= \begin{cases} -\frac{v(t)}{\tau} + I_{\text{ext}} + I_{\text{syn}}(t), & 0 < v(t) < \theta \\ v(t_0^+) = 0, & v(t_0^-) = \theta \end{cases}$ $I_{\text{syn}}(t) = g \sum_{\text{spikes}} f(t - t_{\text{spike}})$ <p>and</p> $f(t) = A[\exp(-t/\tau_1) - \exp(-t/\tau_2)]$	$v(t)$ is the neuron membrane potential; $\theta$ is the threshold for spike generation. $I_{\text{ext}}$ is an external stimulus current; $I_{\text{syn}}$ is the sum of the synaptic currents; and $\tau_1$ and $\tau_2$ are time constants characterizing the synaptic currents.	A spike occurs when the neuron reaches the threshold $\theta$ in $v(t)$ after which the cell is reset to the resting state.	Lapicque, 1907
Rate models	$\dot{a}_i(t) = F_i(a_i(t)) [G_i(a_i(t)) - \sum_j \rho_{ij} Q_j(a_j(t))]$	$a_i(t) > 0$ is the spiking rate of the $i$ th neuron or cluster; $\rho_{ij}$ is the connection matrix; and $F, G, Q$ are polynomial functions.	This is a generalization of the Lotka-Volterra model [see Eq. (9)].	Fukai and Tanaka, 1997; Lotka, 1925; Volterra, 1931
McCulloch and Pitts	$x_i(n+1) = \Theta(\sum_j g_{ij} x_j(n) - \theta)$ $\Theta(x) = \begin{cases} 1, & x > 0 \\ 0, & x \leq 0 \end{cases}$	$\theta$ is the firing threshold; $x_j(n)$ are synaptic inputs at the discrete "time" $n$ ; $x_i(n+1)$ is the output. Inputs and outputs are binary (one or zero); the synaptic connections $g_{ij}$ are 1, -1, or 0.	The first computational model for an artificial neuron; it is also known as a linear threshold device model. This model neglects the relative timing of neural spikes.	McCulloch and Pitts, 1943
Hodgkin-Huxley	$C\dot{v}(t) = g_L[v_L - v(t)] + g_N m(t)^3 h(t)[vN_a - v(t)] + gK n(t)^4 (v_K) - v(t) + I,$ $\dot{m}(t) = \frac{m_\infty(v(t)) - m(t)}{\tau_m(v(t))}$ $\dot{h}(t) = \frac{h_\infty(v(t)) - h(t)}{\tau_h(v(t))}$ $\dot{n}(t) = \frac{n_\infty(v(t)) - n(t)}{\tau_n(v(t))}$	$v(t)$ is the membrane potential, $m(t)$ , and $h(t)$ , and $n(t)$ represent empirical variables describing the activation and inactivation of the ionic conductances; $I$ is an external current. The steady-state values of the conductance variables $m_\infty, h_\infty, n_\infty$ have a nonlinear voltage dependence, typically through sigmoidal or exponential functions.	These ODEs represent point neurons. There is a large list of models derived from this one, and it has become the principal tool in computational neuroscience. Other ionic currents can be added to the right-hand side of the voltage equation to better reproduce the dynamics and bifurcations observed in the experiments.	Hodgkin and Huxley, 1952
FitzHugh-Nagumo	$\dot{x} = \mu x - cx^3 - y + I, \quad \dot{y} = x + by - a$	$x(t)$ is the membrane potential, and $y(t)$ describes the dynamics of fast currents; $I$ is an external current. The parameter values $a, b$ , and $c$ are constants chosen to allow spiking.	A reduced model describing oscillatory spiking neural dynamics including bistability.	FitzHugh, 1961; Nagumo <i>et al.</i> , 1962

TABLE I. (Continued.)

Model	Example	Variables	Remarks	References
Wilson-Cowan	$\mu \frac{\partial E(x,t)}{\partial t} = -E(x,t) + [1-rE(x,t)] \times \mathcal{L}_e[E(x,t) \otimes w_{ee}(x) - I(x,t) \otimes w_{ei}(x) + I_e(x,t)]$ $\mu \frac{\partial I(x,t)}{\partial t} = -I(x,t) + [1-rI(x,t)] \times \mathcal{L}_i[E(x,t) \otimes w_{ie}(x) - I(x,t) \otimes w_{ii}(x) + I_i(x,t)]$	$\{E(x,t), I(x,t)\}$ are the number density of active excitatory and inhibitory neurons at location $x$ of the continuous neural media. $(w_{ee}(x), w_{ie}(x), w_{ei}(x), w_{ii}(x))$ are connectivity distributions among the populations of cells. $\{\mathcal{L}_e, \mathcal{L}_i\}$ are nonlinear responses reflecting different populations of thresholds. The operator $\otimes$ is a convolution involving the connectivity distributions.	The first “mean-field” model. It is an attempt to describe a cluster of neurons, to avoid the inherent noisy dynamical behavior of individual neurons; by averaging to a distribution noise is reduced.	Wilson and Cowan, 1973
Morris-Lecar	$v'(t) = g_L[v_L - v(t)] + n(t)g_n \times [v_n - v(t)] + g_m m_\infty(\dot{v}(t)) [v_m - v(t)] + I,$ $n'(t) = \lambda(v(t)) [n_\infty(v(t)) - n(t)]$ $m_\infty(v) = \frac{1}{2} \left( 1 + \tanh \frac{v - v_m}{v_m^0} \right)$ $n_\infty(v) = \frac{1}{2} \left( 1 + \tanh \frac{v - v_n}{v_n^0} \right)$ $\lambda(v) = \phi_n \cosh \frac{v - v_n}{2v_n^0}$	$v(t)$ is the membrane potential; $n(t)$ describes the recovery activity of a calcium current; $I$ is an external current.	Simplified model that reduces the number of dynamical variables of the HH model. It displays action potential generation when changing $I$ leads to a saddle-node bifurcation to a limit cycle.	Morris and Lecar, 1981
Hindmarsh-Rose	$x'(t) = y(t) + ax(t)^2 - bx(t)^3 - z(t) + I$ $y'(t) = C - xx(t)^2 - y(t)$ $z'(t) = r\{s[x(t) - x_0] - z(t)\}$	$x(t)$ is the membrane potential; $y(t)$ describes fast currents; $z(t)$ describes slow currents; and $I$ is an external current.	Simplified model that uses a polynomial approximation to the right-hand side of a Hodgkin-Huxley model. This model fails to describe the hyperpolarized periods after spiking of biological neurons.	Hindmarsh and Rose, 1984
Phase oscillator models	$\frac{d\theta_i(t)}{dt} = \omega + \sum_j H_{ij}(\theta_i(t) - \theta_j(t))$	$\theta(t)$ is the phase of the $i$ th neuron with approximately periodic behavior; and $H_{ij}$ is the connectivity function determining how neuron $i$ and $j$ interact.	First introduced for chemical oscillators; good for describing strongly dissipative oscillating systems in which the neurons are intrinsic periodic oscillators.	Cohen et al., 1982; Ermentrout and Kopell, 1984; Kuramoto, 1984
Map models	$x_{t+1}(i) = \frac{\alpha}{1+x_t(i)^2} + y_t(i) + \frac{\epsilon}{N} \sum_j x_t(j)$ $y_{t+1}(i) = y_t(i) - \sigma x_t(i) - \beta$	$x_t$ represents the spiking activity and $y_t$ represents a slow variable. A discrete time map.	One of a class of simple phenomenological models for spiking, bursting neurons. This kind of model can be computationally very fast, but has little biophysical foundation.	Cazelles et al., 2001; Rulkov, 2002

respect to initial spiking functions exist, depending on whether the neuron is excitable or repetitively firing in the absence of feedback.

Following Hebb's (1949) ideas most studies of the mechanisms underlying learning and memory focus on changing synaptic efficacy. Learning is associated with changing connectivity in a network. However, the network dynamics also depends on complex interactions among intrinsic membrane properties, synaptic strengths, and membrane-voltage time variation. Furthermore, neuronal activity itself modifies not only synaptic efficacy but also the intrinsic membrane properties of neurons. Papers by Marder *et al.* (1996) and Turriano *et al.* (1996) present examples showing that bistable neurons can provide short-term memory mechanisms that rely solely on intrinsic neuronal properties. While not replacing synaptic plasticity as a powerful learning mechanism, these examples suggest that memory in networks could result from an ongoing interplay between changes in synaptic efficacy and intrinsic neuron properties.

To understand the biological basis for such computational properties we must examine both the dynamics of the ionic currents and the geometry of neuronal morphology.

### 3. Synaptic plasticity

Synapses as well as neurons are dynamical nonlinear devices. Although synapses throughout the CNS share many features, they also have distinct properties. They operate with the following sequences of events: A spike is initiated in the axon near the cell body, it propagates down the axon, and arrives at the presynaptic terminal, where voltage-gated calcium channels admit calcium, which triggers vesicle fusion and neurotransmitter release. The released neurotransmitter then binds to receptors on the postsynaptic neuron and changes their conductance (Nicholls *et al.*, 1992; Kandel *et al.*, 2000). This series of events is regulated in many ways, making synapses adaptive and plastic.

In particular, the strength of synaptic conductivity changes in real time depending on their activity, as Katz observed many years ago (Fatt and Katz, 1952; Katz, 1969). A description of such plasticity was made in 1949 by Hebb (1949). He proposed that "When an axon of cell *A* is near enough to excite a cell *B* and repeatedly or persistently takes part in firing it, some growth process or metabolic change takes place in one or both cells such that *A*'s efficiency, as one of the cells firing *B*, is increased." This neurophysiological postulate has since become a central concept in neuroscience through a series of classic experiments demonstrating Hebbian-like synaptic plasticity. These experiments show that the efficacy of synaptic transmission in the nervous system is activity dependent and continuously modified. Examples of such modification are long-term potentiation and depression (LTP and LTD), which involve increased or decreased conductivity, respectively, of synaptic connections between two neurons, leading to increased or

decreased activity over time. Long-term potentiation and depression are presumed to produce learning by differentially facilitating the association between stimulus and response. The role of LTP and LTD, if any, in producing more complex behaviors is less closely tied to specific stimuli and more indicative of cognition, and is not well understood.

Long-term potentiation was first reported in the hippocampal formation (Bliss and Lomo, 1973). Changes induced by LTP can last for many days. Long-term potentiation has long been regarded, along with its counterpart LTD, as a potential mechanism for short-term-memory formation and learning. In fact, the hypothesis is widely accepted in learning and memory research that activity-dependent synaptic plasticity is induced at appropriate synapses during memory formation and is both necessary and sufficient for the information storage underlying the type of memory mediated by the brain area in which that plasticity is observed [see for a review Martin *et al.* (2000)]. Hebb did not anticipate LTD in 1949, but along with LTP it is thought to play a critical role in "rewiring" biological networks.

The notion of a coincidence requirement for Hebbian plasticity has been supported by classic studies of LTP and LTD using presynaptic stimulation coupled with prolonged postsynaptic depolarization [see, for example, Malenka and Nicoll (1999)]. However, coincidence there was loosely defined with a temporal resolution of hundreds of milliseconds to tens of seconds, much larger than the time scale of typical neuronal activity characterized by spikes that last for a couple of milliseconds. In a natural setting, presynaptic and postsynaptic neurons fire spikes as their functional outputs. How precisely must such spiking activities coincide in order to induce synaptic modifications? Experiments addressing this critical issue led to the discovery of spike-timing-dependent synaptic plasticity (STDP). Spikes initiate a sequence of complex biochemical processes in the postsynaptic neuron during the short time window following synaptic activation. Identifying detailed molecular processes underlying LTP and LTD remains a complex and challenging problem. There is good evidence that it consists of a *competition* between processes removing (LTD) and processes placing (LTP) phosphate groups from on postsynaptic receptors, or increasing (LTP) or decreasing (LTD) the number of such receptors in a dendritic spine. It is also widely accepted that *N*-methyl-*D*-aspartate (NMDA) receptors are crucial for the development of LTP or LTD and that it is calcium influx onto the postsynaptic cell that is critical for both LTP and LTD.

Experiments on synaptic modifications of excitatory synapses between hippocampal glutamatergic neurons in culture (Bi and Poo, 1998, 2001) (see Fig. 4) indicate that if a presynaptic spike arrives at time  $t_{\text{pre}}$  and a postsynaptic spike is observed or induced at  $t_{\text{post}}$  then when  $\tau = t_{\text{post}} - t_{\text{pre}}$  is positive the incremental percentage increase in synaptic strength behaves as

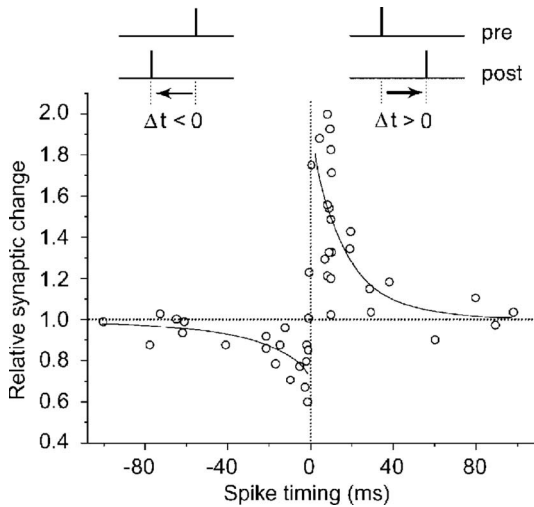


FIG. 4. Spike-timing-dependent synaptic plasticity observed in hippocampal neurons. Each data point represents the relative change in the amplitude of evoked postsynaptic current after repetitive application of presynaptic and postsynaptic spiking pairs (1 Hz for 60 s) with fixed spike timing  $\Delta t$ , which is defined as the time interval between postsynaptic and presynaptic spiking within each pair. Long-term potentiation (LTP) and depression (LTD) windows are each fitted with an exponential function. Modified from Bi, 2002.

$$\frac{\Delta g}{g} \approx a_P e^{-\beta_P \tau}, \quad (1)$$

with  $\beta_P \approx 1/16.8$  ms. When  $\tau < 0$ , the percentage decrease in synaptic strength behaves as

$$\frac{\Delta g}{g} \approx -a_D e^{\beta_D \tau}, \quad (2)$$

with  $\beta_D \approx 1/33.7$  ms.  $a_P$  and  $a_D$  are constants. This is illustrated in Fig. 4.

Many biochemical factors contribute differently to LTP and LTD in different synapses. Here we discuss a phenomenological dynamical model of synaptic plasticity (Abarbanel et al., 2002) which is very useful for modeling neural plasticity; its predictions agree with several experimental results. The model introduces two dynamical variables  $P(t)$  and  $D(t)$  that do not have a direct relationship with the concentration of any biochemical components. Nonlinear competition between these variables imitates the known competition in the postsynaptic cell. These variables satisfy the following simple first-order kinetic equations:

$$\begin{aligned} \frac{dP(t)}{dt} &= f(V_{\text{pre}}(t))[1 - P(t)] - \beta_P P(t), \\ \frac{dD(t)}{dt} &= g(V_{\text{post}}(t))[1 - D(t)] - \beta_D D(t), \end{aligned} \quad (3)$$

where the functions  $f(V)$  and  $g(V)$  are typical logistic or sigmoidal functions which rise from zero to the order of unity when their argument exceeds some threshold. These driving or input functions are a simplification of

the detailed way in which each dynamical process is forced. The  $P(t)$  process is associated with a particular time constant  $1/\beta_P$  while the  $D(t)$  process is associated with a different time constant  $1/\beta_D$ . Experiments show that  $\beta_P \neq \beta_D$ , and this is the primary embodiment of the two different time scales seen in many observations. The two time constants are a coarse-grained representation of the diffusion and leakage processes which dampen and terminate activities. Presynaptic voltage activity serves to release neurotransmitters in the usual manner and this in turn induces the postsynaptic action of  $P(t)$ , which has a time course determined by the time constant  $\beta_P^{-1}$ . Similarly, the postsynaptic voltage, constant or time varying, can be associated with the induction of the  $D(t)$  process.

$P(t)$  and  $D(t)$  compete to produce a change in synaptic strength  $\Delta g(t)$  as

$$\frac{d\Delta g(t)}{dt} = \gamma [P(t)D^\eta(t) - D(t)P^\eta(t)], \quad (4)$$

where  $\eta > 1$  and  $\gamma > 0$ . This dynamical model reproduces some of the key STDP experimental results like, for example, those shown in Fig. 4. It also accounts for the case where the postsynaptic cell is depolarized while a presynaptic spike train is presented to it.

#### 4. Examples of the cooperative dynamics of individual neurons and synapses

To illustrate the dynamical significance of plastic synapses we consider the synchronization of two neurons: a living neuron and an electronic model neuron coupled through a STDP or inverse STDP electronic synapse. Using hybrid circuits of model electronic neurons and biological neurons is a powerful method for analyzing neural dynamics (Pinto et al., 2000; Szücs et al., 2000; LeMasson et al., 2002; Prinz et al., 2004a). The representation of synaptic input to a cell using a computer to calculate the response of the synapse to specified presynaptic input goes under the name “dynamic clamp” (Robinson and Kawai, 1993; Sharp et al., 1993). It has been shown in modeling and in experiments (Nowotny, Zhigulin, et al., 2003; Zhigulin et al., 2003) that coupling through plastic electronic synapses leads to neural synchronization or, more correctly, entrainment that is more rapid, more flexible, and much more robust against noise than synchronization mediated by connections of constant strength. In these experiments the neural circuit consists of a specified presynaptic signal, a simulated synapse (via the dynamic clamp), and a postsynaptic biological neuron from the Aplysia abdominal ganglion. The presynaptic neuron is a spike generator producing spikes of predetermined form at predetermined times. The synapse and its plasticity are simulated by dynamic clamp software (Nowotny, 2003). In each update cycle of  $\sim 100 \mu\text{s}$  the presynaptic voltage is acquired, the spike generator voltage is updated, the synaptic strength is determined according to the learning rule, and the resulting synaptic current is calculated and injected into the living neuron through a current injection electrode. As

one presents the presynaptic signal many times, the synaptic conductance changes from one fixed value to another depending on the properties of the presynaptic signal.

The calculated synaptic current is a function of the presynaptic and postsynaptic potentials of the spike generator  $V_{\text{pre}}(t)$  and the biological neuron  $V_{\text{post}}(t)$ , respectively. It is calculated according to the following model. The synaptic current depends linearly on the difference between the postsynaptic potential  $V_{\text{post}}$  and its reversal potential  $V_{\text{rev}}$ , on an activation variable  $S(t)$ , and on its maximal conductance  $g(t)$ :

$$I_{\text{syn}}(t) = g(t)S(t)[V_{\text{post}}(t) - V_{\text{rev}}]. \quad (5)$$

The activation variable  $S(t)$  is a nonlinear function of the presynaptic membrane potential  $V_{\text{pre}}$  and represents the percentage of neurotransmitter docked on the postsynaptic cell relative to the maximum that can dock. It has two time scales: a docking time and an undocking time. We take it to satisfy the dynamical equation

$$\frac{dS(t)}{dt} = \frac{S_\infty(V_{\text{pre}}(t)) - S(t)}{\tau_{\text{syn}}[S_1 - S_\infty(V_1(t))]} \quad (6)$$

$S_\infty(V)$  is a sigmoid function which we take to be

$$S_\infty(V) = \begin{cases} \tanh[(V - V_{\text{th}})/V_{\text{slope}}] & \text{for } V > V_{\text{th}} \\ 0 & \text{otherwise.} \end{cases} \quad (7)$$

The time scale is  $\tau_{\text{syn}}(S_1 - 1)$  for neurotransmitter docking and  $\tau_{\text{syn}}S_1$  for undocking. For AMPA excitatory receptors, the docking time is about 0.5 ms, and the undocking time is about 1.5 ms. The maximal conductance  $g(t)$  is determined by the learning rule discussed below. In the experiments, the synaptic current is updated at  $\sim 10$  kHz.

To determine the maximal synaptic conductance  $g(t)$  of the simulated STDP synapse, an additive STDP learning rule was used. This is accurate if the time between presented spike pairs is long compared to the time between spikes in the pair. To avoid runaway behavior, the additive rule was applied to an intermediate  $g_{\text{raw}}$  that was then filtered through a sigmoid function. In particular, the change  $\Delta g_{\text{raw}}$  in synaptic strength is given by

$$\Delta g_{\text{raw}}(\Delta t) = \begin{cases} A_+ \frac{\Delta t - \tau_0}{\tau_+} e^{-(\Delta t - \tau_0)/\tau_+} & \text{for } \Delta t > \tau_0 \\ A_- \frac{\Delta t - \tau_0}{\tau_-} e^{(\Delta t - \tau_0)/\tau_-} & \text{for } \Delta t < \tau_0, \end{cases} \quad (8)$$

where  $\Delta t = t_{\text{post}} - t_{\text{pre}}$  is the difference between postsynaptic and presynaptic spike times. The parameters  $\tau_+$  and  $\tau_-$  determine the widths of the learning windows for potentiation and depression, respectively, and the amplitudes  $A_+$  and  $A_-$  determine the magnitude of synaptic change per spike pair. The shift  $\tau_0$  reflects the finite time of information transport through the synapse.

As one can see in Fig. 5, the postsynaptic neuron quickly synchronizes to the presynaptic spike generator which presents spikes with an interspike interval (ISI) of 255 ms (top panel). The synaptic strength continuously

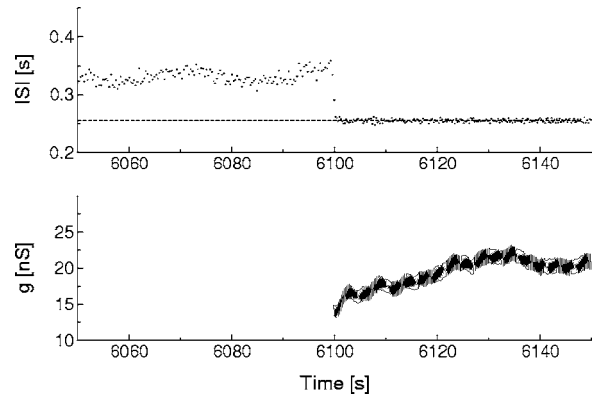


FIG. 5. Example of a synchronization experiment. Top: The interspike intervals (ISIs) of the postsynaptic biological neuron. Bottom: The synaptic strength  $g(t)$ . Presynaptic spikes with ISI of 255 ms were presented to a postsynaptic neuron with periodic oscillations at an ISI of 330 ms. Before coupling with the presynaptic spike generator, the biological neuron spikes tonically at its intrinsic ISI of 330 ms. Coupling was switched on with  $g(t=0)=15$  nS at time 6100 s. As one can see the postsynaptic neuron quickly synchronizes to the presynaptic spike generator (top panel, dashed line). The synaptic strength continuously adapts to the state of the postsynaptic neuron, effectively counteracting adaptation and other modulations of the system. This leads to a very precise and robust synchronization at a nonzero phase lag. The precision of the synchronization manifests itself in small fluctuations of the postsynaptic ISIs in the synchronized state. Robustness and phase lag cannot be seen directly. Modified from Nowotny, Zhigulin, *et al.*, 2003.

adapts to the state of the postsynaptic neuron, effectively counteracting adaptation and other modulations of the system (bottom panel). This leads to a very precise and robust synchronization at a nonzero phase lag. The precision of the synchronization manifests itself in small fluctuations of the postsynaptic ISIs in the synchronized state. Robustness and phase lag cannot be seen directly in Fig. 5. Spike-timing-dependent plasticity is a mechanism that enables synchronization of neurons with significantly different intrinsic frequencies as one can see in Fig. 6. The significant increase in the regime of synchronization associated with synaptic plasticity is a welcome, perhaps surprising, result and addresses the issue raised above about robustness of synchronization in neural circuits.

## B. Robustness and adaptability in small microcircuits

The precise relationship between the dynamics of individual neurons and the mammalian brain as a whole remains extremely complex and obscure. An important reason for this is a lack of knowledge on the detailed cell-to-cell connectivity patterns as well as a lack of knowledge on the properties of the individual cells. Although large-scale modeling of this situation is attempted frequently, parameters such as the number and kind of synaptic connections can only be estimated. By

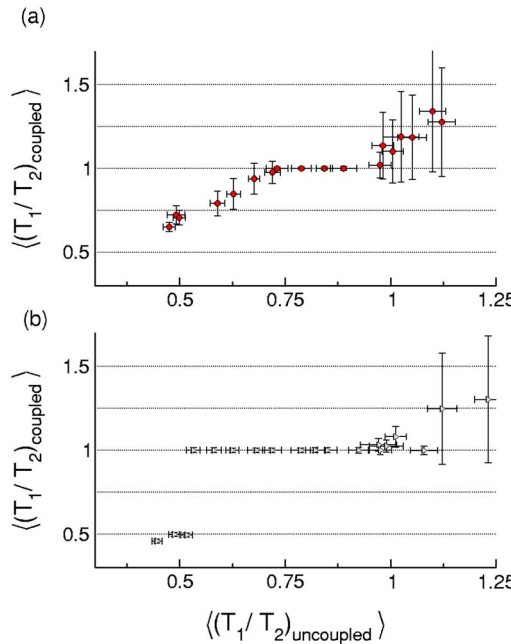


FIG. 6. (Color online) The presynaptic signal generator presents a periodic spike train with ISI of  $T_1$  to a postsynaptic neuron with ISI of  $T_2^0$ , before coupling. When neurons are coupled,  $T_2^0 \rightarrow T_2$ . We plot the ratio of these periods after coupling as a function of the ratio before coupling (a), for a synapse with constant  $g$  and (b) for a synaptic connection  $g(t)$  following the rule in the text. The enlarged domain of one-to-one synchronization in the latter case is quite clear and, as shown by the change in the error bar sizes, the synchronization is much better. This result persists when noise is added to the presynaptic signal and to the synaptic action (not shown). Modified from Nowotny, Zhigulin, et al., 2003.

using the less complex microcircuits (MCs) of invertebrates, a more detailed understanding of neural circuit dynamics is possible.

Central pattern generators are small MCs that can produce stereotyped cyclic outputs without rhythmic sensory or central input (Marder and Calabrese, 1996;

Stein et al., 1997). Thus CPGs are oscillators, and the image of their activity in the corresponding system state space is a limit cycle when oscillations are periodic and a strange attractor in more complex cases. Central pattern generators underlie the production of most motor commands for muscles that execute rhythmic animal activity such as locomotion, breathing, heartbeat, etc. The CPG output is a spatiotemporal pattern with specific phase lags between the temporal sequences corresponding to the different motor units (see below).

The network architecture and the main features of CPG neurons and synapses are known much better than any other brain circuits. Examples of typical invertebrate CPG networks are shown in Fig. 7. Common to many CPG circuits are electrical and inhibitory connections and the spiking-bursting activity of their neurons. The characteristics of the spatiotemporal patterns generated by the CPG, such as burst frequency, phase, length, etc., are determined by the intrinsic properties of each individual neuron, the properties of the synapses, and the architecture of the circuit.

The motor patterns produced by CPGs fall into two categories: those that operate continuously such as respiration (Ramirez et al., 2004) or heartbeat (Cymbalyuk et al., 2002), and those that are produced intermittently such as locomotion (Getting, 1989) or chewing (Selverston, 2005). Although CPGs autonomously establish correct rhythmic firing patterns, they are under constant supervision by descending fibers from higher centers and by local reflex pathways. These inputs allow the animal to constantly adapt its behavior to the immediate environment, which suggests that there is considerable flexibility in the dynamics of motor systems. In addition there is now a considerable body of information showing that anatomically defined small neural circuits can be reconfigured in a more general way by neuromodulatory substances in the blood, or released synaptically so that they are functionally altered to produce different stable spatiotemporal patterns, which must also be flexible in response to sensory inputs on a cycle-by-cycle basis; see

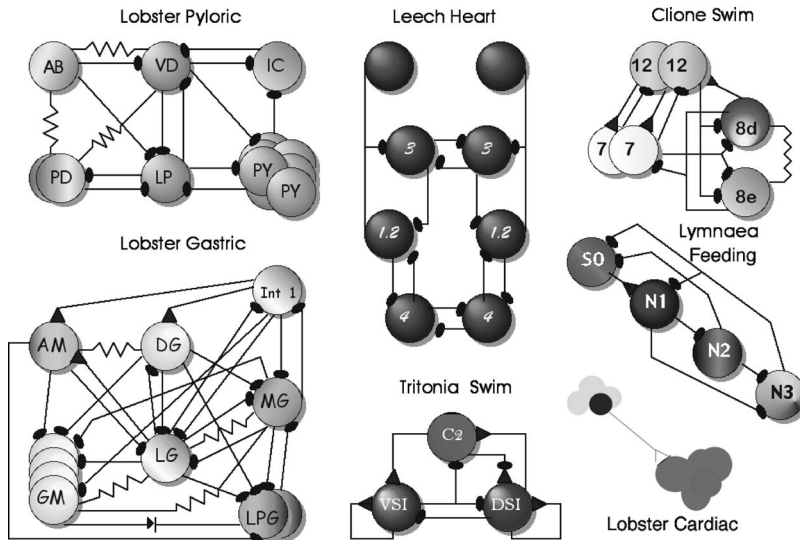


FIG. 7. Examples of invertebrate CPG microcircuits from arthropod, mollusk, and annelid preparations. All produce rhythmic spatiotemporal motor patterns when activated by nonpatterned input. The black dots represent chemical inhibitory synapses. Resistors represent electrical connections. Triangles are chemical excitatory synapses, and diodes are rectifying synapses (electrical synapses in which the current flows only in one direction). Individual neurons are identifiable from one preparation to another.

Simmers and Moulins (1988), for example.

Central pattern generators have similarity with neural MCs in the brain (Silberberg *et al.*, 2005; Solis and Perkel, 2005; Yuste *et al.*, 2005) and are often studied as models of neural network function. In particular, there are important similarities between vertebrate spinal cord CPGs and neocortical microcircuits which have been emphasized by Yuste *et al.* (2005): (i) CPG interactions, which are fundamentally inhibitory, dynamically regulate the oscillations. Furthermore, subthreshold-activated voltage-dependent cellular conductances that promote bistability and oscillations also promote synchronization with specific phase lags. The same cellular properties are also present in neocortical neurons, and underlie the observed oscillatory synchronization in the cortex. (ii) Neurons in spinal cord CPGs show bistable membrane dynamics, which are commonly referred to as plateau potentials. A correlate of bistable membrane behavior, in this case termed “up” and “down” states, has also been described in the striatum and neocortex both *in vivo* and *in vitro* (Sanchez-Vives and McCormick, 2000; Cossart *et al.*, 2003). It is still unclear whether this bistability arises from intrinsic or circuit mechanisms or a combination of the two (Egorov *et al.*, 2002; Shu *et al.*, 2003). (iii) Both CPGs and cortical microcircuits demonstrate attractor dynamics and transient dynamics [see, for example, Abeles *et al.* (1993); Ikegaya *et al.* (2004)]. (iv) Modulations by sensory inputs and neuromodulators are also a common characteristic that is shared between CPGs and cortical circuits. Examples in CPGs include the modulation of oscillatory frequency, of temporal coordination among different populations of neurons, of the amplitude of network activity, and of the gating of CPG input and output (Grillner, 2003). (v) Switching between different states of CPG operation (for example, switching coordinated motor patterns for different modes of locomotion) is under sensory afferent and neurochemical modulatory control. This makes CPGs multifunctional and dynamically plastic. Switching between cortical activity states is also under modulatory control, as shown, for example, by the role of the neurotransmitter dopamine in working memory in monkeys (Goldman-Rakic, 1995). Thus modulation reconfigures microcircuit dynamics and transforms activity states to modify behavior.

The CPG concept was built around the idea that behaviorally relevant spatiotemporal cyclic patterns are generated by groups of nerve cells without the need for rhythmic inputs from higher centers or feedback from structures that are moving. If activated, isolated invertebrate preparations can generate such rhythms for many hours and as a result have been extremely important in trying to understand how simultaneous cooperative interactions between many cellular and synaptic parameters can produce robust and stable spatiotemporal patterns [see Fig. 8(d)]. An example of a three-neuron CPG phase portrait is shown in Figs. 8(a)–8(c). The effect of a hyperpolarizing current leads to changes in the pattern as reflected by the phase portrait in Figs. 8(b) and 8(c).

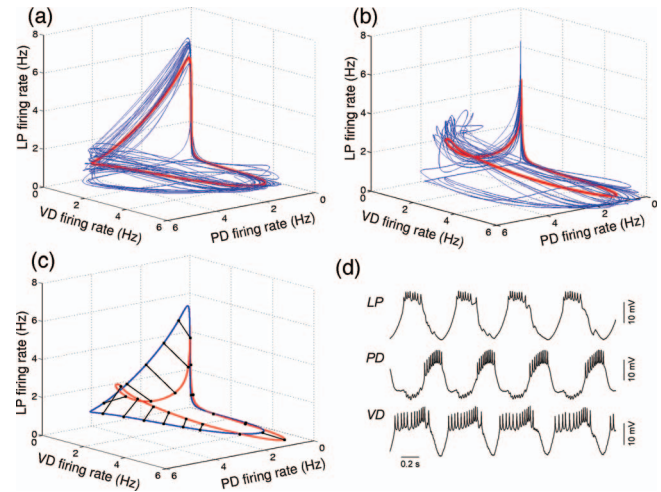


FIG. 8. (Color) Phase portrait of typical CPG output. The data were recorded in the pyloric CPG of the lobster stomatogastric ganglion. Each axis represents the firing rate of one of three pyloric neurons: LP, VD, and PD (see Fig. 7). (a) The orbit of the oscillating pyloric system is shown in blue and the average orbit is shown in red; (b) the same but with a hyperpolarizing dc current injected into the PD; (c) the difference between the averaged orbits; (d) time series of the membrane potentials of the three neurons. Figure provided by T. Nowotny, R. Levi, and A. Szücs.

Neural oscillations arise either through interactions among neurons (network-based mechanism) or through interactions among currents in individual neurons (pacemaker mechanism). Some CPGs use both mechanisms. In the simplest case, one or more neurons with intrinsic bursting activity acts as the pacemaker for the entire CPG circuit. The intrinsic currents may be constitutively active or they may require activation by neuromodulators, so-called conditional bursters. Synaptic connections act to determine the pattern by exciting or inhibiting other neurons at the appropriate time. Such networks are extremely robust and have generally been thought to be present in systems in which the rhythmic activity is active all or most of the time. In the second case, it is the synaptic interactions between nonbursting neurons that generate the rhythmic activity and many schemes for the types of connections necessary to do this have been proposed. Usually reciprocal inhibition serves as the basis for generating bursts in antagonistic neurons and there are many examples of cells in pattern-generating microcircuits connected in this way (see Fig. 7). Circuits of this type are usually found for behaviors that are intermittent in nature and require a greater degree of flexibility than those based on pacemaker cells.

Physiologists know that reciprocal inhibitory connections between oscillatory neurons can produce, as a result of the competition, sequential activity of neurons and rhythmic spatiotemporal patterns (Szekely, 1965; Stent and Friesen, 1977; Rubin and Terman, 2004). However, even for a rather simple MC, consisting of just three neurons, there is no quantitative description. If the connections are symmetric, the MC can reach an attrac-

tor. It is reasonable to hypothesize that asymmetric inhibitory connections are necessary to preserve the order of patterns with more than two phases per cycle. The contradiction, noted earlier, between robustness and flexibility can then be resolved because external signals can modify the effective topology of connections so one can have functionally different networks for different stimuli.

Theoretical analysis and computer experiments with MCs based on the winnerless competition principle (discussed in Sec. IV.C) show that sufficient conditions for the generation of sequential activity do exist and the range of allowed nonsymmetric inhibitory connections is quite wide (Rabinovich et al., 2001; Varona, Rabinovich, et al., 2002; Afraimovich, Rabinovich, et al., 2004). We illustrate this using a Lotka-Volterra rate description of neuron activity:

$$\frac{da_i(t)}{dt} = a_i(t) \left( 1 - \sum_{j=1}^N \rho_{ij}(S_i) a_j(t) \right) + S_i, \quad i = 1, \dots, N, \quad (9)$$

where the rate of each  $N$  neuron is  $a_i(t)$ , the connection matrix is  $\rho_{ij}$ , and the stimuli  $S_i$  are constants here. This model can be justified as a rate neural model as follows (Fukai and Tanaka, 1997). The firing rate  $a_i(t)$  and membrane potential  $v_i(t)$  of the  $i$ th neuron can be described by

$$a_i(t) = G(v_i - \theta), \quad (10)$$

$$\frac{dv_i(t)}{dt} = -\lambda v_i(t) + I_i(t), \quad (11)$$

where  $G(v_i - \theta)$  is a gain function,  $\theta$  and  $\lambda$  are constants, and the input current  $I_i(t)$  to neuron  $i$  is generated by the rates  $a_j(t)$  of the other neurons:

$$I_i(t) = S_i - \sum_j^N \rho_{ij} a_j(t). \quad (12)$$

Here  $S_i$  is the input and  $\rho_{ij}$  is the strength of the inhibitory synapse from neuron  $j$  to neuron  $i$ . We suppose that  $G(x)$  is a sigmoidal function:

$$G(x) = G_0 / [1 + \exp(-\beta x)]. \quad (13)$$

Let us then make two assumptions: (i) the firing rate is always much smaller than its maximum value  $G_0$ ; and (ii) the system is strongly dissipative (this is reasonable because we are considering inhibitory networks). Based on these assumptions, after combining and rescaling Eqs. (10)–(13), we obtain the Lotka-Volterra rate description (9) with an additional positive term on the right side that can be replaced by a constant [see Fukai and Tanaka (1997) for details].

The tests of whether WLC is operating in a reduced pyloric CPG circuit are shown in Fig. 9. This study used estimates of the synaptic strengths shown in Fig. 9(a). Some of the key questions here are these. (i) What is the minimal strength for the inhibitory synapse from the py-

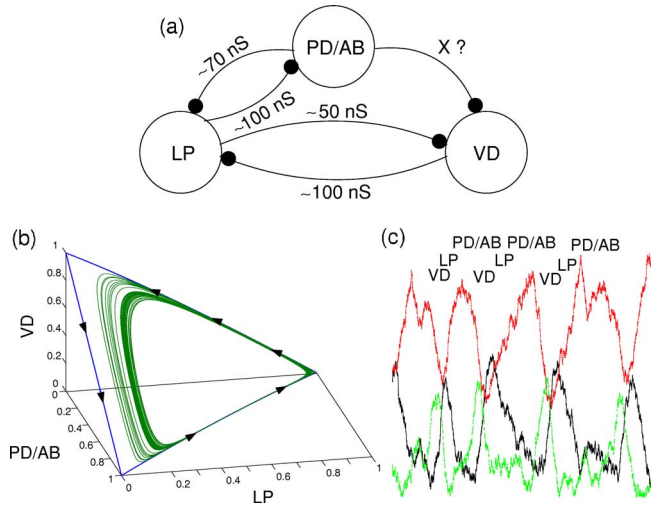


FIG. 9. (Color online) Competition without winner in a model of the pyloric CPG. (a) Schematic diagram of the three-neuron network used for rate modeling. Black dots represent chemical inhibitory synapses with strengths given in nanoseconds ( $X > 160$ ). (b) Phase portrait of the model: The limit cycle corresponding to the rhythmic activity is in the 2D simplex (Zeeman and Zeeman, 2002). (c) Robustness in the presence of noise: Noise introduced into the model shows no effect on the order of activation for each type of neuron. Figure provided by R. Huerta.

loric dilator (PD) neuron or AB group to the VD neuron such that WLC exists? (ii) Does the connectivity obtained from the competition without winner condition produce the order of activation observed in the pyloric CPG? (iii) Is this dynamics robust against noise, in the sense that strong perturbations of the system do not alter the sequence? If the strengths of  $\rho_{ij}$  are taken as

$$\rho_{ij} = \begin{pmatrix} 1 & 1.25 & 0 \\ 0.875 & 1 & 1.25 \\ X/80 & 0.625 & 1 \end{pmatrix},$$

the WLC formulas imply that the sufficient conditions for a reliable and robust cyclic sequence are satisfied if  $X > 160$ . The activation sequence of the rate model with noise shown in Fig. 9(c) is similar to that observed experimentally in the pyloric CPG. When additive Gaussian noise is introduced into the rate equations, the activation order of neurons is not broken, but the period of the limit cycle depends on the level of perturbation. Therefore the cyclic competitive sequence is robust and can be related to the synaptic connectivity seen in real MCs. If individual neurons in a MC are not oscillating, one can consider small subgroups of neurons that may form oscillatory units and apply the WLC principle to these units.

An important question about modeling the rhythmic activity of small inhibitory circuits is how the specific dynamics of individual neurons influences the network rhythm generation. Figure 10 represents the three-dimensional (3D) projection of the many-dimensional phase portrait of a circuit with the same architecture as

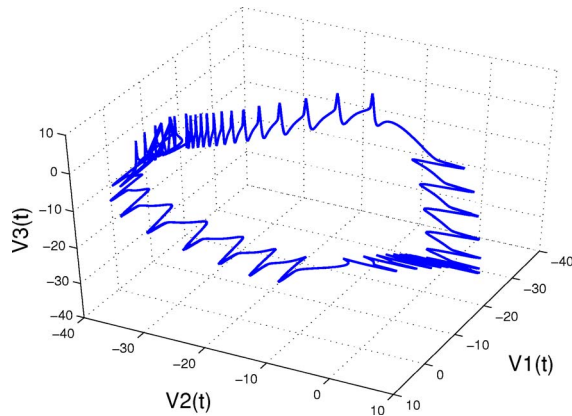


FIG. 10. (Color online) Three-dimensional projection of the many-dimensional phase portrait of a circuit with the same architecture as the one shown in Fig. 9, using Hodgkin-Huxley spiking-burging neuron models. The switching dynamics seen in the rate model is shown in Fig. 9(c), and this circuit is robust when noise is added to it.

shown in Fig. 9(a) but using Hodgkin-Huxley spiking-burging neuron models. The switching dynamics seen in the rate model is shown in Fig. 9(c), and this circuit is robust when noise is added to it.

Pairs of neurons can interact via inhibitory, excitatory, or electrical (gap junction) synapses to produce basic forms of neural activity which can serve as the foundation for MC dynamics. Perhaps the most common (and well-studied) CPG interaction consists of reciprocal inhibition, an arrangement that generates a rhythmic bursting pattern in which neurons fire approximately out of phase with each other (Wang and Rinzel, 1995). This is called a half-center oscillator. It occurs when there is some form of excitation to the two neurons sufficient to cause their firing and some form of decay mechanism to slow high firing frequencies. The dynamical range of the bursting activity varies with the synapse strength and in some instances can actually produce in-phase bursting. Usually reciprocal excitatory connections (unstable if too large) or reciprocal excitatory-inhibitory connections are able to reduce the intrinsic irregularity of neurons (Varona, Torres, Abarbanel, *et al.*, 2001).

Modeling studies with electrically coupled neurons have also produced nonintuitive results (Abarbanel *et al.*, 1996). While electrical coupling is generally thought to provide synchrony between neurons, under certain conditions the two neurons can burst out of phase with each other (Sherman and Rinzel, 1992; Elson *et al.*, 1998, 2002); see Fig. 11 and also Chow and Kopell (2000) and Lewis and Rinzel (2003). An interesting modeling study of three neurons (Soto-Trevino *et al.*, 2001) with synapses that are activity dependent found that the synaptic strengths self-adjusted in different combinations to produce the same three-phase rhythm. There are many examples of vertebrate MCs in which a collection of neurons can be conceptually isolated to perform a particular function or to represent the canonical or modular circuit for a particular brain region [see Shepherd (1998)].

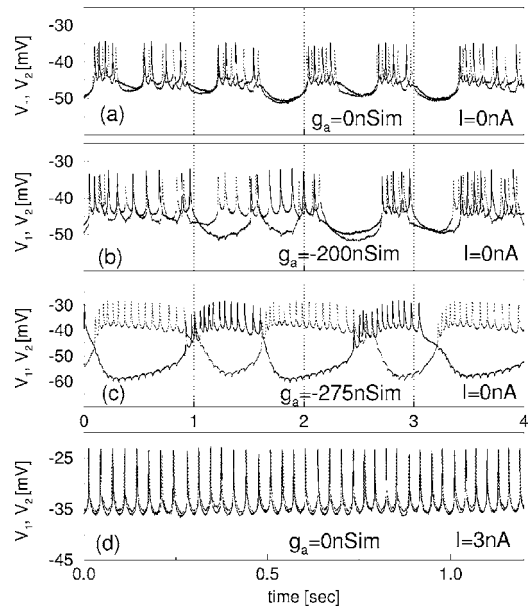


FIG. 11. Artificial electrical coupling between two living chaotic PD cells of the stomatogastric ganglion of a crustacean can demonstrate both synchronous and asynchronous regimes of activity. In this case the artificial electrical synapse was built on top of the existing natural coupling between two PD cells. This shows different synchronization levels (a)–(d) as a function of the artificial coupling  $g_a$  and a dc current  $I$  injected in one of the cells. (a) With their natural coupling  $g_a=0$  the two cells are synchronized and display irregular spiking-burging activity. (b) With an artificial electrical coupling that changes the sign of the current  $g_a=-200$  nS, and thus compensates the natural coupling, the two neurons behave independently. (c) Increasing the negative conductance leads to a regularized antiphase spiking activity (by mimicking mutual inhibitory synapses). (d) With no artificial coupling but adding a dc current two neurons are synchronized, displaying tonic spiking activity. Modified from Elson *et al.*, 1988.

### C. Intercircuit coordination

It is often the case that more or less independent MCs must synchronize in order to perform some coordinated function. There is a growing literature suggesting that large groups of neurons in the brain synchronize oscillatory activity in order to achieve coherence. This may be a mechanism for binding disparate aspects of cognitive function into a whole (Singer, 2001), as we will discuss in Sec. III.D. However, it is more persuasive to examine intercircuit coordination in motor circuits where the phases of different segments or limbs actually control movements. For example, the pyloric and gastric circuits can be coordinated in the crustacean stomatogastric system by a higher-level modulatory neuron that channels the faster pyloric rhythm to a key cell in the gastric mill rhythm (Bartos and Nusbaum, 1997; Bartos *et al.*, 1999) (Fig. 12). In crab stomatogastric MCs, the gastric mill cycle has a period of approximately 10 s while the pyloric period is approximately 1 s. When an identified modulatory projection neuron (MCN1) [Fig. 12(a)] is activated, the gastric mill pattern is largely controlled by

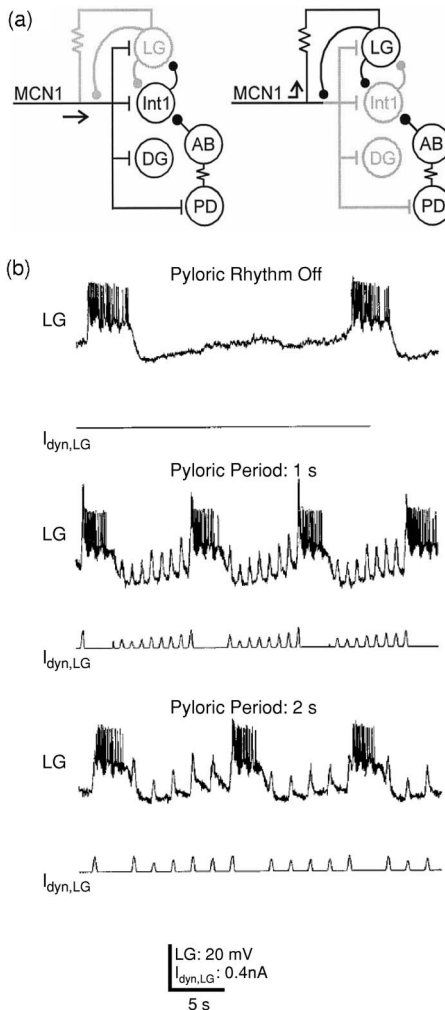


FIG. 12. (a) Schematic circuit diagram underlying MCN1 activation of the gastric mill rhythm of a crustacean. The circuit represents two phases of the rhythm, retraction (left) and protraction (right). Lighter lines represent inactive connections. LG, Int1, and DG are members of the gastric CPG and AB and PD are members of the pyloric CPG. Arrows represent functional transmission pathways from the MCN1 neuron. Bars are excitatory and dots are inhibitory. (b) The gastric mill cycle period; the timing of each cycle is a function of the pyloric rhythm frequency. With the pyloric rhythm turned off, the gastric rhythm cycles slowly (LG). Replacing the AB inhibition of Int1 with current into LG using a dynamic clamp reduces the gastric mill cycle period. Modified from [Bartos et al., 1999](#).

interactions between MCN1 and gastric neurons LG and Int 1 ([Bartos et al., 1999](#)). When Int 1 is stimulated, the AB to LG synapse [see Fig. 12(b)] plays a major role in determining the gastric cycle period and coordination between the two rhythms. The two rhythms become coordinated because LG burst onset occurs with a constant latency after the onset of the triggering pyloric input. These results suggest that intercircuit synapses can enable an oscillatory circuit to control the speed of a slower oscillatory circuit as well as provide a mechanism for intercircuit coordination ([Bartos et al., 1999](#)).

Another type of intercircuit coupling occurs among segmental CPGs. In the crayfish, abdominal appendages

called swimmerets beat in a metachronal rhythm from posterior to anterior with a frequency-independent phase lag of about  $90^\circ$ . Like most rhythms of this kind, the phase lag must remain constant over different frequencies. In theoretical and experimental studies by [Jones et al. \(2003\)](#), it was shown that such phase constancy could be achieved by ascending and descending excitatory and inhibitory synapses, if the right connections were made. It appears realistic to look at rhythmic MCs as recurrent networks with many intrinsic feedback connections so that the information on a complete spatiotemporal pattern is contained in the long-term activity of just a few neurons in the circuit. The number of intercircuit connections necessary for coordination of the rhythms is therefore much smaller than the total number of neurons in the MC.

To investigate coordinating two elements of a population of neurons, one may investigate how various couplings, implemented in a dynamical clamp, might operate in the cooperative behavior of two pyloric CPGs. This is a hybrid and simplified model of the more complex interplay between brain areas whose coordinated activity might be used to achieve various functions. We now describe such a set of experiments.

Artificially connecting neurons from the pyloric CPG of two different animals using a dynamic clamp could lead to different kinds of coordination depending on which neurons are connected and what kind of synapses are used ([Szücs et al., 2004](#)). Connecting the pacemaker group with electrical synapses could achieve same-phase synchrony; connecting them with inhibitory synapses provided much better coordination but out of phase. The two pyloric circuits (Fig. 13) are representative of circuits driven by coupled pacemaker neurons that communicate with each other via both graded and conventional chemical interactions. But while the unit CPG pattern is formed in this way, coordinating fibers must use spike-mediated postsynaptic potentials only. It therefore becomes important to know where in the circuit to input these connections in order to achieve maximum effectiveness in terms of coordinating the entire circuit and ensuring phase constancy at different frequencies. Simply coupling the PDs together electrically is rather ineffective although the bursts (not spikes) do synchronize completely even at high coupling strengths. The fact that the two PDs are usually running at slightly different frequencies leads to bouts of chaos in the two neurons, i.e., a reduction in regularity. More effective synchronization occurs when the pacemaker groups are linked together with moderately strong reciprocal inhibitory synapses in the classic half-center configuration. Bursts in two CPGs are of course  $180^\circ$  out of phase, but the frequencies are virtually identical. The best in-phase synchronization is obtained when the LPs are coupled to the contralateral PDs with inhibitory synapses (Fig. 13).

#### D. Chaos and adaptability

Over the past decades there have been many reports of the observation of chaos in the analysis of various

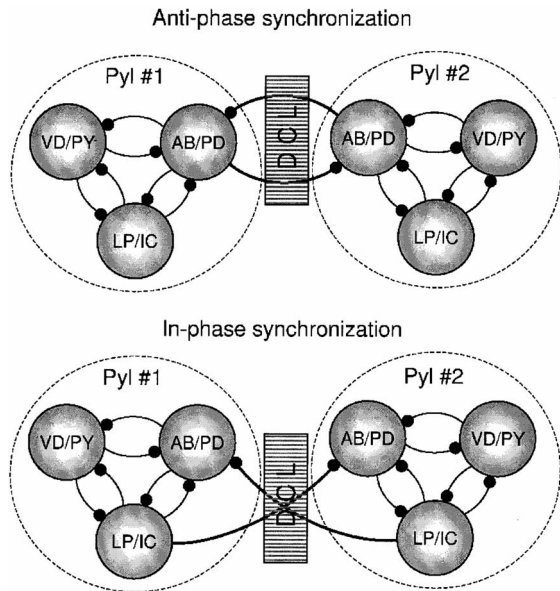


FIG. 13. Coupling of two biological pyloric CPGs Pyl 1 and Pyl 2 by means of dynamic clamp artificial inhibitory synapses. The dynamic clamp is indicated by DCL. Reciprocal inhibitory coupling between the pacemaker groups AB and PD leads to antiphase synchronization while nonreciprocal coupling from the LPs produces in-phase synchronization. Figure provided by A. Szücs.

time courses of data from a variety of neural systems ranging from the simple to the complex (Glass, 1995; Korn and Faure, 2003). Perhaps the outstanding feature of these observations is not the presence of chaos but the appearance of low-dimensional dynamical systems as the origin of spectrally broadband, nonperiodic signals observed in many instances (Rabinovich and Abarbanel, 1998). All chaotic oscillations occur in a bounded state-space region of the system. This state space is captured by the multivariate time course of the vector of dynamical degrees of freedom associated with neural spike generation. These degrees of freedom are comprised of the membrane voltage and the characteristics of the various ion currents in the cell. Using nonlinear dynamical tools one can reconstruct a mathematically faithful proxy state space for the neuron by using the membrane voltage and its time-delayed values as coordinates for the state space (see Fig. 14).

Chaos seems to be almost unavoidable in natural systems comprised of numerous simple or slightly complex subsystems. As long as there are three or more dimensions, chaotic motions are generic in the broad mathematical sense. So neurons are dealt a chaotic hand by nature and may have little choice but to work with it. Accepting that chaos is more or less the only choice, we can ask what benefits accrue to the robustness and adaptability of neural activity.

Chaos itself may not be essential for living systems. However, the multitude of regular regimes of operation that can be accomplished in dynamical systems composed of elements which themselves can be chaotic gives rise to a basic principle that nature may use for the or-

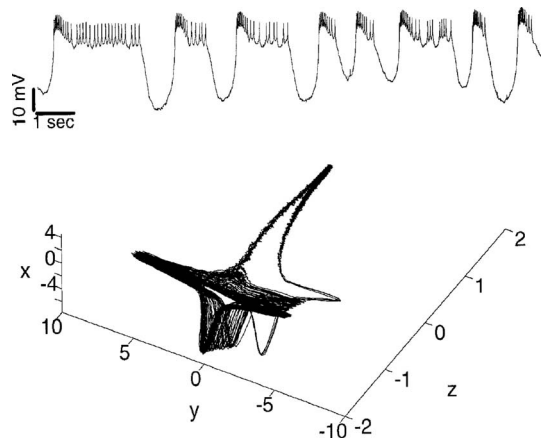


FIG. 14. Chaotic spiking-bursting activity of isolated CPG neurons. Top panel: Chaotic membrane potential time series of a synaptically isolated LP neuron from the pyloric CPG. Bottom panel: State-space attractor reconstructed from the voltage measurements of the LP neuron shown in the top panel using delayed coordinates  $[x(t), y(t), z(t)] = [V(t), V(t-T), V(t-2T)]$ . This attractor is characterized by two positive Lyapunov exponents. Modified from Rabinovich and Abarbanel, 1998.

ganization of neural assemblies. In other words, chaos is not responsible for the work of various neural structures, but rather for the fact that those structures function at the edge of instability, and often beyond it. By recognizing chaotic motions in a system state space as unstable, but bounded, this geometric notion gives credence to the otherwise unappealing idea of system instability. The instability inherent in chaotic motions, or more precisely in nonlinear dynamics of systems with chaos, facilitates the extraordinary ability of neural systems to adapt, make transitions from one pattern of behavior to another when the environment is altered, and consequently create a rich variety of patterns. Thus chaos gives a means to explore the opportunities available to the system when the environment changes, and acts as a precursor to adaptive, reliable, and robust behavior for living systems.

Throughout evolution neural systems have developed different methods of self-control or self-organization. On the one hand, such methods preserve all advantages of the complex behavior of individual neurons, such as allowing regulation of the time period of transitions between operating regimes, as well as regulation of the operation frequency in any given regime. They also preserve the possibility of a rich variety of periodic and nonperiodic regimes of behavior; see Fig. 11 and Elson *et al.* (1988) and Varona, Torres, Huerta, *et al.* (2001). On the other hand, these control or organizational techniques provide the needed predictability of behavioral patterns in neural assemblies.

Organizing chaotic neurons through appropriate wiring associated with electrical, inhibitory, and excitatory connections appears to allow for essentially regular operation of such an assembly (Huerta *et al.*, 2001). As an example we mention the dynamics of an artificial micro-

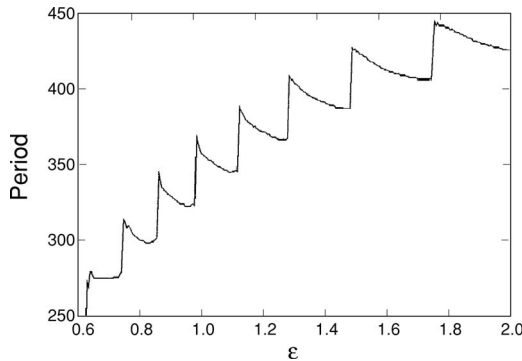


FIG. 15. Average bursting period of the model heartbeat CPG activity as a function of the inhibitory coupling  $\epsilon$ . Modified from [Malkov et al., 1996](#).

circuit that mimics the leech heartbeat CPG ([Calabrese et al., 1995](#)). This CPG model consists of six chaotic neurons implemented with Hindmarsh-Rose equations reciprocally coupled to their neighbors through inhibitory synapses. The modeling showed that in spite of chaotic oscillations of individual neurons the cooperative dynamics is regular and, most importantly, the period of bursting of the cooperative dynamics sensitively depends on the values of the inhibitory connections ([Malkov et al., 1996](#)) (see Fig. 15). This example shows the high level of adaptability of a network consisting of chaotic elements.

Chaotic signals have many of the traditional characteristics attributed to noise. In the present context we recognize that both chaos and noise are able to organize the irregular behavior of individual neurons or neural assemblies, but the principal difference is that dynamical chaos is a controllable irregularity, possessing structure in state space, while noise is an uncontrollable action of dynamical systems. This distinction is extremely important for information processing as discussed below (see Sec. III.B.2 and its final remarks).

There are several possible functions for noise ([Lindner et al., 2004](#)), even seen as high-dimensional essentially unpredictable chaotic motion, in neural network studies. In high-dimensional systems composed here of many coupled nonlinear oscillators, there may be small basins of attraction where, in principle, the system could become trapped. Noise will blur the basin boundaries and remove the possibility that the main attractors could accidentally be missed and highly functional synchronized states lost to neuronal activity. Some noise may persist in the dynamics of neurons to smooth out the actions of the chaotic dynamics active in creating robust, adaptable networks.

Chaos should not be mistaken for noise, as the former has phase-space structure which can be utilized for synchronization, transmission of information, and regularization of the network for performance of critical functions. In the next section we discuss the role of chaos in information processing and information creation.

### III. INFORMATIONAL NEURODYNAMICS

The flow of information in the brain goes from sensory systems, where it is captured and encoded, to central nervous systems, where it is further processed to generate response signals. In the central nervous system command signals are generated and transported to the muscles to produce motor behavior. At all these stages learning and memory processes that need specific representations take place. Thus it is not surprising that the nervous system has to use different coding strategies at different levels of the transport, storage, and use of information. Different transformations of codes have been proposed for the analysis of spiking activity in the brain. The details depend on the particular system under study but some generalization is possible in the framework of analyzing the spatial, temporal, and spatiotemporal codes. There are many unknown factors related to the cooperation between these different forms of information coding. Some key questions are as follows: (i) How can neural signals be transformed from one coding space to another without loss of information? (ii) What dynamical mechanisms are responsible for storing time in memory? (iii) Can neural systems generate new information based on their sensory inputs? In this section, we discuss some important experimental results and new paradigms that can help to address these questions.

#### A. Time and neural codes

Information from sensory systems arrives at sensory neurons as analog changes in light intensity or temperature, or chemical concentration of an odorant, or skin pressure, etc. These analog data are represented in internal neural circuit dynamics and computations by action-potential sequences passed from sensory receivers to higher-order brain processes. Neural codes guarantee the efficiency, reliability, and robustness of the required neural computations ([Machens, Gollisch, et al., 2005](#)).

##### 1. Temporal codes

Two of the central questions in understanding the dynamics of information processing in the nervous system are how information is encoded and how the coding space depends on time-dependent stimuli.

A code in the biophysical context of the nervous system is a specific representation of the information operated on or created by neurons. A code requires a unit of information. However, this is already a controversial issue since, as we have previously discussed, information is conveyed through chemical and electrical synapses, neuromodulators, hormones, etc., which makes it difficult to point out a single universal unit of information. A classical assumption at the cellular level, valid for many neural systems, is that a spike is an all-or-nothing event and thus a good candidate for a unit of information, at least in a computational sense. This is not the only sim-

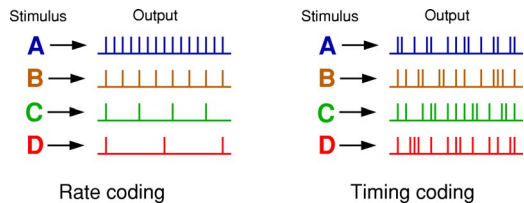


FIG. 16. (Color online) Two possible codes for the activity of a single neuron. In a rate code, different inputs (A–D) are transformed into different output spiking rates. In a timing code, different inputs are transformed into different spiking sequences with precise timing.

plification needed to analyze neural codes for a first approach. A coding scheme needs to determine a coding space and take into account time.

A common hypothesis is to consider a universal time for all neural elements. Although this is the approach we discuss here, we remind the reader that this is also an arguable issue, since neurons can sense time in many different ways: by their intrinsic activity (subcellular dynamics) or by external input (synaptic and network dynamics). Internal and external (network) clocks are not necessarily synchronized and can have different degrees of precision, time scales, and absolute references. Some dynamical mechanisms can contribute to make neural time unified and coherent.

On the one hand, when we consider just a single neuron, a spike as the unit of information, and a universal time, we can talk about two different types of encoding: the frequency of firing can encode information about the stimulus in a rate code; on the other hand, the exact temporal occurrence of spikes can encode the stimulus and its response in a precise timing code. The two coding alternatives are schematically represented in Fig. 16. In this context, a precise timing or temporal code is a code in which relative spike timings (rather than spike counts) are essential for information processing. Several experimental recordings have shown the presence of both types of single-cell coding in the nervous system (Adrian and Zotterman, 1926; Barlow, 1972; Abeles, 1991; McClurkin *et al.*, 1991; Softky, 1995; Shadlen and Newsome, 1998). In particular, fine temporal precision and reliability of spike dynamics are reported in many cell types (Segundo and Perkel, 1969; Mainen and Sejnowski, 1995; deCharms and Merzenich, 1996; de Ryter van Steveninck *et al.*, 1997; Segundo *et al.*, 1998; Mehta *et al.*, 2002; Reinagel and Reid, 2002). Single neurons can display these two codes in different situations.

## 2. Spatiotemporal codes

A population of coupled neurons can have a coding scheme different from the sum of the individual coding mechanisms. Interactions among neurons through their synaptic connections, i.e., their cooperative dynamics, allow for more complex coding paradigms. There is much experimental evidence which shows the existence of so-called population codes that collectively express a complex stimulus better than the individual neurons [see,

e.g., Georgopoulos *et al.* (1986); Wilson and McNaughton (1993); Fitzpatrick *et al.* (1997); Pouget *et al.* (2000)]. The efficacy of population coding has been assessed mainly using measures of mutual information in modeling efforts (Seung and Sompolinsky, 1993; Panzeri *et al.*, 1999; Sompolinsky *et al.*, 2001).

Two elements can be used to build population codes: neuronal identity (i.e., neuronal space) and the time occurrence of neural events (i.e., the spikes). Accordingly, information about the physical world can be encoded in temporal or spatial (combinatorial) codes, or combinations of these two: spike time can represent physical time (a pure temporal code), spike time can represent physical space, neuronal space can represent physical time (a pure spatial code), and neuronal space can represent physical space (Nádasdy, 2000). When we consider a population of neurons, information codes can be spatial, temporal, or spatiotemporal.

Population coding can also be characterized as independent or correlated (deCharms and Christopher, 1998). In an independent code, each neuron represents a separate signal: all information that is obtainable from a single neuron can be obtained from that neuron alone, without reference to the activities of other neurons. For a correlated or coordinated coding messages are carried at least in part by the relative timing of the signals from a population of neurons.

The presence of network coding, i.e., a spatiotemporal dynamical representation of incoming messages, has been confirmed in several experiments. As an example, we discuss here the spatiotemporal representation of episodic experiences in the hippocampus (Lin *et al.*, 2005). Individual hippocampal neurons respond to a wide variety of external stimuli (Wilson and McNaughton, 1994; Dragoi *et al.*, 2003). The response variability at the level of individual neurons poses an obstacle to the understanding of how the brain achieves its robust real-time neural coding of the stimulus (Lestienne, 2001). Reliable encoding of sensory or other network inputs by spatiotemporal patterns resulting from the dynamical interaction of many neurons under the action of the stimulus can solve this problem (Hamilton and Kauer, 1985; Laurent, 1996; Vaadia *et al.*, 1999).

Lin *et al.* (2005) showed that mnemonic short-time episodes (a form of one-trial learning) can trigger firing changes in a set of CA1 hippocampal neurons with specific spatiotemporal relationships. To find such representations in the central nervous system of an animal is an extremely difficult experimental and computational problem. Because the individual neurons that participate in the representation of a specific stimulus and form a temporal neural cluster in different trials can be different, it is necessary to measure simultaneously the activity of a large number of neurons. In addition, because of the variability in the individual neuron responses, the spatiotemporal patterns of different trials may also look different. Thus, to show the functional importance of the spatiotemporal representation of the stimulus, the reader has to use sophisticated methods of data analysis. Lin *et al.* (2005) developed a 96-channel array to record

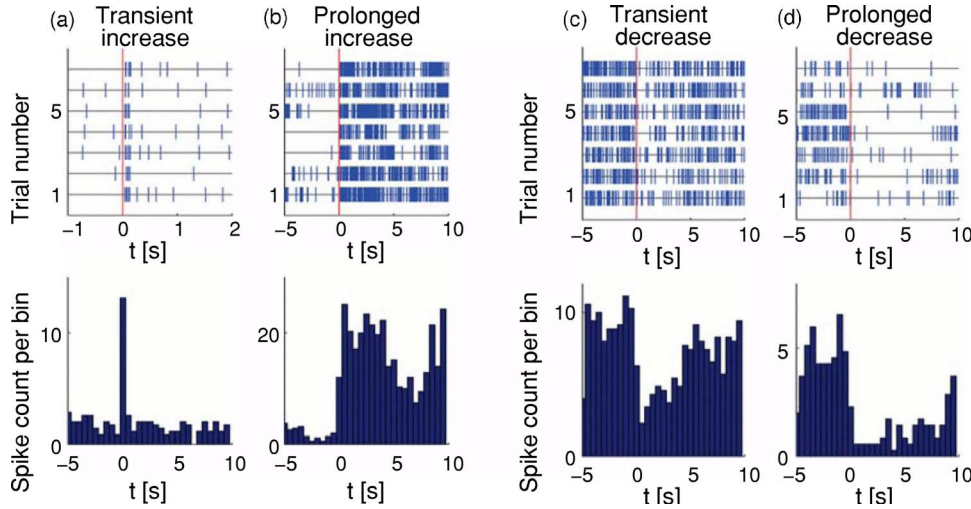


FIG. 17. (Color online) Temporal dynamics of individual CA1 neurons of the hippocampus in response to “startling” events. Spike raster plots [(a)–(d)] upper, seven repetitions each] and corresponding perievent histogram [(a)–(d)] lower, bin width 500 ms] for units exhibiting the four major types of firing changes observed: (a) transient increase, (b) prolonged increase, (c) transient decrease, (d) and prolonged decrease. From Lin et al., 2005.

simultaneously the activity patterns of as many as 260 individual neurons in the mouse hippocampus during various startling episodes (air blow, elevator drop, and earthquake shake). They used multiple-discriminant analysis (Duda et al., 2001) and showed that, even though individual neurons express different temporal patterns in different trials (see Fig. 17), it is possible to identify functional encoding units in the CA1 neuron assembly (see Fig. 18).

The representation of nonstationary sensory information, say, a visual stimulus, can use the transformation of a temporal to a spatial code. The recognition of a specific neural feature can be implemented through the transformation of a spatial code into a temporal one through coincidence detection of spikes. A spatial representation can be transformed into a spatiotemporal one to provide the system with higher capacity and robustness and sensitivity at the same time. Finally, a spatiotemporal code can be transformed into a spatial code in processes related to learning and memory. These possibilities are summarized in Fig. 19.

Morphological constraints of neural connections in some cases impose a particular spatial or temporal code. For example, projection neurons transfer information between areas of the brain along parallel pathways by preserving the input topography as neuronal specificity at the output. In many cases the input topography is transformed to a different topography that is preserved; for example, the retinotopic map of the primary visual areas and somatotopic maps of the somatosensory and motor areas. Other transformations do not preserve topology. These include transformations in place cells in the hippocampus, and the tonotopic representation in the auditory cortex. There is a high degree of convergence and divergence of projections in some of these transformations that can be a computationally optimal design (Garcia-Sanchez and Huerta, 2003). In most of these transformations, the temporal dimension of the stimulus is encoded by spike timing or by the onset of firing-rate transients.

An example of transforming a spatiotemporal code to a pure spatial code was found in the olfactory system of

locusts, and has been modeled by Nowotny, Rabinovich, et al. (2003) and Nowotny et al. (2005). Figure 20 gives a graphical explanation of the connections involved. The complex spatiotemporal code of sequences of transiently synchronized groups of projection neurons in the antennal lobe (Laurent et al., 2001) is sliced into temporal snapshots of activity by feedforward inhibition and coincidence detection in the next processing layer, the mushroom body (Perez-Orive et al., 2002). This snapshot code is presumably integrated over time in the next stages of the mushroom lobes, completing the transformation of the spatiotemporal code in the antennal lobe to a purely spatial code. It was shown in simulations that the temporal information on the sequence of activity in the antennal lobe that could be lost in downstream temporal integration can be restored through slow lateral excitation in the mushroom body (Nowotny, Rabinovich, et al., 2003). This has been reported experimentally (Leitch and Laurent, 1996). With this extra feature the transformation from a spatiotemporal code to a pure spatial code becomes free of information loss.

### 3. Coexistence of codes

Different stages of neural information processing are difficult to study in isolation. In many cases it is hard to distinguish between what is an encoding of an input and what is a static or dynamic, perhaps nonlinear, response to that input. This is a crucial observation that is often missed. Encoding and decoding may or may not be part of a dynamical process. However, the creation of information (discussed in the next section) and the transformation of spatial codes to temporal or spatiotemporal codes are always dynamical processes.

Another, but less frequently addressed, issue about coding is the presence of multiple encodings in single-cell signals (Latorre et al., 2006). This may occur since multifunctional networks may need multiple coexisting codes. The neural signatures in interspike intervals of CPG neurons provide an example (Szücs et al., 2003). Individual fingerprints characteristic of the activity of each neuron coexist with the encoding of information in

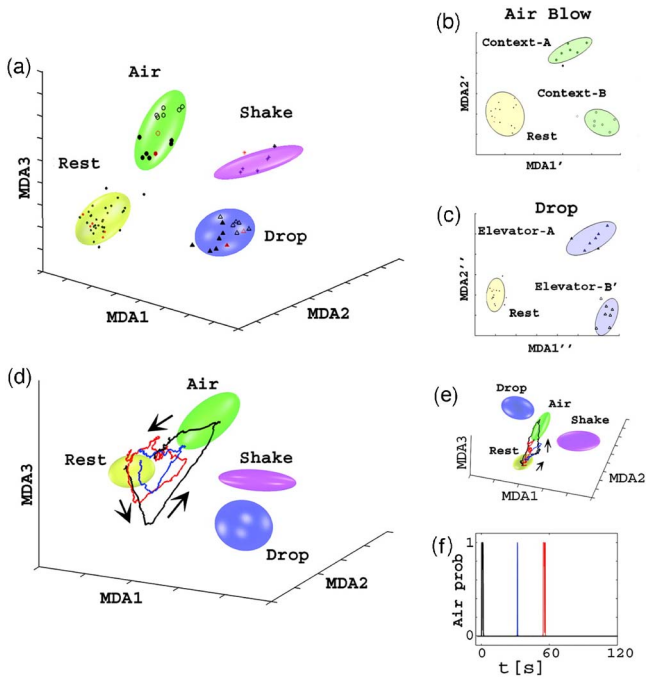


FIG. 18. (Color online) Classification, visualization, and dynamical decoding of CA1 ensemble representations of startle episodes by multiple-discriminant analysis (MDA) methods. (a) Firing patterns during rest, air blow, drop, and shake epochs are shown after being projected to a three-dimensional space obtained by using MDA for mouse A; MDA1–MDA3 denote the discriminant axes. Both training (dark symbols) and test data are shown. After the identification of startle types, a subsequent MDA is further used to resolve contexts (full vs empty symbols) in which the startle occurred for air-blow context (b) and for elevator drop (c). (d) Dynamical monitoring of ensemble activity and the spontaneous reactivation of startle representations. Three-dimensional subspace trajectories of the population activity in the two minutes after an air-blow startle in mouse A are shown. The initial response to an air blow (black line) is followed by two large spontaneous excursions (blue/dark and red/light lines), characterized by coplanar, geometrically similar lower-amplitude trajectories (directionality indicated by arrows). (e) The same trajectories as in (a) from a different 3D angle. (f) The timing ( $t_1=31.6$  s and  $t_2=54.8$  s) of the two reactivations (marked in blue/dark and red/light, respectively) after the actual startle (in black) ( $t=0$  s). The vertical axis indicates the air-blow classification probability. From Lin *et al.*, 2005.

the frequency and phase of the spiking-bursting rhythms. This is an example that shows that codes can be nonexclusive. In bursting activity, coding can exist in slow waves, but also, and simultaneously, in the spiking activity.

In the brain, specific neural populations often send messages through projections to several information “users.” It is difficult to imagine that all of them decode the incoming signals in the same way. In neuroscience the relationship between the encoder and decoder is not a one-to-one map but can be many simultaneous maps from the senders to different receivers, based on different dynamics. This departs from Shannon’s classical

formulation of information theory (Fano, 1961; Gallager, 1968). For example, cochlear afferents in birds bifurcate to two different areas of the brain with different decoding properties. One area extracts information about relative timing from a spike train, whereas the other extracts the average firing rate (Konishi, 1990).

#### 4. Temporal-to-temporal information transformation: Working memory

There is another important code transformation of interest here: the transformation of a finite amount of temporal information to a slow temporal code lasting for seconds, minutes, or hours. We are able to remember a phone number from someone who just called us. Persistent dynamics is one of the mechanisms for this phenomenon, which is usually named short-term memory (STM) or working memory; it is a basic function of the brain. Working memory, in contrast to long-term memory which most likely requires molecular (membrane) or structural (connection) changes in neural circuits, is a dynamical process. The dynamical origins of working memory can vary.

One plausible idea is that STMs are the result of active reverberation in interconnected neural clusters that fire persistently. Since its conceptualization (de Nô, 1938; Hebb, 1949), reverberating activity in microcircuits has been explored in many modeling papers (Grossberg, 1973; Amit and Brunel, 1997a; Durstewitz *et al.*, 2000; Seung *et al.*, 2000; Wang, 2001). Experiments with cultured neuronal networks show that reverberatory activity can be evoked in circuits that have no preexisting anatomical specialization (Lau and Bi, 2005). The reverberation is primarily driven by recurrent synaptic excitation rather than complex individual neuron dynamics such as bistability. The circuitry necessary for reverberating activity can be a result of network self-organization. Persistent reverberatory activity can exist even in the simplest circuit, i.e., an excitatory neuron with inhibitory self-feedback (Connors, 2002; Egorov *et al.*, 2002). In this case, reverberation depends on asynchronous transmitter release and intracellular calcium stores as shown in Fig. 21.

Nature seems to use different dynamical mechanisms for persistent microcircuit activity: cooperation of many interconnected neurons, persistent dynamics of individual neurons, or both. These mechanisms each have distinct advantages. For example, network mechanisms can be turned on and off quickly (McCormick *et al.*, 2003) [see also Brunel and Wang (2001)]. Most dynamical models with persistent activity are related to the analysis of microcircuits with local feedback excitation between principal neurons controlled by disynaptic feedback inhibition. Such basic circuits spontaneously generate two different modes: relative quiescence and persistent activity. The triggering between modes is controlled by incoming signals. The review by Brunel (2003) considers several basic models of persistent dynamics, including bistable networks with excitation only and multistable models for working memory of a discrete set

Transformation of codes	What for	Dynamical mechanism
	Representation of nonstationary sensory information Learning and memory	Context-sensitivity synaptic plasticity
	Labeling for recognition	Coincidence detector
	Capacity robustness sensitivity	Winnerless competition principle (WLC)
	Learning and memory	Spike-time dependent synaptic plasticity

FIG. 19. (Color online) Summary of possible scenarios for the transformation of codes, their functional implications, and the dynamical mechanism involved.

of pictures with structured excitation and global inhibition.

Working memory is used for tasks such as planning, organizing, rehearsing, and movement preparation. Experiments with functional magnetic resonance imaging reveal some aspects of the dynamics of working memory [see, for example, Diwadkar *et al.* (2000) and Nystrom *et al.* (2000)]. It is important to note that working memory has a limited capacity of around four to seven items (Cowan, 2001; Vogel and Michizawa, 2004). An essential feature attributed to working memory is the labile and transient nature of its representations. Because such representations involve many coupled neurons from cortical areas (Curts and D'Esposito, 2003), it is natural to model working memory as the spatiotemporal dynamics of large neural networks.

A popular idea is to model working memory with attractors. Representation of items in working memory by attractors may guarantee its robustness. Although robustness is an important requisite for a working-memory system, its transient properties are also important. Consider a foraging task in which an animal uses visual input to catch prey (Nakahara and Doya, 1998). It is helpful to store the location of the prey in the animal's working memory if the prey goes behind a bush and the sensory cue becomes temporarily unavailable. However, the memory should not be retained forever because the prey may have actually gone away or may have been eaten by another animal. Furthermore, if more prey appears near the animal, the animal should quickly load the location of the new prey into its working memory without being disturbed by the old memory.

This example illustrates that there are more requirements for a working-memory system than solely robust

maintenance. First, the activity should be maintained but not for too long. Second, the activity should be reset quickly when there is a novel sensory cue that needs to be stored. In other words, the neural dynamics involved in working memory for goal-directed behaviors should have the properties of long-term maintenance and quick switching. A corresponding model based on “near-saddle-node” bifurcation dynamics has been suggested by Nakahara and Doya (1998). The authors have analyzed the dynamics of a network of model neural units that are described by the following map (see Fig. 22):

$$y_i(t_{n+1}) = F\left(ay_i(t_n) + b + \sum_{j \neq i} \rho_{ij}y_j(t_n) + \gamma_i I_i(t_n)\right), \quad (14)$$

where  $y_i(t_n)$  is the firing rate of the  $i$ th unit at time  $t_n$ ,  $F(z) = 1/[1 + \exp(-z)]$  is a sigmoid function,  $a$  is the self-connection weight,  $\rho_{ij}$  are the lateral connection weights,  $I_i(t)$  are external inputs,  $b$  is the bias, and  $\gamma_i$  are constants used to scale the inputs  $I_i(t)$ . As the bias  $b$  is increased, the number of fixed points changes sequentially from one to two, three, two, and then back to one. A saddle-node bifurcation occurs when the stable transition curve  $y(t_{n+1}) = F(z)$  is tangent to the fixed point  $y(t_{n+1}) = y(t_n)$  (see Fig. 22). Just near the saddle-node bifurcation the system shows persistent activity. This means that it spends a long time in the narrow channel between the bisectrix and the sigmoid activation curve and then goes to the fixed point quickly. Such dynamical behavior reminds one of the well-known intermittency phenomenon in physics (Landau and Lifshitz, 1987). Because the effect of the sum of the lateral and external inputs in Eq. (14) is equivalent to a change in the bias, the mechanism may satisfy the requirements of the dy-

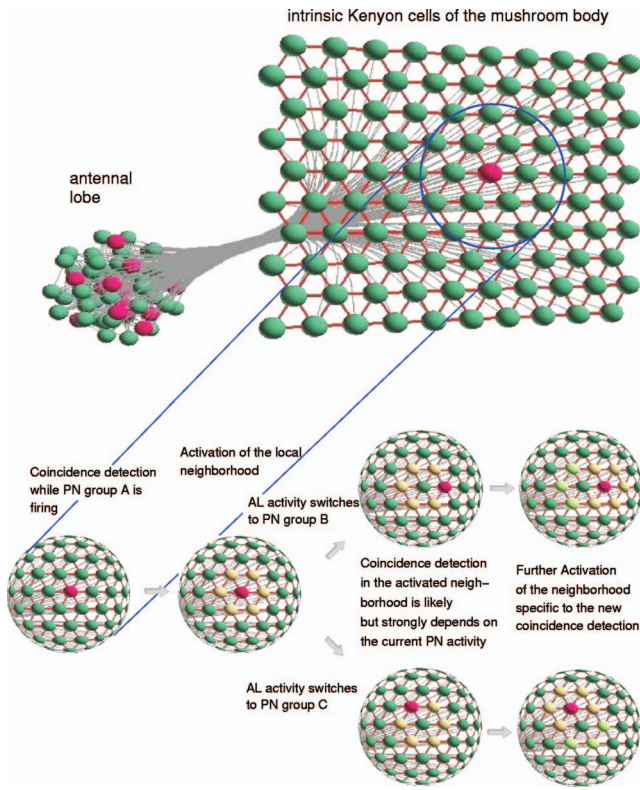


FIG. 20. (Color) Illustration of the transformation of temporal into spatial information. If a coincidence detection occurs, the local excitatory connections activate the neighbors of the active neuron (yellow neurons). Coincidence detection of input is now more probable in these activated neighborhoods than in other Kenyon cells (KCs). Which of the neighbors might fire a spike, however, depends on the activity of the projection neurons (PNs) in the next cycle. It might be a different neuron for active group B of PNs (upper branch) than for active group C (lower branch). In this way local sequences of active KCs form. These depend on the identity of active PNs (coincidence detection) as well as on the temporal order of their activity (activated neighborhoods). Modified from Nowotny, Rabinovich, et al., 2003.

namics of working memory for goal-directed behavior: long-term maintenance and quick switching.

Another reasonable model for working memory consists of competitive networks with stimulus-dependent inhibitory connections [as in Eq. (9)]. One of the advantages of such a model is the ability to have both working memory and stimulus discrimination. This idea was proposed by Machens, Romo, et al. (2005) in relation to the frontal-lobe neural architecture. The network first perceives the stimulus, then holds it in the working memory, and finally makes a decision by comparing that stimulus with another one. The model integrates both working memory and decision making since the number of stable fixed points and the size of the basins of attractors are controlled by the connection matrix  $\rho_{ij}(S)$  which depends on the stimuli  $S$ . The working-memory phase corresponds to the bifurcation boundary, i.e.,  $\rho_{ij} = \rho_{ji} = \rho_{ii}$ . In the state space of the dynamical model, this phase is represented by a stable manifold called a “continuous

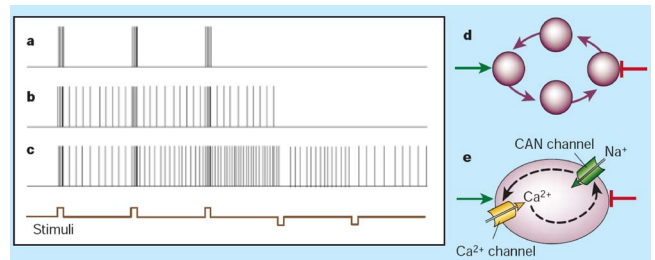


FIG. 21. (Color online) Reverberation can be the dynamical origin for working memory in minimal circuits. (a) Most neurons respond to excitatory stimuli [upward steps in the line below (c)] by spiking only as long as each stimulus lasts. (b) Very rare neurons are bistable: brief excitation leads to persistent spiking, always at the same rate; brief inhibition [downward steps in the line below (c)] can turn it off. (c) Multistable neurons persistently increase or decrease their spiking across a range of rates in response to repeated brief stimuli. (d) In the reverberatory network model of short-term memory discussed in the text, an excitatory stimulus (left arrow) leads to recursive activity in interconnected neurons. Inhibitory stimuli (bar on the right) can halt the activity. (e) Egorov et al. (2002) suggest that graded persistent activity in single neurons [as in (c)] might be triggered by a pulse of internal  $\text{Ca}^{2+}$  ions that enter through voltage-gated channels;  $\text{Ca}^{2+}$  then activates calcium-dependent nonspecific cation (CAN) channels, through which an inward current (largely comprising  $\text{Na}^+$  ions) enters, persistently exciting the neuron. The positive feedback loop (broken arrows) may include the activity of many ionic channels. Modified from Connors, 2002.

attractor.” This is an attractor that consists of continuous sets of fixed points [see Amari (1977) and Seung (1998)]. Thus the stimulus creates a specific fixed point and, at the next stage, the working memory (a continuous attractor) maintains it. During the comparison and decision phase, the second stimulus is mapped onto the same state space as another attractor. The criterion of the decision maker is reflected in the positions of the separatrices that separate the basins of attraction of different

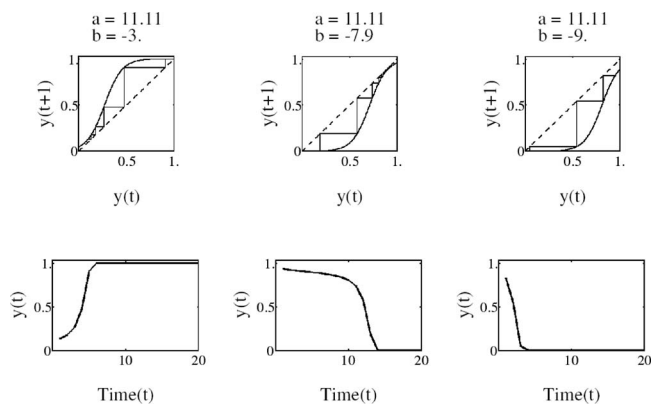


FIG. 22. Temporal responses of self-recurrent units: Near-saddle-node bifurcation with  $a=11.11$ ,  $b=-7.9$  (center panels). Increased bias,  $b=-3.0$  (left panels). Decreased bias  $b=-9.0$  (right panels). Modified from Nakahara and Doya, 1998.

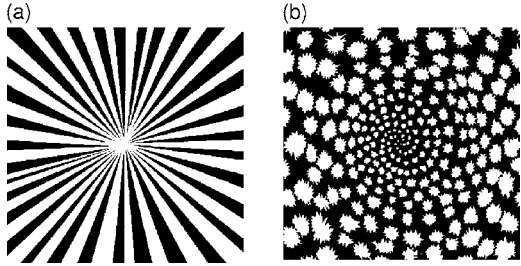


FIG. 23. Hallucinations generated by LSD are an example of a dynamical representation of the internal activity of the visual cortex without an input stimulus. Figure shows examples of (a) funnel and (b) spiral hallucinations. Modified from Bressloff, et al. 2001.

stimuli, i.e., fixed points (see an alternative approach in Rabinovich and Huerta, 2006).

We think that the intersection of the mechanisms responsible for persistent activity of single neurons with the activity of a network with local or nonlocal recurrence provides robustness against noise and perturbations, and at the same time makes working memory more flexible.

## B. Information production and chaos

Information processing in the nervous system involves more than the encoding, transduction, and transformation of incoming information to generate a corresponding response. In many cases, neural information is created by the joint action of the stimulus and the individual neuron and network dynamics. A creative activity like improvisation on the piano or writing a new poem results in part from the production of new information. This information is generated by neural circuits in the brain and does not directly depend on the environment.

Time-dependent visual hallucinations are one example of information produced by neural systems, in this case the visual cortex, themselves. Such hallucinations consist in seeing something that is not in the visual field. There are interesting models, beginning from the pioneering paper of Ermentrout and Cowan (1979), that explain how the intrinsic circuitry of the brain's visual cortex can generate the patterns of activity that underlie hallucinations. These hallucination patterns usually take the form of checkerboards, honeycombs, tunnels, spirals, and cobwebs (see two examples in Fig. 23). Because the visual cortex is an excitable medium it is possible to use spatiotemporal amplitude equations to describe the dynamics of these patterns (see the next section). These models are based on advances in brain anatomy and physiology that have revealed strong short-range connections and weaker long-range connections between neurons in the visual cortex. Hallucination patterns can be quasistatic, periodically repeatable, or chaotically repeatable as in low-dimensional convective turbulence; see for a review Rabinovich et al. (2000). Unpredictability of the specific pattern in the hallucination sequences

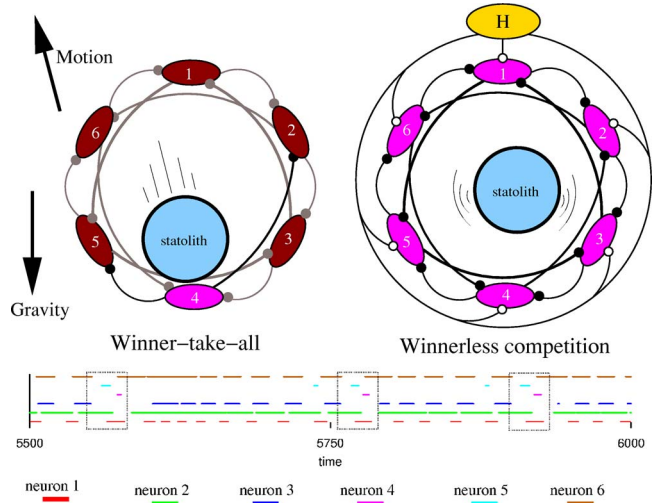


FIG. 24. (Color online) Dual sensory network dynamics. Top panels: Schematic representation of the dual role of a single statocyst, the gravity sensory organ of the mollusk *Clione*. During normal swimming, a stonelike structure, the statolith, hits the mechanoreceptor neurons that react to this excitation. In *Clione*'s hunting behavior, the statocyst receptors receive additional excitation from the cerebral hunting neuron (H) which generates a winnerless competition among them. Bottom panels: Chaotic sequential switching displayed by the activity of the statocyst during hunting mode in a model of a six-receptor network. This panel displays the time intervals in which each neuron is active ( $a_i > 0.03$ ). Each neuron is represented by a different color. The dotted rectangles indicate the activation-sequence locks among units that are active at a given time interval within each network for time windows in which all six neurons are active.

(movie) means the generation of information that in principle can be characterized by the value of the Kolmogorov-Sinai entropy (Scott, 2004).

The creation or production of new information is a theme that has been neglected in theoretical neuroscience, but it is a provocative and challenging point that we discuss in this section. As mentioned before, information production or creation must be a dynamical process. Below we discuss an example that emphasizes the ability of neural systems to produce information-rich output from information-poor input.

## 1. Stimulus-dependent motor dynamics

A simple network with which we can discuss the creation of new information is the gravity-sensing neural network of the marine mollusk *Clione limacina*. *Clione* is a blind planktonic animal, negatively buoyant, that has to maintain continuous motor activity in order to keep its preferred head-up orientation. Its motor activity is controlled by wing CPGs and tail motor neurons that use signals from its gravity-sensing organs, the statocysts (Panchin et al., 1995). A six-receptor neural network model with synaptic inhibition has been built to describe a single statocyst (Varona, Rabinovich, et al., 2002) (see Fig. 24). This is a small sphere in which a statolith, a stonelike structure, moves according to the gravitational

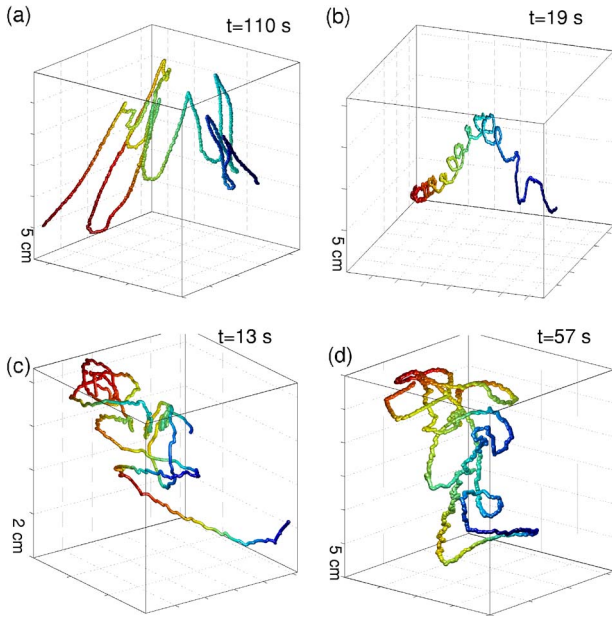


FIG. 25. (Color online) *Clione* swimming trajectories in different situations. (a) Three-dimensional trajectory of routine swimming. Here and in the following figures, different colors (gray tones) are used to emphasize the three-dimensional perception of the trajectories and change according to the  $x$  axis. The indicated time  $t$  is the duration of the trajectory. (b) Swimming trajectory of *Clione* with the statocysts surgically removed. (c) Trajectory of swimming during hunting behavior evoked by the contact with the prey. (d) Trajectory of swimming after immersion of *Clione* in a solution that pharmacologically evokes hunting. Modified from Levi *et al.*, 2004.

field. The statolith excites the neuroreceptors by pressing down on them. When excited, the receptors send signals to the neural systems responsible for wing beating and tail orientation.

The statocysts have a dual role (Levi *et al.*, 2004, 2005). During normal swimming only neurons that are excited by the statolith are active, and this leads to a winner-take-all dynamical mode as a result of inhibitory connections in the network. (Winner-take-all dynamics is essentially the same as the attractor-based computational ideas discussed earlier.) However, when *Clione* is searching for its food, a cerebral hunting neuron excites each neuron of the statocyst (see Fig. 24). This triggers a competition between all statocyst neurons whose signals participate in the generation of a complex motion that the animal uses to scan the immediate space until it finds its prey (Levi *et al.*, 2004, 2005) (see Fig. 25). The following Lotka-Volterra-type dynamics can be used to describe the activity of this network:

$$\frac{da_i(t)}{dt} = a_i(t) \left( \sigma(\mathbf{H}, \mathbf{S}) - \sum_{j=1}^N \rho_{ij} a_j(t) + H_i(t) \right) + S_i(t), \quad (15)$$

where  $a_i(t) \geq 0$  represents the instantaneous spiking rate of the statocyst neurons,  $H_i(t)$  represents the excitatory stimulus from the cerebral hunting interneuron to neu-

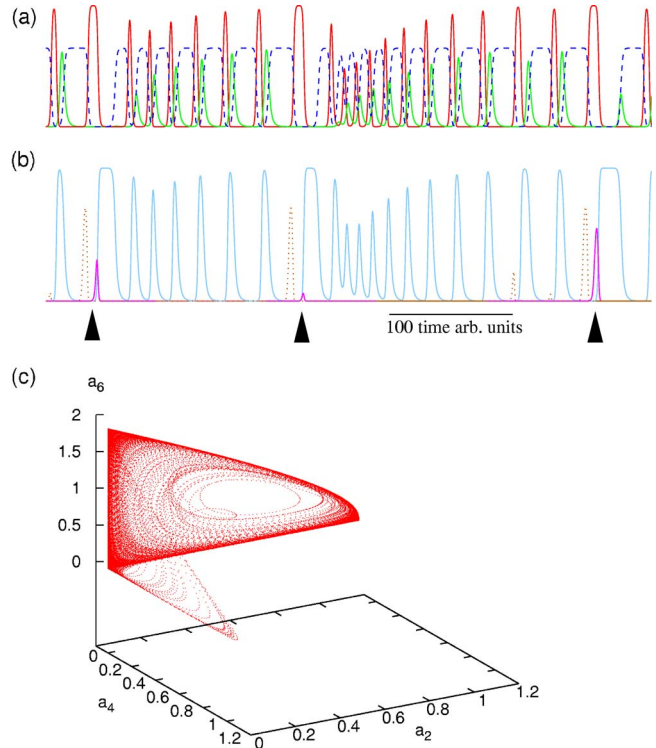


FIG. 26. (Color online) Irregular switching in a network of six statocyst receptors. Traces represent the instantaneous spiking rate of each neuron  $a_i$  [neurons 1,2,3 are shown in (a), neurons 4,5,6 in (b)]. Note that after a neuron is silent for a while, its activity reappears with the same sequence relative to the others (see arrows, and Fig. 24). (c) A projection of the phase portrait of the strange attractor in 3D space; see model (15).

ron  $i$ ,  $S_i(t)$  represents the action of the statolith on the receptor that it is pressing, and  $\rho_{ij}$  is the nonsymmetric statocyst connection matrix. When there is no stimulus from the hunting neuron,  $H_i=0$ , or the statolith,  $S_i=0$ , then  $\sigma(\mathbf{H}, \mathbf{S})=-1$  and all neurons are silent. When the hunting neuron is active  $H_i \neq 0$  and/or the statolith is pressing one of the receptors,  $S_i \neq 0$ ,  $\sigma(\mathbf{H}, \mathbf{S})=+1$ .

During hunting  $H_i \neq 0$ , and we assume that the action of the hunting neuron overrides the effect of the statolith and thus  $S_i \approx 0$ . As a result of the competition, the receptors display a highly irregular, in fact chaotic, switching activity. The phase-space image of the statocyst model in this behavioral mode is a strange attractor [the heteroclinic loops in the phase space of Eq. (15) become unstable; see Sec. IV.C]. For six receptors we have shown (Varona, Rabinovich, *et al.*, 2002) that the observed dynamical chaos is characterized by two positive Lyapunov exponents.

The bottom panel in Fig. 24 is an illustration of the nonsteady switching activity of the receptors. An interesting phenomenon can be seen in this figure and is also pointed out in Fig. 26. Although the timing of each activity is irregular, the sequence of switching among the statocyst receptors is the same for those neurons that are active at a given time window. Dotted rectangles in Fig. 24 point out this fact. The activation-sequence lock

among the statocyst receptor neurons emerges in spite of the highly irregular timing of the switching dynamics and is a feature that can be used for motor coordination (Venaille et al., 2005).

In this example the winnerless competition is triggered by a constant excitation to all statocyst receptors [ $H_i=c_i$ ; see details by Varona, Rabinovich, et al. (2002)]. Thus the stimulus has low information content. Nonetheless, the network of statocyst receptors can use this activity to generate an information-rich signal with positive Kolmogorov-Sinai entropy. This entropy is equal to the value of the new information encoded in the dynamical motion. The statocyst sensory network is thus multifunctional and can generate a complex spatiotemporal pattern useful for motor coordination even when its dynamics are not evoked by gravity, as during hunting.

## 2. Chaos and information transmission

To illustrate the role of chaos in information transmission, we use as an example the inferior olive (IO), which is an input system to the cerebellum. Neurons of the IO may chaotically recode the high-frequency information carried by its inputs into chaotic, low-rate output (Schweighofer et al., 2004). The IO has been proposed as a system that controls and coordinates different rhythms through the intrinsic oscillatory properties of its neurons and the nature of their electrical interconnections (Llinás and Welsh, 1993; de Zeeuw et al., 1998). It has also been implicated in motor learning (Ito, 1982) and in comparing tasks of intended and achieved movements as a generator of error signals (Oscarsson, 1980).

Experimental recordings show that IO cells are electrically coupled and display subthreshold oscillations and spiking activity. Subthreshold oscillations have a relevant role for information processing in the context of a system with extensive electrical coupling. In such systems the spiking activity can be propagated through the network, and, in addition, small differences in hyperpolarized membrane potentials propagate among neighboring cells.

A modeling study suggests that electrical coupling in IO neurons may induce chaos, which would allow information-rich, but low-firing-rate, error signals to reach individual Purkinje cells in the cerebellar cortex. This would provide the cerebellar cortex with essential information for efficient learning without disturbing ongoing motor control. The chaotic firing leads to the generation of IO spikes with different timing. Because the IO has a low firing rate, an accurate error signal will be available for individual Purkinje cells only after repeated trials. Electrical coupling can provide the source of disorder that induces a chaotic resonance in the IO network (Schweighofer et al., 2004). This resonance leads to an increase in information transmission by distributing the high-frequency components of the error inputs over the sporadic, irregular, and non-phase-locked spikes.

The IO single-neuron model consists of two compartments that include a low-threshold calcium current ( $I_{Ca}$ ), an anomalous inward rectifier current ( $I_h$ ), a Hodgkin-Huxley-type sodium current ( $I_{Na}$ ), and a delayed rectifier potassium current ( $I_{Kd}$ ) in the somatic compartment (see Table I). The dendritic compartment contains a calcium-activated potassium current ( $I_{KCa}$ ) and a high-threshold calcium current ( $I_{Ca_h}$ ). This compartment also receives electrical connections from neighboring neurons. Fast ionic channels are located in the soma, and slow channels are located in the dendritic compartment. Some of the channel conductances depend on the calcium concentration. The equations for each compartment of a single neuron can be summarized as

$$C_M \frac{dV(t)}{dt} = -(I_{ion} + I_l + I_{inj} + I_{comp}), \quad (16)$$

where  $C_M$  is the membrane capacitance,  $I_l$  is a leak current,  $I_{inj}$  is the injected stimulus current,  $I_{comp}$  connects the compartments, and  $I_{ion}$  is the sum of the currents above for each compartment. In addition, the dendritic compartment has the electrical coupling current  $I_{ec} = g_c \sum_i [V(t) - V_i(t)]$ , where the index  $i$  runs over the neighbors of each neuron, and  $g_c$  is the electrical coupling conductance.

Each IO neuron is represented by a system of ordinary differential equations (ODEs), and the network is a set of these systems coupled through the electrical coupling currents  $I_{ec}$ . The networks examined consisted of  $2 \times 2$ ,  $3 \times 3$ , and  $9 \times 3$  neurons, where cells are connected to their two, three, or four neighbors depending on their positions in the grid.

This is a complex network, even when it is only  $2 \times 2$ , and one must select an important feature of the dynamics to characterize its behavior. The largest Lyapunov exponent of the network is a good choice as it is independent of initial conditions and tells us about information flow in the network. Figure 27 displays the largest Lyapunov exponent for each network as a function of the electric coupling conductance  $g_c$ . We also see in Fig. 27 that the  $g_c$  producing the largest Lyapunov exponent yields the largest information transfer through the network, evaluated as the average mutual information per spike.

In a more general framework than the IO, it is remarkable that the chaotic activity of individual neurons unexpectedly underlies higher flexibility and, at the same time, greater accuracy and precision in their neural dynamics. The origin of this phenomenon is the potential ability of coupled neurons with chaotic behavior to synchronize their activities and generate rhythms whose period depends on the strength of the coupling or other network parameters [for a review see Rabinovich and Abarbanel (1998) and Aihara (2002)]. Networks with many chaotic neurons can generate interesting transient dynamics, i.e., chaotic itinerancy (CI) (Tsuda, 1991; Rowe, 2002). Chaotic itinerancy results from weak instabilities in the attractors, i.e., attractor sets in whose

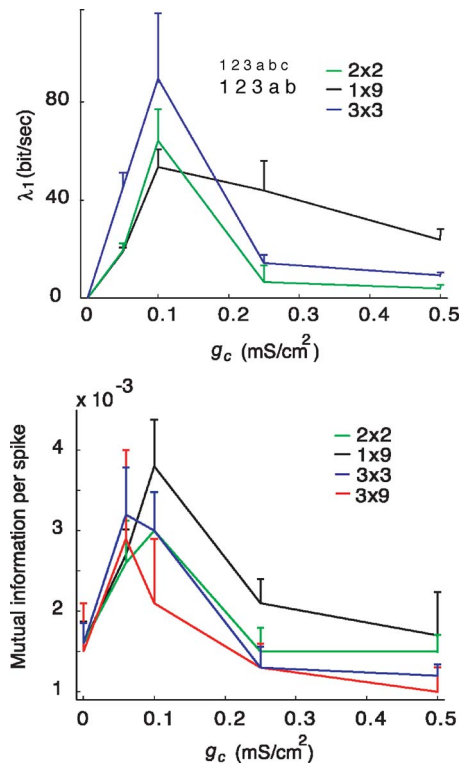


FIG. 27. (Color online) Chaotic dynamics increases information transmission in IO models. Top panel: Largest Lyapunov exponent as a function of the electrical coupling strength  $g_c$  for different IO networks of nonidentical cells. Bottom panel: Network average mutual information per spike as a function of  $g_c$ . Modified from Schweighofer et al., 2004.

neighborhood there are trajectories that do not go to the attractors (Milnor-type attractors). A developed CI motion needs both many neurons and a very high level of interconnections. This is in contrast to the traditional concept of computation with attractors (Hopfield, 1982). Chaotic itinerancy yields computations with transient trajectories; in particular, there can be motion along separatrices as in winnerless competition dynamics (Sec. IV.C). Although CI is an interesting phenomenon, applying it to explain and predict the activity of sensory systems (Kay, 2003), and to any nonautonomous neural circuit dynamics, poses a question that has not been answered yet: How can CI be reproducible and robust against noise and at the same time sensitive to a stimulus?

To conclude this section it is necessary to emphasize that the answer to the question of the functional role of chaos in real neural systems is still unclear. In spite of the attractiveness of such ideas as (i) chaos makes neural circuits more flexible and adaptive, (ii) chaotic dynamics create information and can help to store it (see above), and (iii) the nonlinear dynamical analyses of physiological data (e.g., electroencephalogram time series) can be important for the prediction or control of pathological neural states, it is extremely difficult to confirm these ideas directly in *in vivo* or even *in vitro* experiments. In particular, there are three obstacles that can fundamen-

tally hinder the power of data analyses: (i) finite statistical fluctuations, (ii) external noise, and (iii) nonstationarity of the neural circuit activity [see, for example, Lai et al. (2003)].

### C. Synaptic dynamics and information processing

Synaptic transmission in many networks of the nervous system is dynamical, meaning that the magnitude of postsynaptic responses depends on the history of presynaptic activity (Thompson and Deuchars, 1994; Fuhrmann et al., 2002). This phenomenon is independent of (or in addition to) the plasticity mechanisms of the synapses (discussed in Sec. II.A.3). The role of synapses is often considered to be the simple notification to the postsynaptic neuron of presynaptic cell activity. However, electrophysiological recordings show that synaptic transmission can imply activity-dependent changes in response to presynaptic spike trains. The magnitude of postsynaptic potentials can change rapidly from one spike to another, depending on the particular temporal distribution of the presynaptic signals. Thus each single postsynaptic response can encode information about the temporal properties of the presynaptic signals.

The magnitude of the postsynaptic response is determined by the interspike intervals of the presynaptic activity and by the probabilistic nature of neurotransmitter release. In depressing synapses a short interval between presynaptic spikes is followed by small postsynaptic responses, while long presynaptic interspike intervals are followed by a large postsynaptic response. Facilitating synapses tend to generate responses that grow with successive presynaptic spikes. In this context, several theoretical efforts have tried to explore the capacity of single responses of dynamical synapses to encode temporal information about the timing of presynaptic events.

Theoretical models for dynamical synapses are based on the time variation of the fraction of neurotransmitter released from the presynaptic terminal  $R(t)$ ,  $0 \leq R(t) \leq 1$ . When a presynaptic spike occurs at time  $t_{sp}$ , the fraction  $U$  of available neurotransmitters and the recovery time constant  $\tau_{rec}$  determine the rate of return of resources  $R(t)$  to the available presynaptic pool. In a depressing synapse,  $U$  and  $\tau_{rec}$  are constant. A simple model describes the fraction of synaptic resources available for transmission as (Fuhrmann et al., 2002)

$$\frac{dR(t)}{dt} = \frac{1 - R(t)}{\tau_{rec}} - UR(t)\delta(t - t_{sp}), \quad (17)$$

and the amplitude of the postsynaptic response at time  $t_{sp}$  is proportional to  $R(t_{sp})$ .

For a facilitating synapse,  $U$  becomes a function of time  $U(t)$  increasing at each presynaptic spike and decaying to the baseline level when there is no presynaptic activity:

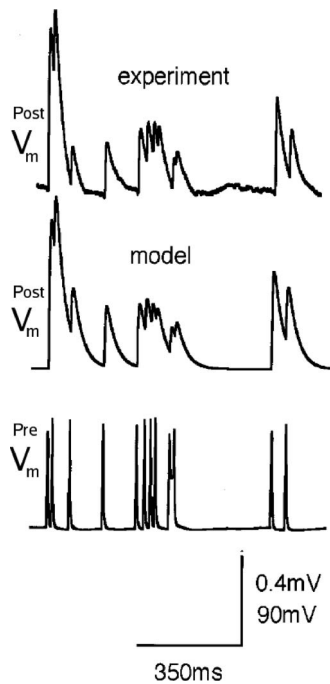


FIG. 28. Dynamical synapses imply that synaptic transmission depends on previous presynaptic activity. This shows the average postsynaptic activity generated in response to a presynaptic spike train (bottom trace) in a pyramidal neuron (top trace) and in a model of a depressing synapse (middle trace). Postsynaptic potential in the model is computed using a passive membrane mechanism  $\tau_m(dV/dt) = -V + R_i I_{\text{syn}}(t)$ , where  $R_i$  is the input resistance. Modified from [Tsodyks and Markram, 1997](#).

$$\frac{dU(t)}{dt} = -\frac{U(t)}{\tau_{\text{facil}}} + U_1[1 - U(t)]\delta(t - t_{\text{sp}}), \quad (18)$$

where  $U_1$  is a constant determining the step increase in  $U(t)$  and  $\tau_{\text{facil}}$  is the relaxation time constant of the facilitation.

Other approaches to modeling dynamical synapses include probabilistic models to account for fluctuations in presynaptic release of neurotransmitters. At a synaptic connection with  $N$  release sites we can assume that at each site there can be, at most, one vesicle available for release, and that the release at each site is an independent event. When a presynaptic spike is produced at time  $t_{\text{sp}}$ , each site containing a vesicle will release it with the same probability  $U(t)$ . Once a release occurs, the site can be refilled during a time interval  $dt$  with probability  $dt/\tau_{\text{rec}}$ . The probabilistic release and recovery can be described by the probability  $P_v(t)$  for a vesicle to be available for release at any time  $t$ :

$$\frac{dP_v(t)}{dt} = \frac{1 - P_v(t)}{\tau_{\text{rec}}} - U(t)P_v(t)\delta(t - t_{\text{sp}}). \quad (19)$$

Figure 28 shows how this formulation permits an accurate description of a depressing synapse in response to a specified presynaptic spike train.

The transmission of sensory information from the environment to decision centers through neural communication channels requires a high degree of reliability and

sensitivity from networks of heterogeneous, inaccurate, and sometimes unreliable components. The properties of the channel itself, assuming the sensor is accurate, must be richer than conventional channels studied in engineering applications. Those channels are passive and, when of high quality, can relay inputs accurately to a receiver. Neural communication channels are composed of dynamically active elements capable of complex autonomous oscillations. Individually, chaotic neurons can create information in a way similar to the study of nonlinear systems with unstable trajectories: Two states of the system, indistinguishable because only finite-resolution observations can occur, may through the action of the instabilities of the nonlinear dynamics find themselves in the future widely separated in state space, and thus distinguishable. Information about different states that was unavailable at one time may become available at a later time.

Biological neural communication pathways are able to recover information from a hidden coding space and to transfer information from one time scale to another because of the intrinsic nonlinear dynamics of synapses. As an example, we discuss a very simple neural information channel composed of sensory input in the form of a spike train that arrives at a model neuron and then moves through a realistic dynamical synapse to a second neuron where the information in the initial sensory signal is read ([Eguia et al., 2000](#)). The model neurons are four-dimensional generalizations of the Hindmarsh-Rose neuron, and a model of chemical synapse derived from first-order kinetics is used. The four-dimensional model neuron has a rich variety of dynamical behaviors, including periodic bursting, chaotic bursting, continuous spiking, and multistability. For many of these regimes, the parameters of the chemical synapse can be tuned so that the information about the stimulus, which is unreadable to the first neuron in the path, can be recovered by the dynamical activity of the synapse, and the second neuron can read it (see Fig. 29).

The quantitative description of this unexpected phenomenon was done by calculating the average mutual information  $I(S, N_1)$  between the stimulus  $S$  and the response of the first neuron  $N_1$ , and  $I(S, N_2)$  between the stimulus and the response of the second neuron  $N_2$ . The result in the example shown in Fig. 29 is  $I(S, N_2) > I(S, N_1)$ . This result indicates how nonlinear synapses and neurons acting as input and output systems along a communication channel can recover information apparently hidden in earlier synaptic connections in the pathway. Here the measure of information transmission used is the average mutual information between elements, and because the channel is active and nonlinear, the average mutual information between the sensory source and the final neuron may be greater than the average mutual information found in an intermediate neuron in the channel (but not greater than the original information).

Another form of synaptic dynamics involved in information processing and especially in learning is STDP (already discussed in Sec. II.A.3). Information transduc-

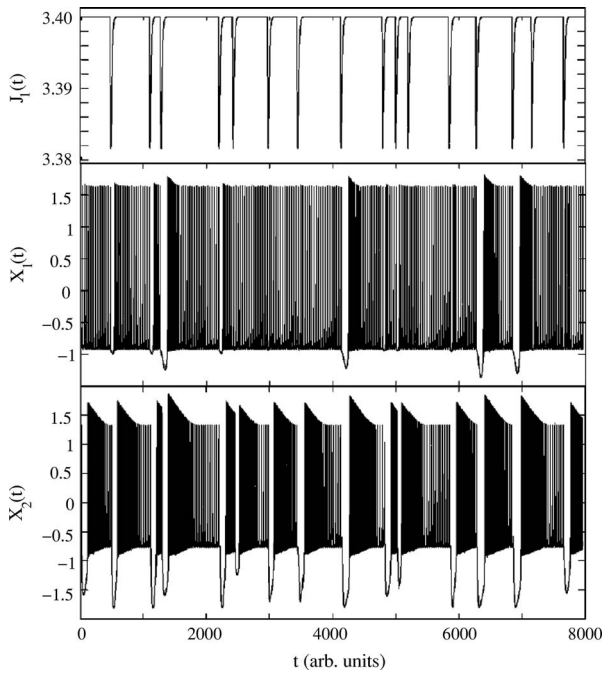


FIG. 29. Example of recovery of hidden information in neural channels. A presynaptic cell receives specified input and connects to a postsynaptic cell through a dynamical synapse. Top panel: the time series of synaptic input to the presynaptic cell  $J_1(t)$ ; middle panel: the membrane potential of the first bursting neuron  $X_1(t)$ ; bottom panel: the membrane potential of the second bursting neuron  $X_2(t)$ . Note that features of the input hidden in the response  $X_1(t)$  are recovered in the response following a dynamical synapse  $X_2(t)$  (note hyperpolarization regions for  $X_2$ ). Modified from [Eguia \*et al.\*, 2000](#).

tion is influenced by STDP ([Chechik, 2003](#); [Hopfield and Brody, 2004](#)), which also plays an important role in binding and synchronization.

#### D. Binding and synchronization

We have discussed the diversity of neuron types and the variability of neural activity. Neural processing requires the fast interaction of many neurons in different neural subsystems. There are several dynamical mechanisms contributing to the complex integration of information that neural systems perform. Among them, the synchronization of neural activity is the one that has captured the most attention. Synchronization of neural activity is also one of the proposed solutions to a widely discussed question in neuroscience: the binding problem, which we describe briefly in this section.

The binding problem was originally formulated as a theoretical problem by von der Malsburg in 1981 [see a review by [von der Malsburg \(1999\)](#), and [Roskies \(1999\)](#); [Singer \(1999\)](#)]. However, examples of binding had already been proposed by [Rosenblatt \(1962\)](#) for the visual system [for a review of the binding problem in vision see [Singer \(1999\)](#), and [Wolfe and Cave \(1999\)](#)]. The binding problem is formulated as the need for a coherent representation of an object provided by the association of all

its features (shape, color, location, speed, etc.). The association of all features or binding allows a unified perception of the object. The binding problem is a generalized task of the nervous system as it seeks to reconstruct any total perception from its components. There are also cognitive binding problems related to cognitive identification and memory. No doubt the binding problem, like many other problems in biology, has multiple solutions. These solutions are most likely implemented through the use of dynamical mechanisms for the control of neural activity.

The most widely studied mechanism proposed to solve the binding problem is temporal synchrony (or temporal correlation) ([Singer and Gray, 1995](#)). It has been suggested by [von der Malsburg and Schneider \(1986\)](#) that synchronization is the basis for perceptual binding. However, there is still criticism of the temporal binding hypothesis ([Ghose and Maunsell, 1999](#); [Riesenhuber and Poggio, 1999](#)). Obviously, neural oscillations and synchronous signals are ubiquitous in the brain, and neural systems can make use of these phenomena to encode, learn, and create effective outputs. There are several lines of experimental evidence that reveal the use of synchronization and activity correlation for binding tasks. Figure 30 shows an example of how neural synchronization correlates with the perceptual segmentation of a complex visual pattern into distinct, spatially overlapping surfaces ([Castelo-Branco \*et al.\*, 2000](#)) (see the figure caption for details). Indeed, modeling studies show that involving time in these processes can lead to the binding of different features. The idea is to use the coincidence of certain events in the dynamics of different neural units for binding. Usually such dynamical binding is represented by synchronous neurons or neurons that are in phase with an external field. However, dynamical events such as phase or frequency variations usually are not very reproducible and robust. As discussed in the next section, it is reasonable to hypothesize that brain circuits displaying sequential switching of neural activity use the coincidence of this switching to implement dynamical binding of different WLC networks.

Any spatiotemporal coding needs the temporal coordination of neural activity among different populations of neurons to provide (i) better recognition of specific features, (ii) faster processing, (iii) higher information capacity, and (iv) feature binding. Neural synchronization has been observed throughout the nervous system, particularly in sensory systems, for example, in the olfactory system ([Laurent and Davidowitz, 1994](#)) and the visual system ([Gray \*et al.\*, 1989](#)). From the point of view of dynamical system theory, transient synchronization is an ideal mechanism for binding neurons into assemblies for several reasons: (i) the synchronized neurons do not necessarily have to be neighbors; (ii) a synchronization event depends on the state of the neuron and the stimulus and can be very selective, that is, neurons from the same network can be temporal members of different cell assemblies at different instants of time; (iii) basic brain rhythms are able to synchronize neurons responsible for

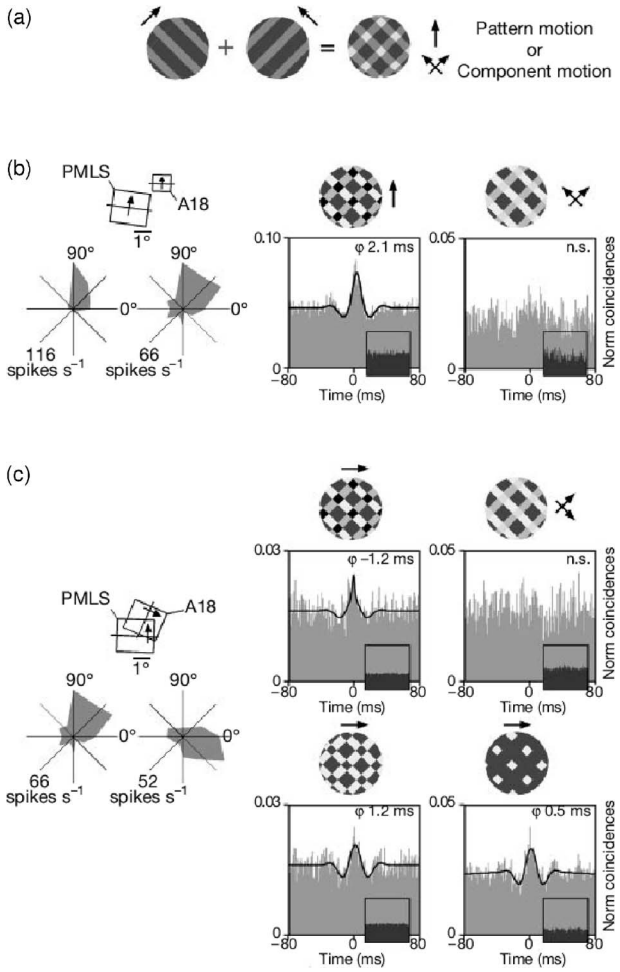


FIG. 30. An example of binding showing dependence of synchrony on transparency conditions and receptive field (RF) configuration in the cat visual cortex. (a) Stimulus configuration. (b) Synchronization between neurons with nonoverlapping RFs and similar directional preferences recorded from areas A18 and PMLS of the cat visual cortex. Left, RF constellation and tuning curves; right, cross correlograms for responses to a nontransparent (left) and transparent plaid (right) moving in the cells' preferred direction. Grating luminance was asymmetric to enhance perceptual transparency. Small dark correlograms are shift predictors. (c) Synchronization between neurons with different direction preferences recorded from A18 (polar and RF plots, left). Top, correlograms of responses evoked by a nontransparent (left) and a transparent (right) plaid moving in a direction intermediate to the cells' preferences. Bottom, correlograms of responses evoked by a nontransparent plaid with reversed contrast conditions (left), and by a surface defined by coherent motion of intersections (right). Scale on polar plots: discharge rate in spikes per second. Scale on correlograms: abscissa, shift interval in ms, bin width 1 ms; ordinate, number of coincidences per trial, normalized. Modified from [Castelo-Branco et al., 2000](#).

the processing of information from different sensory inputs; and (iv) the synchronization is possible even between neural oscillators with strongly different frequencies ([Rabinovich et al., 2006](#)).

In early visual processing neurons that encode features of a complex visual percept are associated in func-

tional assemblies through gamma-frequency synchronization ([Engel et al., 2001](#)). When sensory stimuli are perceptually or attentionally selected, and the respective neurons are bound together to raise their saliency, then gamma-frequency synchronization among these neurons is also enhanced. Gamma-mediated coupling and its modulation by attention are not limited to the visual system: they are also found in the auditory ([Tiitinen et al., 1993](#)) and somatosensory domains ([Desmedt and Tomberg, 1994](#)). Gamma oscillations allow visiomotor binding between posterior and central brain regions ([Rodriguez et al., 1999](#)) and are involved in short-term memory. As a means for dynamically binding neurons into assemblies, gamma-frequency synchronization appears to be the prime mechanism for stabilizing cortical connections among members of a neural assembly over time. On the other hand, neurons can increase or decrease the strength of their synaptic connections depending on the precise coincidence of their activation (STDP), and gamma-frequency synchronization provides the required temporal precision.

[Hatsopoulos et al. \(2003\)](#) and [Jackson et al. \(2003\)](#) revealed the functional significance of neural synchronization and correlations within the motor system. Preeminent among brain actions must be the aggregation of disparate spiking patterns to form spatially and temporally coherent neural codes that then drive alpha motor neurons and their associated muscles. Essentially, motor binding seems to describe exactly what motor structures of the mammalian brain do: provide high-level coordination of simple and complex voluntary movements. Neurons with similar functional output have an increased likelihood of exhibiting neural synchronization.

In contrast to classical synchronization ([Pikovsky et al., 2001](#)), synchronization in the CNS is always transient. The phase-space image of transient synchronization can be a saddle limit cycle in the vicinity of which the system spends finite time. Alternatively, it can be a limit cycle whose basin of attraction decreases in time. In both cases the system is able to leave the synchronization region after a specific stage of processing is completed and proceed with the next task. This is a broad area where the issues and approaches are not settled, and thus it provides an opportunity for innovative ideas to explain the phenomenon.

To conclude this section, we note that the functional role of synchronization in the CNS and the importance of spike-timing coding in general are still a subject of debate. On the one hand, it is possible to build models that use dynamical patterns of spikes for neural computations, e.g., representation, recognition, and decision making. Examples of such spike-timing-based computational models have been discussed by Hopfield and Brody ([Hopfield and Brody, 2001](#); [Brody and Hopfield, 2003](#)). In this work the authors showed, in particular, that spike synchronization across many neurons can be achieved in the absence of direct synaptic interactions between neurons through phase locking to a common underlying oscillatory potential (like gamma oscillation; see above). On the other hand, the real connections of

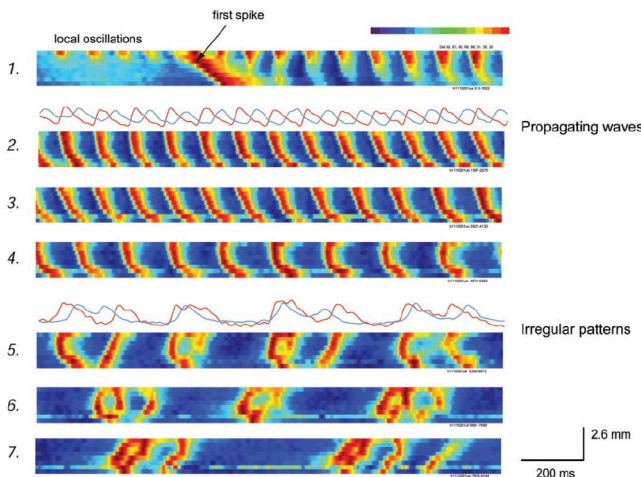


FIG. 31. (Color online) Spontaneous spatiotemporal patterns observed in the neocortex *in vitro* under the action of carbachol. Images composed of optical signals recorded by eight detectors arranged horizontally. The optical signal from each detector was normalized to the maximum on that detector during that period and normalized values were assigned colors according to a linear color scale (at the top right). The traces above images 2 and 5 are optical signals from two optical detectors labeled with this color scale. The *x* direction of the images represents time (12 s) and the *y* direction of each image represents 2.6 mm of space in cortical tissue. Note also that the first spike had a high amplitude but propagated more slowly in the tissue. Modified from [Bao and Wu, 2003](#).

such theoretical models with experiments *in vivo* are not established [see also [Fell \*et al.\* \(2003\)](#) and [O'Reilly \*et al.\* \(2003\)](#)].

#### IV. TRANSIENT DYNAMICS: GENERATION AND PROCESSING OF SEQUENCES

##### A. Why sequences?

The generation and control of sequences is of crucial importance in many aspects of animal life. Working memory, bird songs, finding food in a labyrinth, jumping from one stone to another on the shore—all these are the results of sequential activity generated by the nervous system. Lashley called the problem of coordination of constituent actions into organized sequential spatiotemporal patterns the action syntax problem ([Lashley, 1960](#)). The generation of sequences is also important for intermediate information processing as we discuss below.

The sequences can be cyclic, like many brain rhythms and spatiotemporal patterns generated by CPGs. They can also be irregular, like neocortical theta oscillations (4–10 Hz) generated spontaneously in cortical networks ([Bao and Wu, 2003](#)) (see Fig. 31). The sequences can be finite in time like those generated by a neural circuit under the action of external input as in sensory systems. From a physicist's point of view, any reproducible finite sequence that is functionally meaningful results from the cooperative transient dynamics of the corresponding

neural ensemble or individual neurons. Even brain rhythms demonstrate transient dynamics because the circuit's periodic activity is modulated by nonstationary sensory inputs or signals from the periphery. It is important to emphasize the fundamental role of inhibition in the generation and control of sequences in the nervous system.

In this section we concentrate on the origin of sequence generation and the mechanisms of reproducibility, sensitivity, and functional reorganization of MCs. In the standard study of nonlinear dynamical systems, attention is focused on the long-time behavior of a system. This is typically not the relevant question in neuroscience. Here we must address the transient responses to a stimulus external to the neural system and must consider the short-term binding of a collection of responses, perhaps from different sensory inputs, to facilitate action commands directed to the motor system. If you attempt to swat a fly, it cannot ask you to perform this action many times so that it can average over your actions, allowing it to perform some standard optimal response. Few flies wanting this repetition would survive.

##### B. Spatially ordered networks

###### 1. Stimulus-dependent modes

Many neural ensembles are anatomically organized as slightly inhomogeneous excitable media. Examples of such media are retina ([Tohya \*et al.\*, 2003](#)), IO network ([Leznik and Llinas, 2002](#)), cortex ([Ichinohe \*et al.\*, 2003](#)), and thalamocortical layers ([Contreras \*et al.\*, 1996](#)). All these are neuronal lattices with chemical or electrical connections occurring primarily between neighbors. There are some general dynamical mechanisms of sequence generation in such spatially ordered networks. These mechanisms are usually related to the existence of wave modes such as those shown in Fig. 31 that are modulated by external inputs or stimuli.

Many significant observational and modeling results for this subject are found in the visual system. Visual systems are organized differently for different classes of animals. For example, the mammalian visual cortex has several topographically organized representations of the visual field and neurons at adjacent points in the cortex are excited by stimuli presented at adjacent regions of the visual field. This indicates there is a continuous mapping of the coordinates of the visual field to the coordinates of the cortex ([van Essen, 1979](#)). In contrast to such a mapping connections from the visual field to the visual cortex in the turtle, for example, are more complex: A local spot in the visual field activates many neurons in the cortex but in an ordered way. As a result the excitation of the turtle visual cortex is distributed and not localized, and this suggests the temporal dynamics of several interacting membrane modes (see Fig. 32). In the mammalian cortex a moving stimulus evokes a localized wave or wave front, while in the turtle visual cortex a differentially moving stimulus modulates temporal interactions of the cortical modes differently and is represented by different sequential switchings between them.

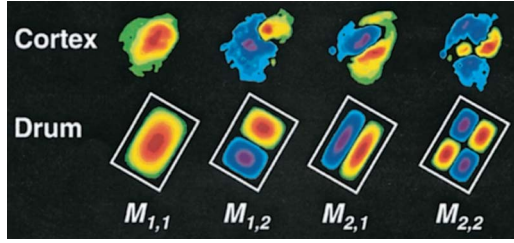


FIG. 32. (Color online) Sequential changing of cortical modes in the turtle visual cortex. Comparison between the spatial organization of the cortical activity in the turtle visual system and the normal modes of a rectangular membrane (drum). From [Senseman and Robbins, 1999](#).

To understand the dynamics of the wave modes, i.e., stability, sensitivity to stimuli, dependence on neuro-modulators, etc., one has to build a model that is based on the experimental information about the possibility of these modes maintaining the topological space structure observed in experiments. In many similar situations one can introduce cooperative or population variables that can be interpreted as the amplitude of such modes depending on time. The corresponding amplitude equations are essentially the widely studied evolution equations of the dynamical theory of pattern formation ([Cross and Hohenberg, 1993](#); [Rabinovich et al., 2000](#)).

For an analysis of the wave mode dynamics of the turtle visual cortex [Senseman and Robbins \(1999\)](#) used the Karhunen-Loeve decomposition and a snapshot of a spatiotemporal pattern at time  $t=t^0$  could be represented as a weighted sum of basic modes  $M_i(x,y)$  with coordinates  $(x,y)$  on the image:

$$u(x,y,t^0) = \sum_i^N a_i(t^0) M_i(x,y), \quad (20)$$

where  $u(x,y,t)$  represents the cooperative dynamics of these modes. The presentation of different visual stimuli, such as spots of light at different points in the visual field, produced spatiotemporal patterns represented by different trajectories in the phase space  $a_1(t), a_2(t), \dots, a_n(t)$ . [Du et al. \(2005\)](#) showed that it is possible to make a reduction in the dimensionality of the wave modes by a second Karhunen-Loeve decomposition, which maps in some time window the trajectory in  $(a_i)$  space into a point in a low-dimensional space (see Fig. 33). The observed transient dynamics is similar to the experimental results on the representation of different odors in the invertebrate olfactory system [see Fig. 46 and [Galan et al. \(2004\)](#)]. [Nenadic et al. \(2002\)](#) used a large-scale computer model of turtle visual cortex to reproduce qualitatively the features of the cortical mode dynamics seen in these experiments.

It is remarkable that not only do spatiotemporal patterns evoked by a direct stimulus look like wave modes, but even spontaneous activity in the sensory cortex is well organized and very different from turbulent flow ([Arieli et al., 1996](#)). This means that the common assumption about the stochastic and uncorrelated sponta-

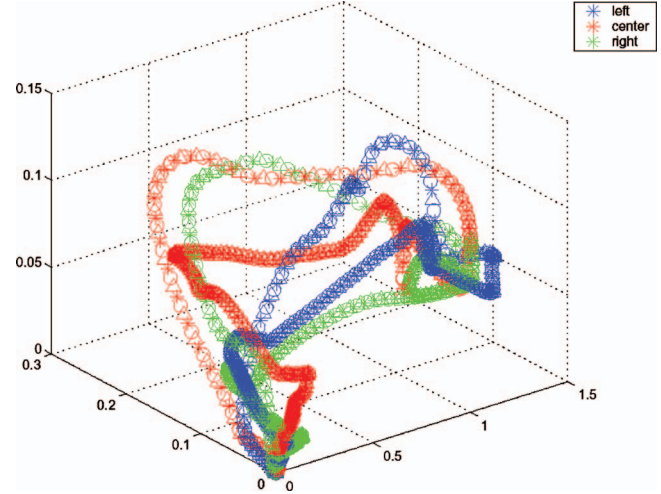


FIG. 33. (Color) Space representation of cortical responses in the turtle visual cortex to left, center, and right stimuli. From [Du et al., 2005](#).

neous activity of neighboring neurons in neural networks [see, for example, [van Vreeswijk and Sompolinsky \(1996\)](#); [Amit and Brunel \(1997b\)](#)] is not always correct. Local field potentials and recordings from single neurons indicate the presence of highly synchronous ongoing activity patterns or wave modes (see Fig. 34). The spontaneous activity of a single neuron connected with others, in principle, can be reconstructed using the evoked patterns of network activity ([Tsodyks et al., 1999](#)).

There are some illustrative models of wave modes that we note here. In 1977 [Amari \(1977\)](#) found spatially localized regions of high neural activity (“bumps”) in network models consisting of a single layer of coupled excitatory and inhibitory rate neurons. [Laing et al. \(2002\)](#) extended Amari’s results to a nonmonotonic connection function (“Mexican hat” with oscillating tails) (shown in Fig. 35) and a neural layer in two spatial dimensions:

$$\begin{aligned} \frac{\partial u(x,y,t)}{\partial t} &= -u(x,y,t) \\ &+ \int_{\Omega} \int \omega(x-q, y-p) f(u(q,p,t)) dq dp, \end{aligned} \quad (21)$$

$$f(u) = 2e^{-\pi/(u-th)^2} \Theta(u-th), \quad (22)$$

$$\omega(x,y) = e^{-b\sqrt{x^2+y^2}} [b \sin(\sqrt{x^2+y^2}) + \cos(\sqrt{x^2+y^2})]. \quad (23)$$

An example of a typical localized mode in such neural media with local excitation and long-range inhibition is represented in Fig. 36. Different modes (with different numbers of bumps) can be switched from one to another by transient external stimuli. Multiple items can be stored in this model because of the oscillating tails of the

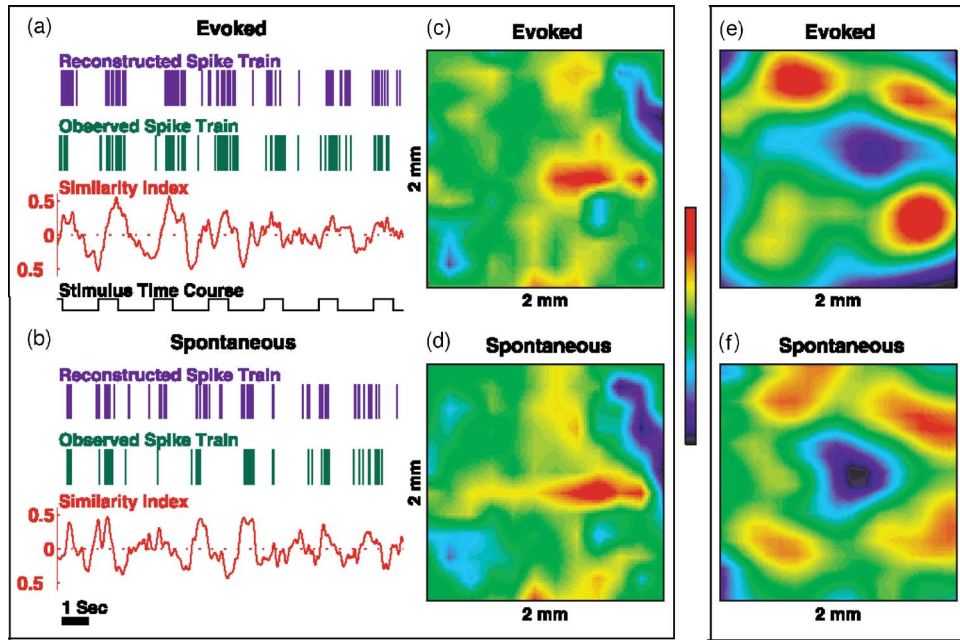


FIG. 34. (Color online) Relation between the spiking activity of a single neuron and the population state of cortical networks. (a) From bottom to top: stimulus time course; correlation coefficient of the instantaneous snapshot of population activity with the spatial pattern obtained by averaging over all patterns observed at the times corresponding to spikes evoked by the optimal orientation of the stimulus called the neuron's preferred cortical state (PCS) pattern; observed spike train of evoked activity with the optimal orientation for that neuron; reconstructed spike train. The similarity between the reconstructed and observed spike trains is evident. Also, strong upswings in the values of correlation coefficients are evident each time the neuron emits bursts of action potentials. Every strong burst is followed by a marked downswing in the values of the correlation coefficients. (b) The same as (a), but for a spontaneous activity recording session from the same neuron (eyes closed). (c) The neuron's PCS, calculated during evoked activity and used to obtain both (a) and (b). (d) The cortical state corresponding to spontaneous action potentials. The two patterns are nearly identical (correlation coefficient 0.81). (e) and (f) Another example of the similarity between the neuron's PCS (e) and the cortical state corresponding to spontaneous activity (f) from a different cat obtained with the high-resolution imaging system (correlation coefficient 0.74). Modified from Tsodyks et al., 1999.

effective connection strength. This is the result of the common activity of the excitatory and inhibitory connections between neurons. Inhibition plays a crucial role for the stability of localized modes (Laing et al., 2002).

Localized modes with different numbers of bumps remind one of complex localized patterns in a dissipative nonequilibrium media (Rabinovich et al., 2000). Based

on this analogy, it is reasonable to hypothesize that different modes may coexist in a neural layer and their interaction and annihilation can explain the sequential effectiveness of the different events. This suggests they could be a model of sequential working memory (see below).

Many rhythms of the brain can take the form of waves: spindle waves (7–14 Hz) seen at the onset of sleep (Kim et al., 1995), slower delta rhythms of deeper sleep, the synchronous discharge during an epileptic sei-

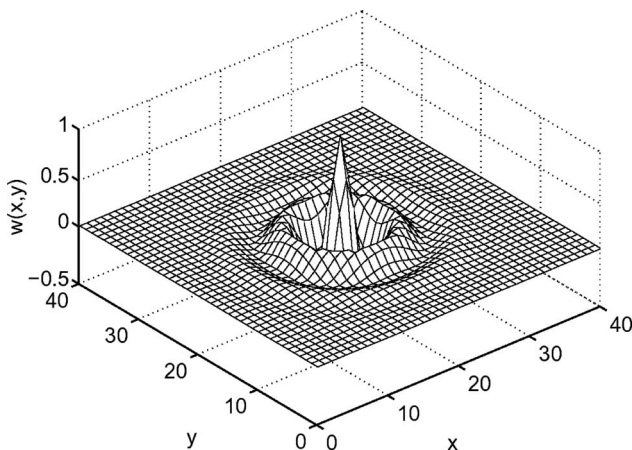


FIG. 35. Connection function  $\omega(x,y)$ , centered at the center of the domain. Modified from Laing et al., 2002.

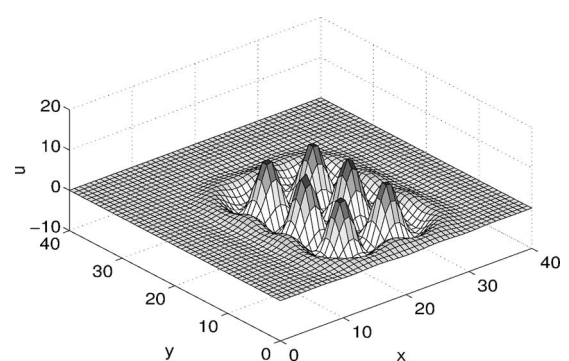


FIG. 36. Six-bump stable solution of the model (21)–(23):  $b = 0.45$ ,  $\tau = 0.1$ ,  $th = 1.5$ . Modified from Laing et al., 2002.

zure (Connors and Amitai, 1997), waves of excitation associated with sensory processing, 40-Hz oscillations, and others. In thalamocortical networks the same clusters of neurons are responsible for different modes of rhythmic activity. What is the dynamical origin of such multifunctionality? There is no unique answer to this question, and there are several different mechanisms that can be responsible for it (we have already discussed this for small invertebrate networks; see Sec. II.B). Terman et al. (1996) studied the transition between spindling and delta sleep rhythms. The authors showed that these two rhythms make different uses of the fast inhibition and slow inhibition generated by thalamic reticularis cells. These two types of inhibition are mediated in the cortex by GABA(A) and GABA(B) receptors, respectively (Schutter, 2002; Tams et al., 2003).

The wave mode equation discussed above is familiar to physicists and can be written both when interactions between neuron populations are homogeneous and isotropic (Ermentrout, 1998) and when the neural layer is partitioned into domains or hypercolumns like the primary visual cortex (V1) of cats and primates, which has a crystallinelike structure at the millimeter length scale (Bressloff, 2002; Bressloff and Cowan, 2002).

In the next section we discuss the propagation of patterns of synchronous activity along spatially ordered neural networks.

## 2. Localized synfire waves

Auditory and visual sensory systems have a very high temporal resolution. For example, the retina is able to resolve sequential temporal patterns with a precision in the millisecond range. Does the transmission of sensory information from the periphery to the cortex maintain such high resolution? If the answer is yes, what are the dynamical mechanisms responsible for this? These questions are still open.

There are several neurophysiological experiments that show the ability of neural systems to transmit temporally modulated responses of sensory networks with high precision over several processing levels. For example, cross correlations between simultaneously recorded responses of retinal cells relay neurons within the thalamus, and cortical neurons show that the oscillatory patterning is reliably transmitted to the cortex with a resolution in the millisecond range [see for reviews Singer (1999) and Nase et al. (2003)]. A similar phenomenon was observed by Kimpo et al. (2003) who showed evidence for the preserved timing of spiking activity through multiple steps of a neural control loop in the bird brain. The dynamical origin of such precise message propagation, independent of the rate fluctuation, is often attributed to synchronization of the many neurons in the overall circuit (Abeles, 1991; Diemann et al., 1999).

We now discuss briefly the dynamics of waves of synchronous neural firing, i.e., synfire waves. One modeling study (Diesmann et al., 1999) has shown that the stable propagation of localized synfire waves, short-lasting synchronous spiking activity, is possible along a sequence of

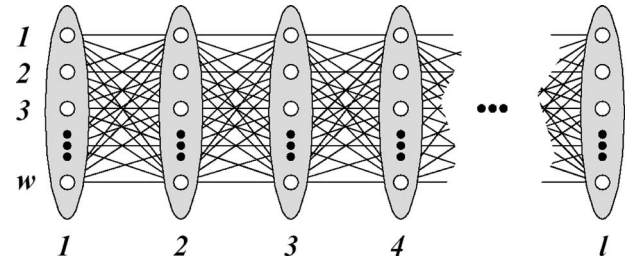


FIG. 37. Sequence of pools of excitatory neurons, connected in a feedforward way by so-called divergent and convergent connections. The network is called a synfire chain if it supports the propagation of synchronous spike patterns. Modified from Geewaltig et al., 2001.

layers or pools of neurons in a feedforward cortical network such as the one shown in Fig. 37, a synfire chain (Abeles, 1991). The degree of temporal accuracy of spike times among the pools' members determines whether subsequent pools can reproduce (or even improve) this accuracy [Fig. 38(a)], or whether synchronous excitation disperses and eventually dies out as in Fig. 38(b) for a smaller number of spikes in the volley. Thus in the context of synfire network function the quality of timing is judged on whether synchronous spiking is sustained or whether it dies out.

Diesmann et al. (1999), Cateau and Fukai (2001), Kistler and de Zeeuw (2002), and Nowotny and Huerta (2003) have shown that if the pool size is more than a critical value determined by the connectivity between layers, the wave activity initiated at the first pool propagates from one pool to the next, forming a synfire wave. Nowotny and Huerta (2003) have theoretically proven that no other states exist beyond synchronized or unsynchronized volleys as shown in the experiments by Reyes (2003).

The synfire feedforward chain (Fig. 37) is an oversimplified model for analyzing synfire waves because in reality any network with synfire chains is embedded in a larger cortical network that also has inhibitory neurons

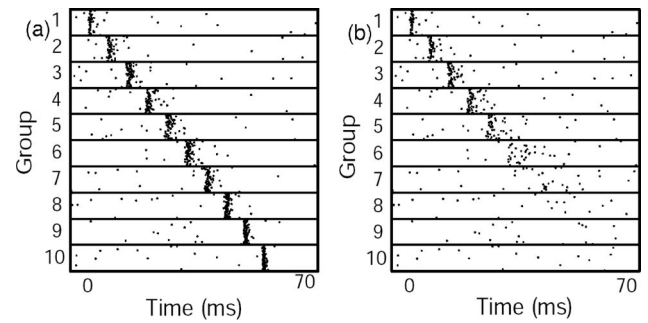


FIG. 38. Propagation of firing activity in synfire chains. (a) Stable and (b) unstable propagation of synchronous spiking in a model of cortical networks. Raster displays of propagating spike volley along fully connected synfire chain. Panels show the spikes in ten successive groups of 100 neurons each (synaptic delays arbitrarily set to 5 ms). Initial spike volley (not shown) was fully synchronized, containing (a) 50 or (b) 48 spikes. Modified from Diesmann et al., 1999.

and many recurrent connections. This problem is discussed in detail by [Aviel \*et al.\* \(2003\)](#).

### C. Winnerless competition principle

#### 1. Stimulus-dependent competition

Here we consider a paradigm of sequence generation that does not depend on the geometrical structure of the neural ensemble in physical space. It can, for example, be a two-dimensional layer with connections between neighbors or a three-dimensional network with sparse random connections. This paradigm can be helpful for the explanation and prediction of many dynamical phenomena in neural networks with excitatory and inhibitory synaptic connections. The paradigm is called the winnerless competition principle. We have touched on aspects of WLC networks earlier, and here we expand on their properties and their possible use in neuroscience.

“Survival of the fittest” is a cliché that is often associated with the term competition. However, competition is not merely a means of determining the winner, as in a winner-take-all network. It is also a multifunctional instrument that nature uses at all levels of the neuronal hierarchy. Competition is also a mechanism that maintains the highest level of variability and stability of neural dynamics, even if it is a transient behavior.

Over two hundred years ago the mathematicians Borda and de Condorcet were interested in the process of plurality elections at the French Royal Academy of Sciences. They considered voting dynamics in a case of three candidates *A*, *B*, and *C*. If *A* beats *B* and *B* beats *C* in a head-to-head competition, we might reasonably expect *A* to beat *C*. Thus predicting the results of the election is easy. However, this is not always the case. It may happen that *C* beats *A*, resulting in a so-called Condorcet triangle, and there is no real winner in such a competitive process ([Borda, 1781](#); [Saari, 1995](#)). This example is also called a “voting paradox.” The dynamical image of this phenomenon is a robust heteroclinic cycle (see Fig. 39). In some specific cases the heteroclinic cycle is even structurally stable ([Guckenheimer and Holmes, 1988](#); [Krupa, 1997](#); [Stone and Armbruster, 1999](#); [Ashwin \*et al.\*, 2003](#); [Postlethwaite and Dawes, 2005](#)).

The competition without a winner is also known in hydrodynamics: Busse and Heikes discovered that convective roll patterns in a rotating plane layer exhibit sequential changes of the roll’s direction as a result of the competition between patterns with different roll orientations. No pattern becomes a winner and the system exhibits periodic or chaotic switching dynamics ([Busse and Heikes, 1980](#)). For review see [Rabinovich \*et al.\* \(2000\)](#). The same phenomenon has been discovered in a genetic system, i.e., in experiments with a synthetic network of three transcriptional regulators ([Elowitz and Leibler, 2000](#)). Specifically, these authors described three repressor genes *A*, *B*, and *C* organized in a closed chain with unidirectional inhibitory connections such that *A*, *B*, and *C* beat each other. This network behaves like a

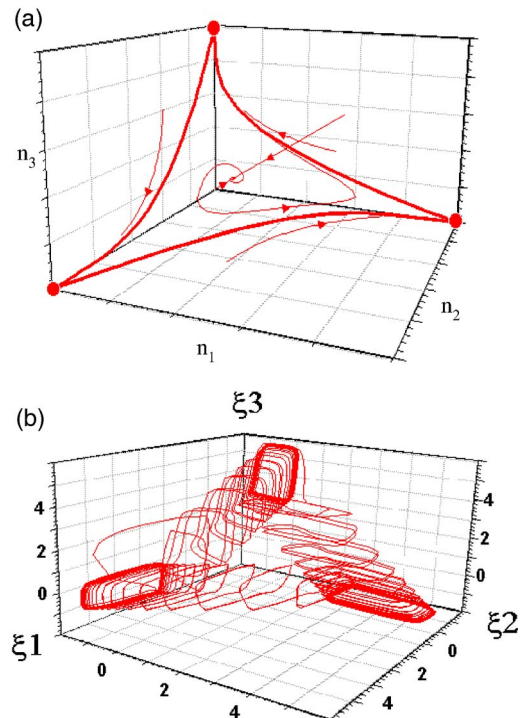


FIG. 39. (Color online) Illustration of WLC dynamics. Top panel: Phase portrait corresponding to the autonomous WLC dynamics of a three-dimensional case. Bottom panel: Projection of a nine-dimensional heteroclinic orbit of three inhibitory coupled FitzHugh-Nagumo spiking neurons in a three-dimensional space (the variables  $\xi_1$ ,  $\xi_2$ ,  $\xi_3$  are linear combinations of the actual phase variables of the system). From [Rabinovich \*et al.\*, 2001](#).

clock: it periodically induces synthesis of green fluorescent proteins as an indicator of the state of individual cells on a time scale of hours.

In neural systems such clock competitive dynamics can result from the inhibitory connections among neurons. For example, [Jefferys \*et al.\* \(1996\)](#) showed that hippocampal and neocortical networks of mutually inhibitory interneurons generate collective 40-Hz rhythms (gamma oscillations) when excited tonically. Another example of neural competition without a winner was discussed by [Ermentrout \(1992\)](#). The author studied the dynamics of a single inhibitory neuron connected to a small cluster of loosely coupled excitatory cells and observed the emergence of a limit cycle through a heteroclinic cycle. For autonomous dynamical systems competition without a winner is a well-known phenomenon.

We use the term WLC principle for the nonautonomous transient dynamics of neural systems receiving external stimuli and exhibiting sequential switching among temporal winners. The main point of the WLC principle is the transformation of incoming inputs into spatiotemporal outputs based on the intrinsic switching dynamics of the neuronal ensemble (see Fig. 40). In the phase space of the network, such switching dynamics are represented by a heteroclinic sequence whose architecture depends on the stimulus. Such a sequence consists of

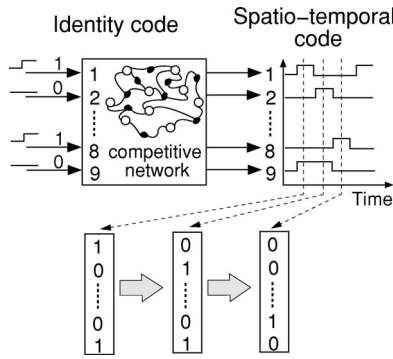


FIG. 40. Transformation of the identity spatial input into spatiotemporal output based on the intrinsic sequential dynamics of a neural ensemble with WLC.

many saddle equilibria or saddle cycles and many heteroclinic orbits connecting them, i.e., many separatrices. The sequence can serve as an attracting set if every semistable set has only one unstable direction [see also [Ashwin and Timme \(2005\)](#)].

The key points on which WLC networks are based are the following: (i) the stimulus-dependent heteroclinic sequence corresponding to a specific order of switching has a large basin of attraction, i.e., the sequence is robust; and (ii) the topology of the heteroclinic sequence sensitively depends on the incoming signals, i.e., WLC dynamics have a high resolution.

In this manner stimulus-dependent sequential switching of neurons or groups of neurons (clusters) is able to resolve the fundamental contradiction between sensitivity and robustness in sensory recognition. Any kind of sequential activity can be programmed, in principle, by a network with stimulus-dependent nonsymmetric inhibitory connections. It can be the creation of spatiotemporal patterns of motor activity, the transformation of the spatial information into spatiotemporal information for successful recognition (see Fig. 40), and many other computations.

The generation of sequences in inhibitory networks has already been discussed when we analyzed the dynamics of CPGs (see Sec. II.B) focusing on rhythmic activity. The mathematical image in phase space of the rhythmic sequential switching shown in Figs. 8 and 9 is a limit cycle in the vicinity of the heteroclinic contour [cf. Fig. 39(a)].

WLC dynamics can be described in the framework of neural models at different levels. These could be rate models, Hodgkin-Huxley-type models, or even simple map models (see Table I). For spiking neurons or groups of synchronized spiking neurons in a network with non-symmetrical lateral inhibition WLC may lead to switching between active and inactive states. The mathematical image of such switching activity is also a heteroclinic loop, but in this case the separatrices do not connect saddle equilibrium points [Fig. 39(a)] but saddle limit cycles as shown in Fig. 39(b). The WLC dynamics in a model network of nine spiking neurons with inhibitory connections is shown in Fig. 41. Similar results based on

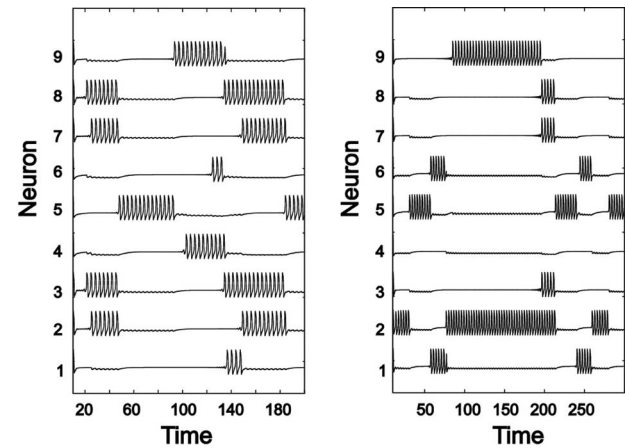


FIG. 41. Spatiotemporal patterns generated by a network of nine FitzHugh-Nagumo neurons with inhibitory connections. The left and right panels correspond to two different stimuli. From [Rabinovich et al., 2001](#).

a map model of neurons have been reported by [Casado \(2003\)](#).

An important advantage of WLC networks is that they can produce different spatiotemporal patterns in response to different stimuli, and, remarkably, neurons spontaneously form synchronized clusters despite the absence of excitatory synaptic connections. For a discussion of synchronization with inhibition see also [van Vreeswijk et al. \(1994\)](#) and [Elson et al. \(2002\)](#).

Finally WLC networks also possess a strikingly different capacity or ability to represent in a distinguishable manner a number of different patterns. In an attractor computation network of the Hopfield variety, a network with  $N$  attractors has been shown to have a capacity of approximately  $N/7$ . In a simple WLC network with  $N$  nodes, this capacity has been shown ([Rabinovich et al., 2001](#)) to be of order  $e(N-1)!$ , which is a remarkable gain in capacity.

## 2. Self-organized WLC networks

It is generally accepted that there is insufficient genetic information available to account for all the synaptic connectivity in the brain. How then can the functional architecture of WLC circuits be generated in the process of development?

One possible answer has been found by Huerta and Rabinovich. Starting with a model circuit consisting of 100 rate model neurons connected randomly with weak inhibitory synapses, new synaptic strengths are computed for the connections using Hebb learning rules in the presence of weak noise. The neuron rates  $a_i(t)$  satisfy a Lotka-Volterra model familiar from our earlier discussion. In this case the matrix  $\rho_{ij}(t)$  is a dynamical variable:

$$\frac{da_i(t)}{dt} = a_i(t) \left( \sigma(S) - \sum_j \rho_{ij}(t) a_j(t) \right) + \xi_i(t). \quad (24)$$

$\sigma(S)$  is a function dependent on the stimulus  $S$ ,  $\rho_{ij}(t)$  are the strengths of the inhibitory connections determined

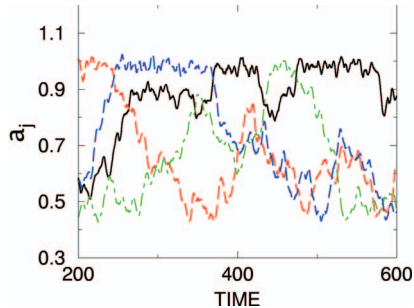


FIG. 42. (Color) Result of simulating a network of 100 neurons subject to the learning rule  $g(a_i, a_j) = a_i a_j [10 \tanh(a_j - a_i) + 1]$ . The activity of representative neurons in this network is shown in different colors. The system starts from random initial conditions for the connections. The noise level is  $\eta = 0.01$ . For simplicity, the switching activity of only four of the 100 neurons is shown.

by some learning rules, and  $\xi_i(t)$  is Gaussian noise with  $\langle \xi_i(t) \xi_j(t') \rangle = \eta \delta_{ij} \delta(t - t')$ . The learning is described by the equations

$$\frac{d\rho_{ij}(t)}{dt} = \rho_{ij}(t) g(a_i(t), a_j(t), S) - [\rho_{ij}(t) - \gamma], \quad (25)$$

where  $g(a_i, a_j, S)$  represents the strengthening of interactions from neuron  $i$  to neuron  $j$  as a function of the external stimulus  $S$ . The parameter  $\gamma$  represents the lower bound of the coupling strengths among neurons. Figure 42 shows the activity of representative neurons in a network built with this model. After the self-organization phase, this network displays WLC switching dynamics.

Winnerless competition dynamics can also be the result of local self-organization in networks of HH model neurons that display STDP with inhibitory synaptic connections as shown in Fig. 43. Such mechanisms of self-organization, as shown by Nowotny and Rabinovich, can be appropriate for networks that generate not only rhythmic activity but also transient heteroclinic sequences.

### 3. Stable heteroclinic sequence

The phase-space image of nonrhythmic WLC dynamics is a trajectory in the vicinity of a stable heteroclinic sequence (SHS) in the state space of the system. Such a sequence (see Fig. 44) is an open chain of saddle fixed points connected by one-dimensional separatrices which retain nearby trajectories in its vicinity. The flexibility of WLC dynamics is provided by their dependence on the identity of participating neural clusters of stimuli. Sequence generation in chainlike or layerlike networks of neurons may result from a feedforward wavelike propagation of spikes like waves in synfire chains (see above). In contrast, WLC dynamics does not need a specific spatial organization of the network. However, the image of a wave is a useful one, because in the case of WLC a wave of neural activity propagates in state space along the SHS. Such a wave is initiated by a stimulus. The

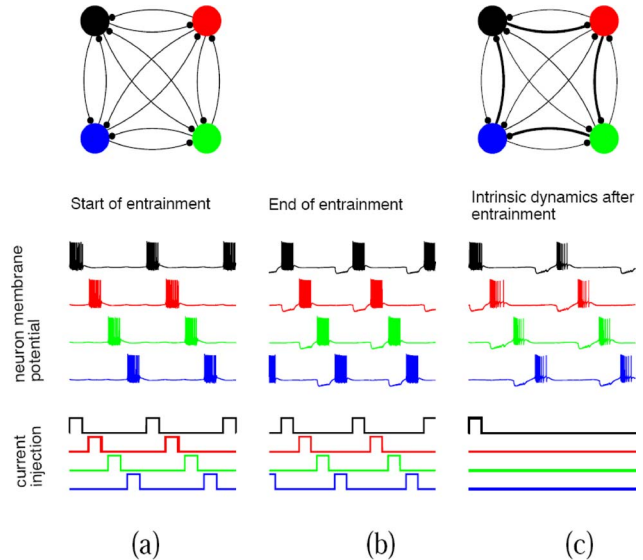


FIG. 43. (Color online) Example of WLC dynamics entrained in a network by a local learning rule. In isolation, the four HH neurons in the network are rebound bursters, i.e., they fire a brief burst of spikes after being strongly inhibited. The all-to-all inhibitory synapses in the small network are governed by a STDP learning rule which strengthens the synapse for positive time delays between postsynaptic and presynaptic activity and weakens it otherwise. Such STDP of inhibitory synapses has been observed in the entorhinal cortex of rats (Haas *et al.*, 2006). (a) Before entrainment the neurons just follow the input signal of periodic current pulses. (b) The resulting bursts strengthen the forward synapses corresponding to the input sequence making them eventually strong enough to cause rebound bursts. (c) After entrainment activating any one of the neurons leads to an infinite repetition of the trained sequence carried by the successive rebound bursts of the neurons.

speed of the sequential switching depends on the noise level  $\eta$ . Noise controls the distance between trajectories realized by the system and the SHS. For trajectories that get closer to the SHS the time that the system spends near semistable states (saddles), i.e., the interval between switching, becomes longer (see Fig. 44).

The mechanism of reproducing transient sequential neural activity has been analyzed by Aframovich, Zhigulin, *et al.* (2004) (see Fig. 44). It is quite general and does not depend on the details of the neuronal model. Saddle points in the phase space of the neural network can be replaced by saddle limit cycles or even chaotic sets that describe neural activity in more detail, as in typical spiking or spiking-bursting models. This feature is important for neural modeling because it may help to build a bridge between the concepts of neural competition and synchronization of spikes.

We can formulate the necessary conditions for the connectivity of a WLC network that must be satisfied in order for the network to exhibit reproducible sequential dynamics along the heteroclinic chain. As before, we base our discussion on the rate model

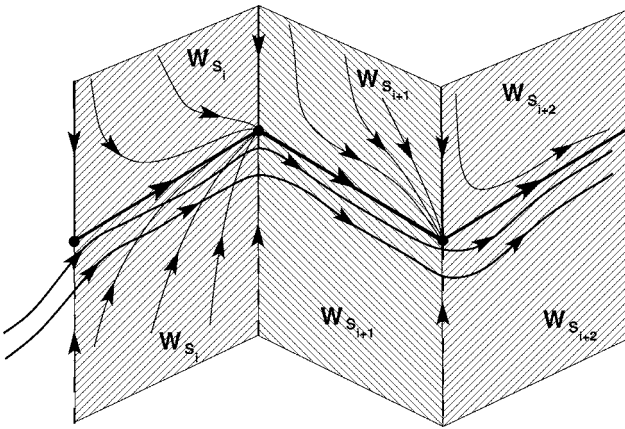


FIG. 44. A stable open heteroclinic sequence in a neural circuit with WLC.  $W_{s_i}$  is a stable manifold of the  $i$ th saddle fixed point (heavy dots). The trajectories in the vicinity of the SHS represent sequences with different timings. The time intervals between switches is proportional to  $T \sim |\ln \eta| / \lambda_u$ , where  $\lambda_u$  is a positive Lyapunov exponent that characterizes the one-dimensional unstable separatrices of the saddle points (Stone and Holmes, 1990). Modified from Aframovich, Zhigulin, et al., 2004.

$$\frac{da_i(t)}{dt} = a_i(t) \left( \sigma_i(\vec{S}^l) - \sum_j^N \rho_{ij}(\vec{S}^l) a_j(t) \right) + \xi_i(t), \quad (26)$$

where  $\xi_i(t)$  is an external Gaussian noise. In this model it is assumed that the stimulus  $\vec{S}^l$  influences the matrix  $\rho_{ij}$  and increments  $\sigma_i$  only in the subnetwork  $N^l$ . Each increment  $\sigma_i$  controls the time constant of an initial exponential growth from the resting state  $a_i(t)=0$ . As shown by Aframovich, Zhigulin, et al. (2004) to assure that the SHS is in the phase space of the system (26) the following inequalities must be satisfied:

$$\frac{\sigma_{i_{k-1}}}{\sigma_{i_k}} < \rho_{i_{k-1}i_k} < \frac{\sigma_{i_{k-1}}}{\sigma_{i_k}} + 1, \quad (27)$$

$$\frac{\sigma_{i_{k+1}}}{\sigma_{i_k}} - 1 < \rho_{i_{k+1}i_k} < \frac{\sigma_{i_{k+1}}}{\sigma_{i_k}}, \quad (28)$$

$$\rho_{ii_k} > \rho_{i_{k-1}i_k} + \frac{\sigma_i - \sigma_{i_{k-1}}}{\sigma_{i_k}}. \quad (29)$$

$\sigma_{i_m}$  is the increment of the  $m$ th saddle whose unstable manifold is one dimensional;  $\rho_{i_{k+1}i_k}$  is the strength of the inhibitory connection between neighboring saddles in the heteroclinic chain. The computer modeling result of a network with parameters that satisfy (27)–(29) is shown in Fig. 45.

In the next section we discuss some experiments that support the SHS paradigm.

#### 4. Relation to experiments

The olfactory system may serve as one example of a neural system that generates transient, but trial-to-trial

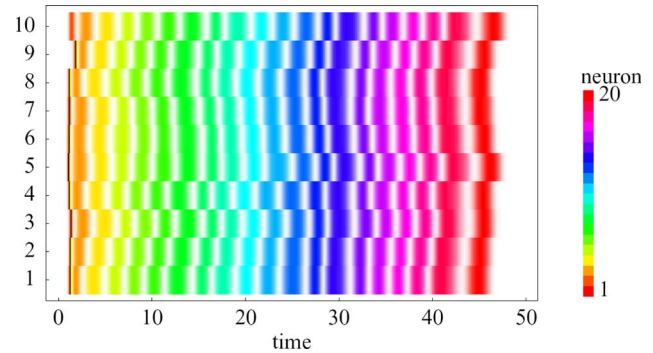


FIG. 45. (Color online) Time series of the activity of a WLC network during ten trials (only 20 neurons are shown): simulations of each trial were started from a different random initial condition. In this plot each neuron is represented by a different color and its level of activity by the saturation of the color. From Aframovich, Zhigulin, et al., 2004.

reproducible, sequences of neuronal activity which can be explained with the WLC principle. The complex intrinsic dynamics in the antennal lobe (AL) of insects transform static sensory stimuli into spatiotemporal patterns of neural activity (Laurent et al., 2001). Several experimental results about the reproducibility of the transient spatiotemporal AL dynamics have been published (Stopfer et al., 2003; Galan et al., 2004; Mazor and Laurent, 2005) (see Fig. 46). In experiments described by Galan et al. (2004) bees were presented with different odors, and neural activity in the AL was recorded using calcium imaging. The authors analyzed the transient trajectories in the projection neuron activity space and found that trajectories representing different trials of stimulation with the same odor were very similar. It was shown that after a time interval of about 800 ms different odors are represented in phase space by different static attractors, i.e., the transient spatiotemporal patterns converge to different spatial patterns of activity. However, the authors emphasize that due to the reproducibility of the transient dynamics some odors were recognized in the early transient stage as soon as 300 ms after the onset of the odor presentation. It is highly likely that the transient trajectories observed in these experiments represent realizations of a SHS.

The generation of reproducible sequences plays also a key role in the high vocal center (HVC) of the songbird system (Hahnloser et al., 2002). Like a CPG, this neural system is able to generate sparse spatiotemporal patterns without any rhythmic stimuli *in vitro* (Solis and Perkel, 2005). In its projections to the premotor nucleus RA, HVC in an awake singing bird sends sparse bursts of high-frequency signals once for each syllable of the song. These bursts have an interspike interval about 2 ms and last about 8 ms within a syllable time scale of 100–200 ms. The bursts are shown for several HVC → RA projection neurons in Fig. 47. The HVC also contains many inhibitory interneurons (Mooney and Prather, 2005). The interneurons burst densely throughout the vocalizations, in contrast to the bursting of the RA-projecting HVC neurons at single precise timings. A

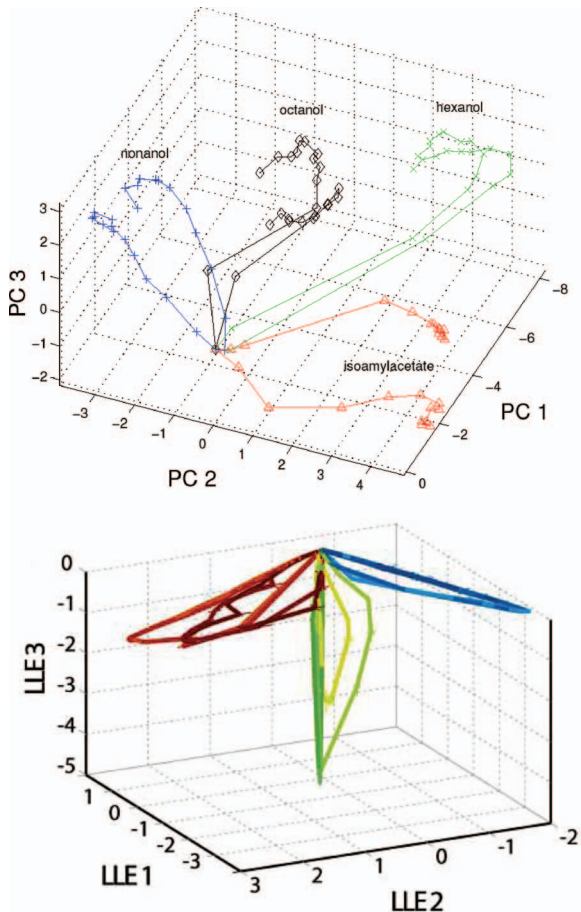


FIG. 46. (Color) Transient AL dynamics. Top panel: Trajectories of the antennal lobe activity during poststimulus relaxation in one bee. Modified from [Galan \*et al.\*, 2004](#). Bottom panel: Visualization of trajectories representing the response of a PN population in a locust AL over time. Time-slice points were calculated from 110 PN responses to four concentrations (0.01, 0.05, 0.1, 1) of three odors, projected onto three dimensions using locally linear embedding, an algorithm that computes low-dimensional, neighborhood-preserving embeddings of high-dimensional inputs ([Roweis and Saul, 2000](#)). Modified from [Stopfer \*et al.\*, 2003](#).

plausible hypothesis is that HVC's synaptic connections are nonsymmetric and WLC can be a mechanism of the neural spatiotemporal pattern generation of the song. This would provide a basis for the reproducible patterned output from the HVC when it receives a song command stimulus.

#### D. Sequence learning

Sequence learning and memory as sequence generation require temporal asymmetry in the system. Such asymmetry can result from specific properties of the network connections, in particular, asymmetry of the connections, or can result from temporal asymmetry in the dynamical features of individual neurons and synapses, or both. The specific dynamical mechanisms of sequence learning depend on the time scale of the sequence that

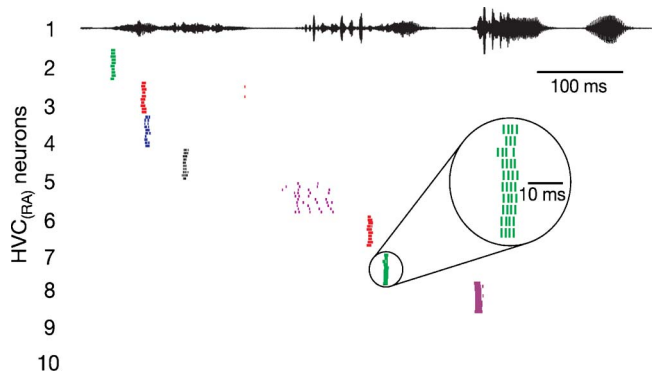


FIG. 47. (Color online) HVC songbird patterns. Spike raster plot of ten HVC(RA) neurons recorded in one bird during singing. Each row of tick marks shows spikes generated during one rendition of the song or call; roughly ten renditions are shown for each neuron. Modified from [Hahnloser \*et al.\*, 2002](#).

this neural system needs to learn. Learning of fast sequences, 20–30 ms and faster, needs precise synchronization of the spikes or phases of neural waves. One possible mechanism for this can be the learning of synfire waves. For slow sequences, like autonomous repetitive behavior, it would be preferable to learn relevant behavioral events that typically occur on the time scale of hundreds of milliseconds or slower and the switching (transitions) between them. Networks whose dynamics are based on WLC are able to do such a job. We consider here slow sequence learning and spatial sequential memory (SSM).

The idea is that sequential memory is encoded in a multidimensional dynamical system with a SHS. Each of the saddle points represents an event in a sequence to be remembered. Once the state of the system approaches one fixed point representing a certain event, it is drawn along an unstable separatrix toward the next fixed point, and the mechanism repeats itself. The necessary connections are formed in the learning phases by different sensory inputs originated by sequential events.

[Seliger \*et al.\* \(2003\)](#) have discussed a model of the SSM in the hippocampus. It is well accepted that the hippocampus plays the central role in acquisition and processing information related to representing motion in physical space. The most spectacular manifestation of this role is the existence of so-called place cells which repeatedly fire when an animal is in a certain spatial location ([O'Keefe and Dostrovsky, 1971](#)). Experimental research also favors an alternative concept of spatial memory based on a linked collection of stored episodes ([Wilson and McNaughton, 1993](#)). Each episode comprises a sequence of events, which, besides spatial locations, may include other features of the environment (orientation, odor, sound, etc.). It is plausible to describe the corresponding learning with a population model that represents neural activity by rate coding. [Seliger \*et al.\* \(2003\)](#) have proposed a two-layer dynamical model of SSM that can answer the following key questions: (i) How is a certain event, e.g., an image of the environment, recorded in the structure of the synaptic connections be-

tween multiple sensory neurons (SNs) and a single principal neuron (PN) during learning? (ii) What kind of cooperative dynamics forces individual PNs to fire sequentially, in a way that would correspond to a specific sequence of snapshots of the environment? (iii) How complex should this network be in order to store a certain number of different episodes without mixing different events or storing spurious episodes?

The two-layer structure of the SSM model is reminiscent of the projection network implementation of the normal form projection algorithm (NFPA); see [Baird and Eeckman \(1993\)](#). In the NFPA model, the dynamics of the network is cast in terms of normal form equations which are written for amplitudes of certain normal forms corresponding to different patterns stored in the system. The normal form dynamics can be chosen to follow certain dynamical rules. [Baird and Eeckman \(1993\)](#) have shown that a Hopfield-type network with improved capacity can be built using this approach. Furthermore, it has been suggested ([Baird and Eeckman, 1993](#)) that specific choices of the coupling matrix for the normal form dynamics can lead to multistability among more complex attracting sets than simple fixed points, such as limit cycles or even chaotic attractors. For example, quasiperiodic oscillations can be described by a normal form that corresponds to a multiple Hopf bifurcation ([Guckenheimer and Holmes, 1986](#)). As shown below, a model of SSM after learning is completed can be viewed as a variant of the NFPA with a specific choice of normal form dynamics corresponding to winnerless competition among different patterns.

To illustrate these ideas consider a two-level network of  $N_s$  SNs [ $x_i(t)$ ] and  $N_p$  principal neurons [ $a_i(t)$ ]. One can reasonably assume that sensory neurons do not have their own complex dynamics and are slaved either to external stimuli in the learning or storing regime or to the PNs in the retrieval regime. In the learning regime,  $x_i(t)$  is a binary input pattern consisting of 0's and 1's. During the retrieval phase,  $x_i(t)=\sum_{j=1}^{N_p} P_{ij} a_j(t)$ , where  $P_{ij}$  is the  $N_s \times N_p$  projection matrix of connections among SNs and PNs.

The PNs are driven by SNs during the learning phase, but they also have their own dynamics controlled by inhibitory interconnections. When learning is complete, the direct driving from SNs is disconnected. The equations for the PN rates  $a_i(t)$  read

$$\frac{da_i(t)}{dt} = a_i(t) - a_i(t) \sum_{j=1}^{N_p} V_{ij} a_j(t) + \alpha a_i \sum_{j=1}^{N_s} P_{ij}^T x_j(t) + \xi(t), \quad (30)$$

where  $\alpha \neq 0$  in the learning phase and  $\alpha=0$  in the retrieval phase, and  $P_{ij}^T$  is the projection matrix. The coupling between SNs and PNs is bidirectional. The last term on the right-hand side of Eq. (30) represents small positive external perturbations which can input signals from other parts of the brain that control learning and retrieval dynamics.

After a certain pattern is presented to the model, the sensory stimuli reset the state of the PN layer according to the projection rule  $a_i(t)=\sum_{j=1}^{N_p} P_{ij}^T x_j(t)$ , but  $a_i(t)$  change according to Eq. (30).

The dynamics of SNs and PNs during the learning and retrieval phases have two learning processes: (i) forming the projection matrix  $P_{ij}$  which is responsible for connecting a group of sensory neurons of the first layer corresponding to a certain stored pattern to a single PN which represents this pattern at the PN level; and (ii) learning of the competition matrix  $V_{ij}$  which is responsible for the temporal (logical) ordering of the sequential memory.

The slow learning dynamics of the projection matrix is controlled by the following equation:

$$\dot{P}_{ij} = \epsilon a_i (\beta x_j - P_{ij}) \quad (31)$$

with  $\epsilon \ll 1$ . We assume that initially all  $P_{ij}$  connections are nearly identical  $P_{ij}=1+\eta_{ij}$ , where  $\eta_{ij}$  are small random perturbations,  $\sum_j \eta_{ij}=0$ ,  $\langle \eta_{ij}^2 \rangle = \eta_0^2 \ll 1$ . Additionally, we assume that initially the matrix  $V_{ij}$  is purely competitive:  $V_{ii}=1$  and  $V_{ij}=V_0 > 1$  for  $i \neq j$ .

Suppose we want to memorize a certain pattern **A** in our projection matrix. We apply a set of inputs  $A_i$  corresponding to the pattern **A** of the SNs. As before, we assume that external stimuli render the SNs in one of two states: excited,  $A_i=1$ , and quiescent,  $A_i=0$ . The initial state of the PN layer is fully excited:  $a_i(0)=\sum_j P_{ij} A_j$ . According to the competitive nature of interactions between PNs after a short transient, only one of them, the neuron **A** which corresponds to the maximum  $a_i(0)$ , remains excited and the others become quiescent. Which neuron becomes responsible for the pattern **A** is actually random, as it depends on the initial projection matrix  $P_{ij}$ . It follows from Eq. (31) that for small  $\epsilon$  synapses of suppressed PNs do not change, whereas synapses of the single excited neuron evolve such that connections between excited SNs and PNs neurons amplify toward  $\beta > 1$ , and connections between excited PNs and quiescent SNs decay to zero. As a result, the first input pattern will be recorded in one of the matrix  $P_{ij}$  rows, while other rows will remain almost unchanged. Now suppose that we want to record a second pattern different from the first one. We can repeat the procedure described above, namely, apply external stimuli associated with pattern **B** to the SNs, project them to the initial state of the PN layer,  $a_i(0)=\sum_j P_{ij} B_j$ , and let the system evolve. Since synaptic connections from SNs suppressed by the first pattern to neuron **A** have been eliminated, a new set of stimuli corresponding to pattern **B** will excite neuron **A** more weakly than most of the others, and competition will lead to selection of one PN **B** different from neuron **A**. In this way we can record as many patterns as there are PNs.

The sequential order of the patterns recorded in the projection network is determined by the competition matrix  $V_{ij}$ , Eq. (30). Initially it is set to  $V_{ij}=V_0 > 1$  for  $i \neq j$  and  $V_{ii}=1$  which corresponds to winner-take-all competition. The goal of sequential spatial learning is to

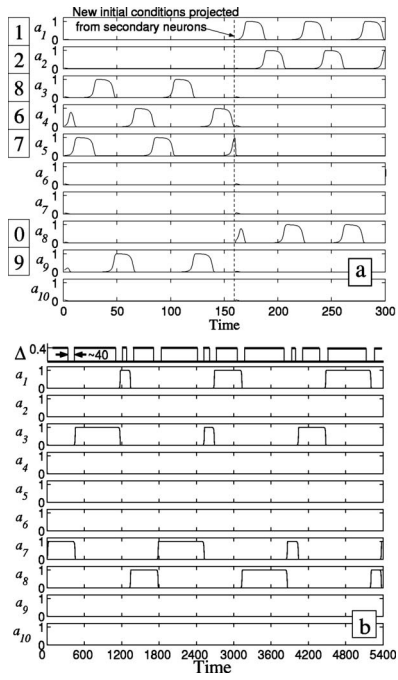


FIG. 48. Amplitudes of principal neurons during the memory retrieval phase in a two-layer dynamical model of sequential spatial memory. (a) Periodic retrieval, two different test patterns presented; (b) aperiodic retrieval with modulated inhibition (see text). Modified from Seliger et al., 2003.

record the transition of pattern **A** to pattern **B** in the form of suppressing the competition matrix element  $V_{BA}$ . We suppose that the slow dynamics of the nondiagonal elements of the competition matrix are controlled by the delay-differential equation

$$\dot{V}_{ij} = \epsilon a_i(t) a_j(t - \tau) (V_1 - V_{ij}), \quad (32)$$

where  $\tau$  is constant. Equation (32) shows that only the matrix elements corresponding to  $a_i(t) \neq 0$  and  $a_j(t - \tau) \neq 0$  are changing toward the asymptotic value  $V_1 < 1$  corresponding to the desired transition. Since most of the time, except for short transients, only one PN is excited, only one of the connections  $V_{ij}$  is changing at any time. As a result, an arbitrary, nonrepeating, sequence of patterns can be recorded.

When a test pattern  $\mathbf{T}$  is presented to the sensory layer,  $x_i(0) = T(i)$ ,  $a_i(0) = \sum_j P_j T_j$ , and  $\mathbf{T}$  resembles one of the recorded patterns, this will initiate a periodic sequence of patterns corresponding to the previously recorded sequence in the network. Figure 48 shows the behavior of principal neurons after different initial patterns resembling different digits have been presented. In both cases, the system quickly settles onto a cyclic generation of patterns associated with a given test pattern. At any given time, except for a short transient time between patterns, only a single PN is on, corresponding to a particular pattern.

## E. Sequences in complex systems with random connections

The level of cellular and network complexity in the nervous system leads one to ask: How do evolution and genetics build a complex brain? Comparative studies of the neocortex indicate that early mammalian neocortices were composed of only a few cortical fields and in primates the neocortex expanded dramatically; the number of cortical fields increased and the connectivity between them became very complex. The architecture of the microcircuitry of the mammalian neocortex remains largely unknown in terms of cell-to-cell connections; however, the connections of groups of neurons with other groups are becoming better understood thanks to new anatomical techniques and the use of slice techniques. Many parts of the neocortex developed under strict genetic control as precise networks with connections that appear similar from animal to animal. Kozlowski et al. (2001) discussed visual networks in this context. However, the local connectivity can be probabilistic or random as a consequence of experience-dependent plasticity and self-organization (Chklovskii et al., 2004). In particular, the imaging of individual pyramidal neurons in the mouse barrel cortex over a period of weeks (Maravall et al., 2004) showed that sensory experience drives the formation and elimination of synapses and that these changes might underlie adaptive remodeling of neural circuits.

Thus the brain appears as a compromise between existing genetic constraints and the need to adapt, i.e., networks are formed by both genetics and activity-dependent or self-organizing mechanisms. This makes it very difficult to determine the principles of network architecture and to build reasonable dynamical models that are able to predict the reactions of a complex neural system to changes in the environment; we have to take into account that even self-organized networks are under genetic control but in a different sense. For example, genetics can control the average balance between excitatory and inhibitory synaptic connections, sparseness of the connections, etc. The point of view that the infant cortex is not a completely organized machine is based on the supposition that there is insufficient storage capacity in the DNA to control every neuron and every synapse. This idea was formulated first by Alan Turing in 1948 (Ince, 1992).

A simple calculation reveals that the total size of the human genome can specify the connectivity of about  $10^5$  neurons. The human brain actually contains around  $10^{11}$  neurons. Let us say that we have  $N$  neurons. Each neuron requires  $Np \log_2 N$  bits to completely specify its connections, where  $p$  is the average number of connections. Therefore we need at least  $N^2 p \log_2 N$  bits to specify the entire on-off connectivity matrix of  $N$  neurons. If the connectivity degree  $p$  is not very sparse then we just need  $N^2$  bits. So, if we solve  $\min(N^2, N^2 p \log_2 N) = 3.3 \times 10^9$  base pairs in the human genome using a connectivity degree of 1%, we obtain a maximum of  $10^5$  neurons that can be completely specified. Since we do not know how much of the genome is used for brain connec-

tivity, it is not possible to narrow down the estimation. Nevertheless, it does not make sense to expect the whole genome to specify all connections in the brain. This simple estimate makes clear that learning and synaptic plasticity have a very important role in determining the connectivity of brain circuits.

The dynamics of complex network models are difficult to dissect. The mapping of the corresponding local and global bifurcations in a low-dimensional system has been extensively studied. To perform such analysis in high-dimensional systems is very demanding if not impossible. Average measures, such as mean firing rates, average membrane potential, correlations, etc., can help us to understand the dynamics of the network as a function of a few variables. One of the first models to use a mean-field approach was the Wilson-Cowan model (Wilson and Cowan, 1973). Individual neurons in the model resemble integrate-and-fire neurons with a membrane integration time  $\mu$  and a refractory period  $r$ . Wilson and Cowan's main hypothesis is that the unreliable individual responses, when grouped together, can lead to more reliable operations. The Wilson-Cowan formalism can be reduced to the following equations:

$$\begin{aligned} \mu \frac{\partial E(x,t)}{\partial t} = & -E(x,t) + [1 - rE(x,t)] \\ & \times \mathcal{L}_e \left[ \int E(y,t) w_{ee}(y,x) dy \right. \\ & \left. - \int I(y,t) w_{ei}(y,x) dy + S_e(x,t) \right], \end{aligned} \quad (33)$$

$$\begin{aligned} \mu \frac{\partial I(x,t)}{\partial t} = & -I(x,t) + [1 - rI(x,t)] \\ & \times \mathcal{L}_i \left[ \int E(y,t) w_{ie}(y,x) dy \right. \\ & \left. - \int I(y,t) w_{ii}(y,x) dy + S_i(x,t) \right], \end{aligned} \quad (34)$$

where  $E(x,t)$  and  $I(x,t)$  are the proportions of firing neurons in the excitatory and inhibitory population, the coordinate  $x$  is a continuous variable that represents the position in the cortical surface,  $w_{ee}$ ,  $w_{ei}$ ,  $w_{ie}$ , and  $w_{ii}$  are the connectivity weights, and  $S_e$  and  $S_i$  are external inputs to the excitatory and inhibitory populations, respectively. The gain functions  $\mathcal{L}_e$  and  $\mathcal{L}_i$  basically reflect the expected proportions of excitatory and inhibitory neurons receiving at least threshold excitation per unit of time. One subtle trick used in the derivation of this model is that the membrane integration time is introduced through synaptic connections. The model expressed in this form attempts to eliminate the uncertainty of single neurons by grouping them according to those with reliable common responses. We are still left with the problem of what to expect in a network of clusters connected randomly to each other. Here we will discuss it in more detail.

In a random network of excitatory and inhibitory neurons, it is not uncommon to find oscillatory activity (Jin, 2002; Huerta and Rabinovich, 2004). However, it is more interesting to study the transient behavior of neural recurrent networks. These are fast behaviors and important for sensory processing and for the control of motor commands. In studying this one needs to address two main issues: (i) whether it is possible to consistently find networks with random connections, described by equations similar to Eqs. (33) and (34), behaving regularly, and (ii) whether transient behavior in these networks is reproducible.

Huerta and Rabinovich (2004) showed, using the Wilson-Cowan formalism, periodic sequential activity (limit cycles) is more likely to be found in regions of the control parameter space where inhibitory and excitatory synapses are slightly out of balance. However, reproducible transient dynamics is more likely found in the region of parameter space far from balanced excitation and inhibition. In particular, the authors investigated the model

$$\mu \frac{dx_i(t)}{dt} = \Theta \left( \sum_{j=1}^{N_E} w_{ij}^{EE} x_j(t) - \sum_{j=1}^{N_I} w_{ij}^{EI} y_j(t) + S_i^E \right) - x_i(t), \quad (35)$$

$$\mu \frac{dy_i(t)}{dt} = \Theta \left( \sum_{j=1}^{N_E} w_{ij}^{IE} x_j(t) - \sum_{j=1}^{N_I} w_{ij}^{II} y_j(t) + S_i^I \right) - y_i(t), \quad (36)$$

where  $x(t)$  and  $y_i(t)$  represent the fractions of active neurons in cluster  $i$  of the excitatory and inhibitory populations, respectively. The numbers of excitatory and inhibitory clusters are  $N_E$  and  $N_I$ . The labels  $E$  and  $I$  are used to denote quantities associated with the excitatory or inhibitory populations, respectively. The external inputs  $S_{E,I}$  are instantaneous kicks applied to a fraction of the total population at time zero. The gain function is  $\Theta(z) = \{\tanh[(z-b)/\sigma] + 1\}/2$ , with a threshold  $b=0.1$  below the excitatory and inhibitory synaptic strength of a single connection. Clusters are taken to have very sharp thresholds of excitability by choosing  $\sigma=0.01$ . There is a wide range of values that generates similar results. The time scale is set as done by Wilson and Cowan (1973),  $\mu=10$  ms. The connectivity matrices  $w_{ij}^{XY}$  have entries drawn from a Bernoulli process (Huerta and Rabinovich, 2004). The main control parameters in this problem are the probabilities of connections from population to population.

Now we can answer the following question: What kind of activity can a network with many neurons and random connections produce? Intuition suggests that the answer has to be a complex multidimensional dynamics. However, this is not the case (Fig. 49): most observable stimulus-dependent dynamics are more simple and reproducible; periodic, transient, or chaotic (also low dimensional).

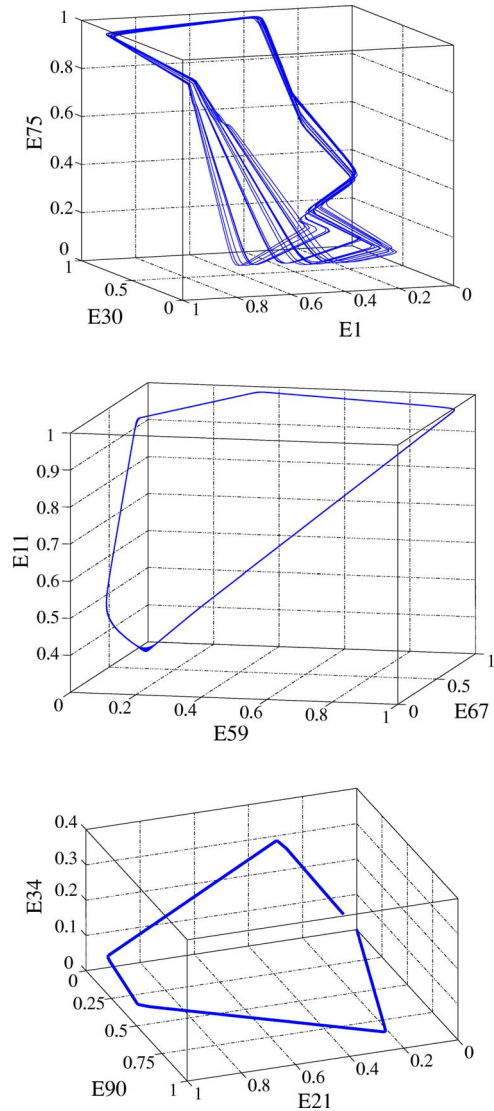


FIG. 49. (Color online) Three-dimensional projections of simulations of random networks of 200 neurons. For illustrative purposes we show three types of dynamics that can be generated by a random network: (top) chaos, (middle) limit cycle (both in the areas of parameter space that are close to balanced), and (bottom) transient dynamics (far from balanced).

This is a very important point for understanding cortex dynamics that involves the cooperative activity of many complex networks (units or microcircuits). From the functional point of view, the stimulus-dependent dynamics of the cortex can be considered as a coordinated behavior of many units with low-dimensional transient dynamics. This is the basis of a new approach to cortex modeling named the “liquid-state machine” ([Maass \*et al.\*, 2002](#)).

#### F. Coordination of sequential activity

Coordination of different sequential behaviors is crucially important for survival. From the modeling point of view it is a very complex problem. The IO (a network

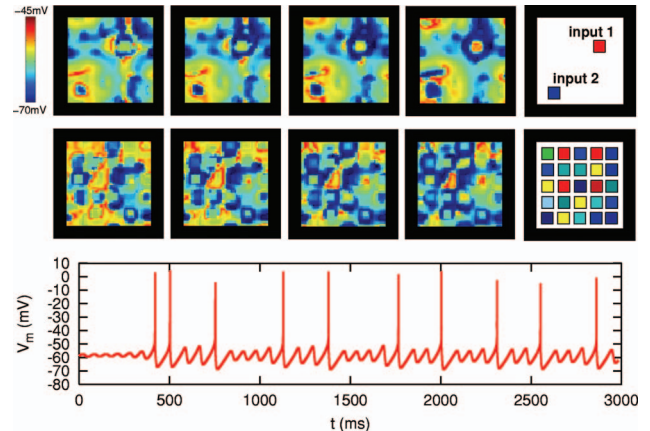


FIG. 50. (Color) Spatiotemporal patterns of coordinated rhythms induced by stimuli in a model of the inferior olive. Several structures with different frequencies can coexist simultaneously in a commensurate representation of the spiking frequencies when several stimuli are present. Incommensurate stimuli are introduced in the form of current injections in different clusters of the network. (Panels on the right show the positions of the input clusters.) These current injections induce different spiking frequencies in the neurons. Colors in these panels represent different current injections, and thus different spiking frequencies in the input clusters. Top row shows the activity of a network with two different input clusters. Bottom row shows the activity of a network with 25 different input clusters. Sequences develop in time from left to right. Regions with the same color have synchronous behavior. Color bar maps the membrane potential. Red corresponds to spiking neurons ( $-45\text{ mV}$  is above the firing threshold in the model). Dark blue means hyperpolarized activity. Bottom panel shows the activity of a single neuron with subthreshold oscillations and spiking activity. Modified from [Varona, Aguirre, \*et al.\*, 2002](#).

already discussed in Sec. III.B.2) has been suggested as a system that coordinates motor voluntary movements involving several simultaneous rhythms ([Llinás and Welsh, 1993](#)). Here an example of how subthreshold oscillations coordinate different incommensurate rhythms in a commensurate fashion is shown. In the IO, neurons are electrically coupled to their close neighbors. Their activity is characterized by subthreshold oscillations and spiking activity (see Fig. 50). The cooperative dynamics of the IO under the action of several incommensurate inputs has been modeled by [Varona, Aguirre, \*et al.\* \(2002\)](#). The results of these large-network simulations show that the electrical coupling of IO neurons produces quasisynchronized subthreshold oscillations. Because spiking activity can happen only on top of these oscillations, incommensurate inputs can produce regions with different commensurate spiking frequencies. Several spiking frequencies are able to coexist in these networks. The coexistence of different rhythms is related to the different clusterization of the spatiotemporal patterns.

Another important question related to coordination of several sequential behaviors concerns the dynamical principles that can be a basis for fast neuronal planning and reaction to a changing environment. One might

think that the WLC principle can be generalized in order to organize the sequential switching according to (i) the learned skill and (ii) the dynamical sensory inputs. The corresponding mathematical model might be similar to Eqs. (26)–(29) together with a learning rule similar to Eq. (25). Stimuli  $S'$  change sequentially and the timing of each step (the time that the system spends moving from the vicinity of one saddle to the vicinity of the next one; see Fig. 51) should be coordinated with the time of change in the environment. In recurrent networks, as a result of learning, the stimulus can go sequentially to the specific goal of an optimal heteroclinic sequence among many such sequences that exist in the phase space of the model. What is important is that at the same time, i.e., in parallel with the choosing of the rest of the motor plan, the already existing part of the motor activity plan is executed.

The two ideas just discussed can be applied to the cerebellar circuit, which is an example of a complex recurrent network (see Fig. 52). To give an impression of the complexity of the cerebellar cortex we note that it is organized into three layers: the molecular layer, the Purkinje cell layer, and the granule cell layer. Only two significant inputs reach the cerebellar cortex: mossy fibers and climbing fibers. Mossy fibers are in the majority (4:1) and carry a wealth of sensory and contextual information of multiple modalities. They make specialized excitatory synapses in structures called “glomeruli” with the dendrites of numerous granule cells. Granule cell axons form parallel fibers that run transversely in the molecular layer, making excitatory synapses with Purkinje cells. Each Purkinje cell receives  $\approx 150\,000$  synapses. These synapses are thought to be major storage sites for the information acquired during motor learning. The Purkinje cell axon provides the only output from the cerebellar cortex. This is via the deep cerebellar nuclei. Each Purkinje cell receives just one climbing fiber input from the inferior olive, but this input is very powerful because it involves several hundreds of synaptic contacts. The climbing fiber is thought to have a role in teaching in the cerebellum. The Golgi cell is excited by mossy fibers and granule cells and exercises an inhibitory feedback control upon granule cell activity. Stellate and basket cells are excited by parallel fibers in order to provide feedforward inhibition to Purkinje cells.

The huge number of inhibitory neurons and the architecture of the cerebellar networks (de Zeeuw et al., 1998) support the generalized WLC mechanism for coordination. A widely discussed hypothesis is that the specific circuitry of the IO, cerebellar cortex, and deep cerebellar nuclei called the slow loop (see Fig. 52) can serve as a dynamical working memory or as a neuronal clock with  $\approx 100$ -ms cycle time which would make it easy to connect it to behavioral time scales (Kistler and de Zeeuw, 2002; Melamed et al., 2004).

Temporal coordination and, in particular, synchronization of neural activity is a robust phenomenon, frequently observed across populations of neurons with diverse membrane properties and intrinsic frequencies. In the light of such diversity the question of how precise

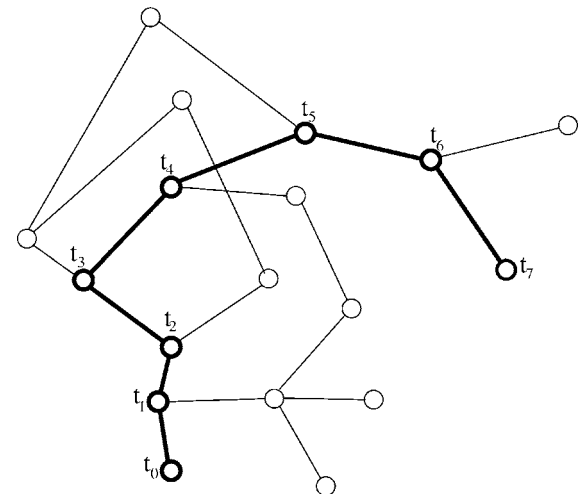


FIG. 51. Illustration of the learned sequential switching in a recurrent network with WLC dynamics: Thin lines, possible learned sequences; thick line, sequential switching chosen online by the dynamical stimulus.

synchronization can be achieved in heterogeneous networks is critical. Several mechanisms have been suggested and many of them require an unreasonably high degree of network homogeneity or very strong connectivity to achieve coherent neural activity. As discussed above (Sec. II.A.4), in a network of two synaptically coupled neurons STDP at the synapse leads to the dynamical self-adaptation of the synaptic conductance to a value that is optimal for the entrainment of the postsynaptic neuron. It is interesting to note that just a few STDP synapses are able to make the entrainment of a

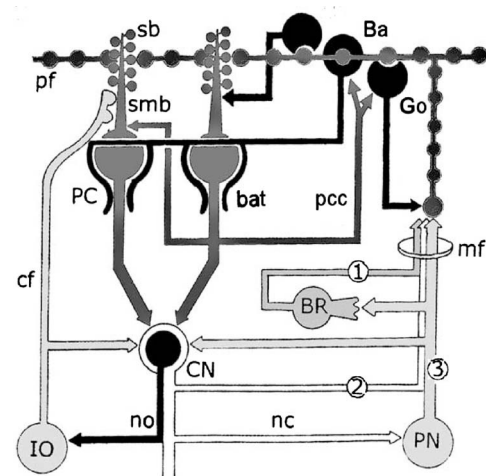


FIG. 52. A schematic representation of the mammalian cerebellar circuit. Arrows indicate the direction of transmission across each synapse. Sources of mossy fibers: Ba, basket cell; BR, brush cell; cf, climbing fiber; CN, cerebellar nuclei; Go, Golgi cell; IO, inferior olive; mf, mossy fiber; pf, parallel fiber; PN, pontine nuclei; sb and smb, spiny and smooth branches of P cell dendrites, respectively; PC, Purkinje cell; bat, basket cell terminal; pcc, P cell collateral; no, nucleo-olivary pathway; nc, collateral of nuclear relay cell. Modified from Voogd and Glickstein, 1998.

heterogeneous network of electrically coupled neurons more effective (Zhigulin and Rabinovich, 2004). It has been shown that such a network oscillates with a much higher degree of coherence than when it is subject to stimulation that is mediated by STDP synapses as compared with stimulation through static synapses. The observed phenomenon depends on the number of stimulated neurons, the strength of electrical coupling, and the degree of heterogeneity. In reality, long-term plasticity depends not only on spike timing (STDP) but also on the firing rate and the cooperativity among different neuronal inputs (Sjöström *et al.*, 2001). This makes modeling self-organization and learning more challenging.

Real behavior in nonstationary or complex environments, as already discussed, requires switching between different sequential activities. Jancke *et al.* (2000) have identified distributed regions in different parts of the cortex that are involved in the switching among sequential movements. It is important for dynamical modeling that this differential pattern of activation is not seen for simple repetitive movements. Thus such movements are too simple to evoke additional activation. This means that a dynamical model that aims to describe the sequential behavior in general has to correctly describe the switching from a low-dimensional subspace to a high-dimensional state space, and vice versa. There are no general methods for describing multidimensional dissipative nonlinear systems with such transient but reproducible dynamics. We think that the WLC principle might be the first step in this direction.

## V. CONCLUSION

Physicists, mathematicians, and physiologists all agree that an important attribute of any dynamical model of CNS activity is that not only should it be able to fit the available anatomical and physiological data, but it should also be capable of explaining function and predicting behavior. However, the ways in which physicists and mathematicians, on one hand, and physiologists, on the other hand, use modeling are based on their own experience and views and thus are different. In this review we tried to bring these different viewpoints closer together and, using many examples from the sensory, motor, and central nervous systems, discussed just a few principles like reproducibility, adaptability, robustness, and sensitivity.

Let us return to the questions formulated at the beginning of the review:

- What can nonlinear dynamics learn from neuroscience?
- What can neuroscience learn from nonlinear dynamics?

After reading this review, we hope the reader can join us in integrating the key messages in our presentation. Perhaps we may offer our compact formulation.

Addressing the first question of what nonlinear dynamics can learn from neuroscience:

- The most important activities of neuronal systems are transient and cannot be understood by analyzing attractor dynamics alone. These need to be augmented by reliable descriptions of stimulus-dependent transient motions in state space as this comprises the heart of most neurobiological activity. Nonetheless, because the dynamics of realistic neuronal models are strongly dissipative, their stimulus-dependent transient behavior is strongly attracted to some low-dimensional manifolds embedded in the high-dimensional state space of the neural network. It is a strong stimulus to nonlinear dynamics to develop a theory of reasonably low-dimensional transient activity and, in particular, to consider the local and global bifurcations of such objects as homoclinic and heteroclinic trajectories.
- For many dynamical problems of neuroscience, in contrast to traditional dynamical approaches, the initial conditions do matter crucially. Persistent neuronal activity (i.e., dynamical memory), stimulus-dependent transient competition, stimulus-dependent transient synchronization, and stimulus-dependent synaptic plasticity are all aspects of this. Clearly, addressing these important phenomena will require an expansion in our approaches to dynamical systems.

Addressing the second question of what neuroscience can learn from nonlinear dynamics:

- Dynamical models confirm the key role of inhibition in neuronal systems. The function of inhibition is not just to organize a balance with excitation in order to stabilize a network but much more: (a) inhibitory networks can generate rhythms, such as reproducible and adaptive motor rhythms in CPGs, or gamma rhythms in the brain; (b) they are responsible for the transformation of an identity sensory code to a spatiotemporal code important for better recognition in an acoustically cluttered environment; and (c) thanks to inhibition, neural systems can be at the same time very sensitive to their input and robust against noise.
- Dynamical chaos is not just a fundamental phenomenon but also important for the survival of living organisms. Neuronal systems may use chaos for the organization of nontrivial behavior such as the irregular hunting-swimming of *Clione* and for the organization of higher brain functions.
- The improvement in yield, stability, and longevity of multielectrode recordings, new imaging techniques, combined with new data processing methods, have allowed neurophysiologists to describe brain activities as the dynamics of spatiotemporal patterns in some virtual space. We think this is a basis for building a bridge between transient large-scale brain activity and animal behavior.

And finally as we pursue the investigation of dynamical principles in neuroscience, we hope that eventually not to see these two questions apart from one another

but as an integrated approach to deep and complex scientific problems.

## ACKNOWLEDGMENTS

We thank Ramon Huerta and Thomas Nowotny for their help, and Rafael Levi and Valentin Zhigulin for useful comments. This work was supported by NSF Grant No. NSF/EIA-0130708, and Grant No. PHY 0414174; NIH Grant No. 1 R01 NS50945 and Grant No. NS40110; MEC BFI2003-07276, and Fundación BBVA.

## GLOSSARY

<i>AL</i>	antennal lobe, the first site of sensory integration from the olfactory receptors of insects.
AMPA receptors	transmembrane receptor for the neurotransmitter glutamate that mediates fast synaptic transmission.
bumps	spatially localized regions of high neural activity.
CA1	subsystem of the hippocampus with a very active role in general memory.
carbachol	chemical that induces oscillations in <i>in vitro</i> preparations.
<i>Clione</i>	marine mollusk whose nervous system is frequently used in neurophysiology studies.
CNS	central nervous system.
CPG	central pattern generator, a small neural circuit that can produce stereotyped rhythmic outputs without rhythmic sensory or central input.
depolarization	any change in the neuron membrane potential that makes it more positive than when the cell is in its resting state.
dynamic clamp	a computer setup to insert virtual conductances into a neural membrane typically used to add synaptic input to a cell by calculating the response current to a specific presynaptic input.
GABA	neurotransmitter of typically inhibitory synapses; they can be mediated by fast GABA(A) or slow GABA(B) receptors.
heteroclinic loop	a closed chain of heteroclinic trajectories.
heteroclinic trajectory	trajectory that lies simultaneously on the stable manifold of one saddle point (or limit cycle) and the unstable manifold of another saddle (or limit cycle) connecting them.
HH	Hodgkin-Huxley neuron model.
HVC	high vocal center in the brain of songbirds.
hyperpolarization	any change in the neuron membrane potential that makes it more negative than when the cell is in its resting state.
interneurons	neurons whose axons remain within a particular brain region as contrasted with projection neurons, which have axons projecting to other brain regions, or with motoneurons, which innervate muscles.
IO	inferior olive, a neural system that is an input to the cerebellar cortex presumably involved in motor coordination.
KCs	Kenyon cells, interneurons of the mushroom body of insects.
Kolmogorov-Sinai entropy	a measure of the degree of predictability of further states visited by a chaotic trajectory started within a small region in a state space.
LP	lateral pyloric neuron of the crustacean stomatogastric CPG.
LTD	long-term depression, activity-dependent decrease of synaptic efficacy transmission.
LTM	long-term memory.
LTP	long-term potentiation, activity-dependent reinforcement of synaptic efficacy transmission.
Lyapunov exponents $\lambda_j$	the rate of exponential divergence from perturbed initial conditions in the $j$ th direction of the state space. For trajectories belonging to a strange attractor the spectrum $\lambda_j$ is independent of initial conditions and characterizes the stable chaotic behavior.
MCs	microcircuits; circuits composed of a small number of neurons that perform specific operational tasks.
mushroom body	lobed subsystem of the insect brain involved in classification, learning, and memory of odors.
mutual information	a measure of the independence of two signals $X$ and $Y$ , i.e., the information of $X$ that is shared by $Y$ . In the discrete case, if the joint probability density function of $X$ and $Y$ is $p(x,y) = P(X=x, Y=y)$ , the probability

neuromodulators	density function of $X$ alone is $f(x)=P(X=x)$ , and the probability density function of $Y$ alone is $g(y)=P(Y=y)$ , then the mutual information of $X$ and $Y$ is given by $I(X,Y) = \sum_{x,y} p(x,y)\log_2[p(x,y)/f(x)g(y)]$ . a substance other than a neurotransmitter, released by neurons that can affect the intrinsic and synaptic dynamics of other neurons.	synfire chain	other. There are at least three different types of synapses: excitatory and inhibitory chemical synapses and electrical synapses or gap junctions.
neurotransmitters	chemicals that are used to relay at the synapses the signals between neurons.	WLC	propagation of synchronous spiking activity in a sequence of layers of neurons belonging to a feedforward network.
pacemaker	neuron or circuit that has endogenous rhythmic activity.		winnerless-competition principle for the nonautonomous transient dynamics of neural systems receiving external stimuli and exhibiting sequential switching among temporal “winners.”
PD	pyloric dilator neuron of the crustacean CPG.		
phase synchronization (locking)	the onset of a certain relationship between the phases of coupled self-sustained oscillators.		
place cell	a type of neuron found in the hippocampus that fires strongly when an animal is in a specific location in an environment.		
plasticity	changes that occur in the organization of synaptic connections or intracellular dynamics.		
PN Purkinje cell	projection or principal neurons. main cell type of the cerebellar cortex.		
RA	premotor nucleus of the songbird brain.		
receptor	a protein on the cell membrane that binds to a neurotransmitter, neuromodulator, or other substance, and initiates the cellular response to the ligand.		
receptor neuron	sensory neuron.		
SHS	stable heteroclinic sequence.		
SN	sensory neuron.		
SSM	sequential spatial memory.		
statocyst	balance organ in some invertebrates that consists of a sphere-like structure containing a mineralized mass (statolith) and several sensory neurons also called statocyst receptors.		
STDP	spike-timing-dependent plasticity.		
STM	short-term memory.		
structural stability	condition in which small changes in the parameters do not change the topology of the phase portrait in the state space.		
synapse	specialized junction through which neurons signal to one another.		

## REFERENCES

- Abarbanel, H., R. Huerta, and M. I. Rabinovich, 2002, Proc. Natl. Acad. Sci. U.S.A. **99**, 10132.
- Abarbanel, H. D. I., 1997, *Analysis of Observed Chaotic Data* (Springer, New York).
- Abarbanel, H. D. I., R. Huerta, M. I. Rabinovich, N. F. Rulkov, P. F. Rowat, and A. I. Selverston, 1996, Neural Comput. **8**, 1567.
- Abarbanel, H. D. I., M. Rabinovich, and M. Sushchik, 1993, *Introduction to Nonlinear Dynamics for Physicists* (World Scientific, Singapore).
- Abeles, M., 1991, *Corticonics: Neural Circuits of the Cerebral Cortex* (Cambridge University Press, Cambridge, England).
- Abeles, M., H. Bergman, E. Margalit, and E. Vaadia, 1993, J. Neurophysiol. **79**, 1629.
- Adrian, E. D., and Y. Zotterman, 1926, J. Physiol. (London) **61**, 151.
- Afraimovich, V., V. Zhigulin, and M. Rabinovich, 2004, Chaos **14**, 1123.
- Afraimovich, V. S., M. I. Rabinovich, and P. Varona, 2004, Int. J. Bifurcation Chaos Appl. Sci. Eng. **14**, 1195.
- Aihara, K., 2002, Proc. IEEE **90**, 919.
- Amari, S., 1977, Biol. Cybern. **27**, 77.
- Amit, D., and N. Brunel, 1997a, Cereb. Cortex **7**, 237.
- Amit, D. J., and N. Brunel, 1997b, Cereb. Cortex **7**, 237.
- Andronov, A., 1933, in *The First All-Union Conference on Auto-oscillations* (GTTI, Moscow Leningrad), pp. 32–71.
- Andronov, A., A. Vitt, and S. Khaikin, 1949, *Theory of Oscillations* (Princeton University Press, Princeton, NJ).
- Andronov, A. A., and L. Pontryagin, 1937, Dokl. Akad. Nauk SSSR **14**, 247.
- Arbib, M. A., P. Érdi, and J. Szentágothai, 1997, *Neural Organization: Structure, Function, and Dynamics* (Bradford Book/MIT, Cambridge, MA).
- Arieli, A., A. Sterkin, A. Grinvald, and A. Aertsen, 1996, Science **273**, 1868.
- Arnold, V., V. Afraimovich, Y. Ilyashenko, L. Shilnikov, and N. Kazarinooff, 1999, *Bifurcation Theory and Catastrophe Theory* (Springer, New York).
- Ashby, W. R., 1960, *Design for a Brain*, 2nd ed. (Wiley, New York).
- Ashwin, P., M. Field, A. Ruckridge, and R. Sturman, 2003, Chaos **13**, 973.
- Aswin, P., and M. Timme, 2005, Nature (London) **436**, 36.

- Aviel, Y., C. Mehring, M. Abeles, and D. Horn, 2003, *Neural Comput.* **15**, 1321.
- Baird, B., and F. Eeckman, 1993, in *Associative Neural Memories: Theory and Implementation*, edited by M. H. Hassoun (Oxford University Press, New York), p. 135.
- Bao, W., and J.-Y. Wu, 2003, *J. Neurophysiol.* **90**, 333.
- Barlow, H. B., 1972, *Perception* **1**, 371.
- Bartos, M., Y. Manor, F. Nadim, E. Marder, and M. P. Nusbaum, 1999, *J. Neurosci.* **19**, 6650.
- Bartos, M., and M. P. Nusbaum, 1997, *J. Neurosci.* **17**, 2247.
- Bi, G., 2002, *Biol. Cybern.* **87**, 319.
- Bi, G., and M. Poo, 1998, *J. Neurosci.* **18**, 10464.
- Bi, G., and M. Poo, 2001, *Annu. Rev. Neurosci.* **24**, 139.
- Bliss, T. V., and T. Lomo, 1973, *J. Physiol. (London)* **232**, 331.
- Block, H. D., 1962, *Rev. Mod. Phys.* **34**, 123.
- Bondarenko, V., G. S. Cymbalyuk, G. Patel, S. Deweerth, and R. Calabrese, 2003, *Neurocomputing* **52-54**, 691.
- Borda, J. C., 1781, *Mémoire sur les élections au scrutin* (Histoire de l'Academie Royale des Sciences, Paris).
- Bressloff, P., 2002, *Phys. Rev. Lett.* **89**, 088101.
- Bressloff, P., and J. D. Cowan, 2002, *Neural Comput.* **14**, 493.
- Bressloff, P., J. Cowan, M. Golubitsky, P. Thomas, and M. Weiner, 2001, *Philos. Trans. R. Soc. London, Ser. B* **356**, 299.
- Brody, C., and J. Hopfield, 2003, *Neuron* **37**, 843.
- Brunel, N., 2003, *Cereb. Cortex* **13**, 1151.
- Brunel, N., and X. Wang, 2001, *J. Comput. Neurosci.* **11**, 63.
- Busse, F., and K. Heikes, 1980, *Science* **208**, 173.
- Calabrese, R., F. Nadim, and O. Olsen, 1995, *J. Neurobiol.* **27**, 390.
- Canavier, C., D. Baxter, J. Clark, and J. Byrne, 1993, *J. Neurophysiol.* **69**, 2252.
- Canavier, C., J. Clark, and J. Byrne, 1990, *Biophys. J.* **57**, 1245.
- Casado, J., 2003, *Phys. Rev. Lett.* **91**, 208102.
- Castelo-Branco, M., R. Goebel, S. Neuenschwander, and W. Singer, 2000, *Nature (London)* **405**, 685.
- Cateau, H., and T. Fukai, 2001, *Neural Networks* **14**, 675.
- Cazelles, B., M. Courbage, and M. I. Rabinovich, 2001, *Europhys. Lett.* **56**, 504.
- Chay, T., 1985, *Physica D* **16**, 223.
- Chechik, G., 2003, *Neural Comput.* **15**, 1481.
- Chklovskii, D. B., B. W. Mel, and K. Svoboda, 2004, *Nature (London)* **431**, 78.
- Chow, C., and N. Kopell, 2000, *Neural Comput.* **12**, 1643.
- Cohen, A., P. Holmes, and R. Rand, 1982, *J. Math. Biol.* **13**, 345.
- Cohen, M. A., and S. Grossberg, 1983, *IEEE Trans. Syst. Man Cybern.* **13**, 815.
- Connors, B., 2002, *Nature (London)* **420**, 133.
- Connors, B. W., and Y. Amitai, 1997, *Neuron* **18**, 347.
- Contreras, D., A. Destexhe, T. Sejnowski, and M. Steriade, 1996, *Science* **274**, 771.
- Coombes, S., and A. Osbaldestin, 2000, *Phys. Rev. E* **62**, 4057.
- Cossart, R., D. Aronov, and R. Yuste, 2003, *Nature (London)* **423**, 283.
- Cowan, N., 2001, *Behav. Brain Sci.* **24**, 87.
- Crawford, J., 1991, *Rev. Mod. Phys.* **63**, 991.
- Crevier, D., and M. Meister, 1998, *J. Neurophysiol.* **79**, 1869.
- Cross, M., and P. Hohenberg, 1993, *Rev. Mod. Phys.* **65**, 851.
- Curts, C. E., and M. D'Esposito, 2003, *Trends Cogn. Sci.* **7**, 415.
- Cymbalyuk, G., O. Gaudry, M. Masino, and R. Calabrese, 2002, *J. Neurosci.* **22**, 10580.
- deCharms, R., and M. Merzenich, 1996, *Nature (London)* **361**, 610.
- deCharms, R. C., 1998, *Proc. Natl. Acad. Sci. U.S.A.* **95**, 15166.
- de Nô, R. L., 1938, *J. Neurophysiol.* **1**, 207.
- de Ryter van Steveninck, R., G. Lewen, S. Strong, R. Koberle, and W. Bialek, 1997, *Science* **275**, 1805.
- Desmedt, J., and C. Tomberg, 1994, *Neurosci. Lett.* **168**, 126.
- de Zeeuw, C. I., J. I. Simpson, C. C. Hoogenraad, N. Galjart, S. K. E. Koekkoek, and T. J. H. Ruigrok, 1998, *Trends Neurosci.* **21**, 391.
- Diesmann, M., M.-O. Gewaltig, and A. Aertsen, 1999, *Nature (London)* **402**, 529.
- Diwadkar, V. A., P. A. Carpenter, and M. Just, 2000, *Neuroimage* **11**, 85.
- Doboli, S., A. A. Minai, and P. Best, 2000, *Neural Comput.* **12**, 1009.
- Dragoi, G., K. Harris, and G. Buzsaki, 2003, *Neuron* **39**, 843.
- Du, X., B. K. Ghosh, and P. Ulinski, 2005, *IEEE Trans. Biomed. Eng.* **52**, 566.
- Duda, R., E. Hart, and D. Stork, 2001, *Pattern Classification* (Wiley, New York).
- Durstewitz, D., J. Seamans, and T. Sejnowski, 2000, *Nat. Neurosci.* **3**, 1184.
- Egorov, A., B. Hamann, E. Fransen, M. Hasselmo, and A. Alonso, 2002, *Nature (London)* **420**, 173.
- Eguia, M. C., M. I. Rabinovich, and H. D. I. Abarbanel, 2000, *Phys. Rev. E* **62**, 7111.
- Elhilali, M., J. Fritz, D. Klein, J. Z. Simon, and S. Shamma, 2004, *J. Neurosci.* **24**, 1159.
- Elowitz, M., and S. Leibler, 2000, *Nature (London)* **403**, 335.
- Elson, R. C., A. I. Selverston, H. D. I. Abarbanel, and M. I. Rabinovich, 2002, *J. Neurophysiol.* **88**, 1166.
- Elson, R. C., A. I. Selverston, R. Huerta, N. F. Rulkov, M. I. Rabinovich, and H. D. I. Abarbanel, 1998, *Phys. Rev. Lett.* **81**, 5692.
- Engel, A. K., P. Fries, and W. Singer, 2001, *Nat. Rev. Neurosci.* **2**, 704.
- Ermentrout, B., 1992, *Neural Networks* **5**, 415.
- Ermentrout, G., and J. Cowan, 1979, *Biol. Cybern.* **34**, 137.
- Ermentrout, G. B., 1998, *Rep. Prog. Phys.* **61**, 353.
- Ermentrout, G. B., and N. Kopell, 1984, *SIAM J. Math. Anal.* **15**, 215.
- Fano, R. M., 1961, Ed., *Transmission of Information: A Statistical Theory of Communications* (MIT, New York).
- Fatt, P., and B. Katz, 1952, *J. Physiol. (London)* **117**, 109.
- Fell, J., G. Fernandez, P. Klaver, C. Elger, and P. Fries, 2003, *Brain Res. Rev.* **42**, 265.
- Feudel, U., A. Neiman, X. Pei, W. Wojtenek, H. Braun, M. Huber, and F. Moss, 2000, *Chaos* **10**, 231.
- FitzHugh, R., 1961, *Biophys. J.* **1**, 445.
- Fitzpatrick, D. C., R. Batra, T. R. Sanford, and S. Kuwada, 1997, *Nature (London)* **388**, 871.
- Foss, J., A. Longtin, B. Mensour, and J. Milton, 1996, *Phys. Rev. Lett.* **76**, 708.
- Freeman, W., 1972, *Progress in Theoretical Biology* (Academic, New York), Vol. 2.
- Freeman, W., 2000, *Neurodynamics: An Exploration in Mesoscopic Brain Dynamics* (Springer, New York).
- Fuhrmann, G., I. Segev, H. Markram, and M. Tsodyks, 2002, *J. Neurophysiol.* **87**, 140.
- Fukai, T., and S. Tanaka, 1997, *Neural Comput.* **9**, 77.
- Galan, R. F., S. Sachse, C. G. Galizia, and A. V. M. Herz, 2004, *Neural Comput.* **16**, 999.

- Gallager, R. G., 1968, Ed., *Information Theory and Reliable Communication* (Wiley, New York).
- Garcia-Sanchez, M., and R. Huerta, 2003, *J. Comput. Neurosci.* **15**, 5.
- Gavrilov, N., and A. Shilnikov, 2000, *Am. Math. Soc. Transl.* **200**, 99.
- Georgopoulos, A. P., A. B. Schwartz, and R. E. Kettner, 1986, *Science* **233**, 1416.
- Gerstner, W., and W. Kistler, 2002, *Spiking Neuron Models* (Cambridge University Press, Cambridge, England).
- Getting, P., 1989, *Annu. Rev. Neurosci.* **12**, 185.
- Gewaltig, M.-O., M. Diesmann, and A. Aertsen, 2001, *Neural Networks* **14**, 657.
- Ghose, G., and J. Maunsell, 1999, *Neuron* **24**, 79.
- Glass, L., 1995, *The Handbook of Brain Theory and Neural Networks* (MIT, Cambridge), pp. 186–189.
- Goldman-Rakic, P., 1995, *Neuron* **14**, 477.
- Goroff, D., 1992, Ed., *New Methods of Celestial Mechanics* (AIP, New York).
- Gray, C., P. Konig, A. Engel, and W. Singer, 1989, *Nature* (London) **338**, 334.
- Grillner, S., 2003, *Nat. Rev. Neurosci.* **4**, 573.
- Grossberg, S., 1973, *Stud. Appl. Math.* **52**, 213.
- Gu, H., M. Yang, L. Li, Z. Liu, and W. Ren, 2003, *Phys. Lett. A* **319**, 89.
- Guckenheimer, J., S. Gueron, and R. Harris-Warrick, 1993, *Philos. Trans. R. Soc. London, Ser. B* **341**, 345.
- Guckenheimer, J., and P. Holmes, 1986, *Nonlinear Oscillations, Dynamical Systems, and Bifurcations of Vector Fields* (Springer, New York).
- Guckenheimer, J., and P. Holmes, 1988, *Math. Proc. Cambridge Philos. Soc.* **103**, 189.
- Hass, J., T. Nowotny, and H. D. I. Abarbanel, 2006, *J. Neurophysiol.*, doi:10.1152/jn.00551.2006.
- Hahnloser, R. H., A. A. Kozhevnikov, and M. S. Fee, 2002, *Nature* (London) **419**, 65.
- Hamilton, K., and J. Kauer, 1985, *Brain Res.* **338**, 181.
- Hatsopoulos, N., L. Paninski, and J. Donoghue, 2003, *Exp. Brain Res.* **149**, 478.
- Hebb, R., 1949, *The Organization of Behavior* (Wiley, New York).
- Hindmarsh, J. L., and R. M. Rose, 1984, *Proc. R. Soc. London, Ser. B* **221**, 87.
- Hodgkin, A. L., and A. F. Huxley, 1952, *J. Physiol. (London)* **117**, 500.
- Hopfield, J., and C. Brody, 2001, *Proc. Natl. Acad. Sci. U.S.A.* **98**, 1282.
- Hopfield, J., and C. Brody, 2004, *Proc. Natl. Acad. Sci. U.S.A.* **101**, 337.
- Hopfield, J. J., 1982, *Proc. Natl. Acad. Sci. U.S.A.* **79**, 2554.
- Huang, X., W. C. Troy, Q. Yang, H. Ma, C. R. Laing, S. J. Schiff, and J.-Y. Wu, 2004, *J. Neurosci.* **24**, 9897.
- Huerta, R., and M. I. Rabinovich, 2004, *Phys. Rev. Lett.* **93**, 238104.
- Huerta, R., M. Rabinovich, H. H. D. I. Abarbanel, and M. Bazhenov, 1997, *Phys. Rev. E* **55**, R2108.
- Huerta, R., P. Varona, M. Rabinovich, and H. Abarbanel, 2001, *Biol. Cybern.* **84**, L1.
- Ichinohe, N., F. Fujiyama, T. Kaneko, and K. S. Rockland, 2003, *J. Neurosci.* **23**, 1372.
- Ikegaya, Y., G. Aaron, R. Cossart, D. Aronov, I. Lampl, D. Ferster, and R. Yuste, 2004, *Science* **304**, 559.
- Ince, D., 1992, Ed., *Mechanical Intelligence: Collected Works of A. M. Turing* (North-Holland, Amsterdam).
- Ito, M., 1982, *Annu. Rev. Neurosci.* **5**, 275.
- Izhikevich, E., 2004, *IEEE Trans. Neural Netw.* **15**, 1063.
- Izhikevich, E., 2006, *Dynamical Systems in Neuroscience: The Geometry of Excitability and Bursting* (MIT, Cambridge, MA).
- Jackson, A., V. Gee, S. Baker, and R. Lemon, 2003, *Neuron* **38**, 115.
- Jancke, L., M. Himmelbach, N. Shah, and K. Zilles, 2000, *Neuroimage* **12**, 528.
- Jefferys, J., R. Traub, and M. Whittington, 1996, *Trends Neurosci.* **19**, 202.
- Jin, D. Z., 2002, *Phys. Rev. Lett.* **89**, 208102.
- Jones, S. R., B. Mulloney, T. J. Kaper, and N. Kopell, 2003, *J. Neurosci.* **60**, 3457.
- Kandel, E. R., J. H. Schwartz, and T. M. Jessell, 2000, *Principles of Neural Science* (McGraw-Hill, New York).
- Kaplan, D., and L. Glass, 1995, *Understanding Nonlinear Dynamics* (Springer, New York).
- Katz, B., 1969, *The Release of Neurotransmitter Substances* (Thomas, Springfield, IL).
- Kay, L., 2003, *Chaos* **13**, 1057.
- Kepes, A., and J. Lisman, 2003, *Network Comput. Neural Syst.* **14**, 103.
- Kim, U., T. Bal, and D. A. McCormick, 1995, *J. Neurophysiol.* **74**, 1301.
- Kimpo, R. R., F. E. Theunissen, and A. J. Doupe, 2003, *J. Neurosci.* **23**, 5730.
- Kistler, W. M., and C. I. de Zeeuw, 2002, *Neural Comput.* **14**, 2597.
- Koch, C., 1999, *Biophysics of Computation* (Oxford University Press, New York).
- Konishi, M., 1990, *Cold Spring Harbor Symp. Quant. Biol.* **55**, 575.
- Korn, H., and P. Faure, 2003, *C R. Seances Soc. Biol. Fil* **326**, 787.
- Kozloski, J., F. Hamzei-Sichani, and R. Yuste, 2001, *Science* **293**, 868.
- Krupa, P., 1997, *J. Nonlinear Sci.* **7**, 129.
- Kuramoto, Y., 1984, *Chemical Oscillations, Waves, and Turbulence* (Springer, New York).
- Kuznetsov, Y., 1998, *Elements of Applied Bifurcation Theory*, 2nd ed. (Springer, New York).
- Lai, Y. C., M. A. F. Harrison, M. G. Frei, and I. Osorio, 2003, *Phys. Rev. Lett.* **91**, 068102.
- Laing, C. R., W. C. Troy, B. Gutkin, and G. B. Ermentrout, 2002, *SIAM J. Appl. Math.* **63**, 62.
- Landau, L. D., and E. M. Lifshitz, 1987, *Fluid Mechanics* (Pergamon, New York).
- Lapicque, L., 1907, *J. Physiol. Pathol. Gen.* **9**, 620.
- Lashley, K., 1960, in *The Neuropsychology of Lashley*, edited by F. A. Beach, D. O. Hebb, C. T. Morgan, and H. W. Nissen (McGraw-Hill, New York), pp. 506–521.
- Latorre, R., F. B. Rodriguez, and P. Varona, 2006, *Biol. Cybern.* **95**, 169.
- Lau, P., and G. Bi, 2005, *Proc. Natl. Acad. Sci. U.S.A.* **102**, 10333.
- Laurent, G., 1996, *Trends Neurosci.* **19**, 489.
- Laurent, G., and H. Davidowitz, 1994, *Science* **265**, 1872.
- Laurent, G., M. Stopfer, R. W. Friedrich, M. I. Rabinovich, and H. D. I. Abarbanel, 2001, *Annu. Rev. Neurosci.* **24**, 263.
- Leitch, B., and G. Laurent, 1996, *J. Comp. Neurol.* **372**, 487.

- LeMasson, G., S. R.-L. Masson, D. Debay, and T. Bal, 2002, Nature (London) **417**, 854.
- Lestienne, R., 2001, Prog. Neurobiol. (Oxford) **65**, 545.
- Levi, R., P. Varona, Y. I. Arshavsky, M. I. Rabinovich, and A. I. Selverston, 2004, J. Neurophysiol. **91**, 336.
- Levi, R., P. Varona, Y. I. Arshavsky, M. I. Rabinovich, and A. I. Selverston, 2005, J. Neurosci. **25**, 9807.
- Lewis, T., and J. Rinzel, 2003, J. Comput. Neurosci. **14**, 283.
- Leznik, E., and R. Llinás, 2002, Ann. N.Y. Acad. Sci. **978**, 529.
- Lin, L., R. Osan, S. Shoham, W. Jin, W. Zuo, and J. Tsien, 2005, Proc. Natl. Acad. Sci. U.S.A. **102**, 6125.
- Lindner, B., J. García-Ojalvo, A. Neiman, and L. Schimansky-Geier, 2004, Phys. Rep. **392**, 2004.
- Llinás, R., and J. P. Welsh., 1993, Curr. Opin. Neurobiol. **3**, 958.
- Loebel, A., and M. Tsodyks, 2002, J. Comput. Neurosci. **13**, 111.
- Lotka, A. J., 1925, *Elements of Physical Biology* (Williams & Wilkins Co., Baltimore).
- Maass, W., T. Natschläger, and H. Markram, 2002, Neural Comput. **14**, 2531.
- Machens, C., T. Göllisch, O. Kolesnikova, and A. Herz, 2005, Neuron **47**, 447.
- Machens, C., R. Romo, and C. Brody, 2005, Science **307**, 1121.
- Maeda, Y., and H. Makino, 2000, BioSystems **58**, 93.
- Maeda, Y., K. Pakdaman, T. Nomura, S. Doi, and S. Sato, 1998, Biol. Cybern. **78**, 265.
- Mainen, Z., and T. Sejnowski, 1995, Science **268**, 1503.
- Malenka, R. C., and R. A. Nicoll, 1999, Science **285**, 1870.
- Malkov, V., M. Rabinovich, and M. M. Sushchik, 1996, *Proceedings of Nizhny Novgorod University*, edited by V. D. Shalfeev (Nizhny Novgorod University, Nizhny Novgorod), p. 72.
- Mandelblat, Y., Y. Etzion, Y. Grossman, and D. Golomb, 2001, J. Comput. Neurosci. **11**, 43.
- Maravall, M., I. Y. Y. Koh, W. Lindquist, and K. Svoboda, 2004, Cereb. Cortex **10**, 1093.
- Marder, E., and R. L. Calabrese, 1996, Physiol. Rev. **76**, 687.
- Marder, E., L. A. G. Turrigiano, Z. Liu, and J. Golowasch, 1996, Proc. Natl. Acad. Sci. U.S.A. **93**, 13481.
- Martin, S. J., P. D. Grimwood, and R. G. M. Morris, 2000, Annu. Rev. Neurosci. **23**, 649.
- Mazor, O., and G. Laurent, 2005, Neuron **48**, 661.
- McClurkin, J. W., L. M. Optican, B. J. Richmond, and T. J. Gawne, 1991, Science **253**, 675.
- McCormick, D., Y. Shu, A. Hasenstaub, M. Sanches-Vives, M. Badoual, and T. Bal, 2003, Cereb. Cortex **13**, 1219.
- McCulloch, W. S., and W. Pitts, 1943, Bull. Math. Biophys. **5**, 115.
- Mehta, M. R., A. K. Lee, and M. A. Wilson, 2002, Nature (London) **417**, 741.
- Melamed, O., W. Gerstner, W. Maas, M. Tsodyks, and H. Markram, 2004, Trends Neurosci. **27**, 11.
- Mooney, R., and J. Prather, 2005, J. Neurosci. **25**, 1952.
- Morris, C., and H. Lecar, 1981, Biophys. J. **35**, 193.
- Nádasdy, Z., 2000, J. Physiol. (Paris) **94**, 505.
- Nagumo, J., S. Arimoto, and S. Yoshizawa, 1962, Proc. IRE **50**, 2061.
- Nakahara, H., and K. Doya, 1998, Neural Comput. **10**, 113.
- Nase, G., W. Singer, H. Monyer, and A. K. Engel, 2003, J. Neurophysiol. **90**, 1115.
- Nenadic, Z., B. K. Ghosh, and P. Ulinski, 2002, IEEE Trans. Biomed. Eng. **49**, 753.
- Nicholls, J. G., A. R. Martin, and B. G. Wallace, 1992, *From Neuron to Brain: A Cellular and Molecular Approach to the Function of the Nervous System* (Sinauer Associates, Sunderland, MA).
- Nowotny, T., 2003, URL [http://inls.ucsd.edu/\\$sim\\$nowotny/dynclamp.html](http://inls.ucsd.edu/$sim$nowotny/dynclamp.html)
- Nowotny, T., and R. Huerta, 2003, Biol. Cybern. **89**, 237.
- Nowotny, T., R. Huerta, H. Abarbanel, and M. Rabinovich, 2005, Biol. Cybern. **93**, 436.
- Nowotny, T., M. I. Rabinovich, R. Huerta, and H. D. I. Abarbanel, 2003, J. Comput. Neurosci. **15**, 271.
- Nowotny, T., V. P. Zhigulin, A. I. Selverston, H. D. I. Abarbanel, and M. I. Rabinovich, 2003, J. Neurosci. **23**, 9776.
- Nystrom, L. E., T. S. Braver, F. W. Sabb, M. R. Delgado, D. C. Noll, and J. D. Cohen, 2000, NeuroImage **11**, 424.
- O'Keefe, J., and J. Dostrovsky, 1971, Brain Res. **34**, 171.
- O'Reilly, R., R. Busby, and R. Soto, 2003, *The Unity of Consciousness—Binding, Integration and Dissociation* (Oxford University Press, Oxford), Chap. 3, p. 2.5.
- Oscarsson, O., 1980, in *The Inferior Olivary Nucleus*, edited by J. Courville, C. de Montigny, and Y. Lamarre (Raven, New York), pp. 279–289.
- Ott, E., 1993, *Chaos in Dynamical Systems* (Cambridge University Press, Cambridge, England).
- Panchin, Y., Y. Arshavsky, T. Deliagina, L. Popova, and G. Orlovsky, 1995, J. Neurophysiol. **73**, 1924.
- Panzeri, S., S. Schultz, A. Treves, and E. Rolls, 1999, Proc. R. Soc. London, Ser. B **266**, 1001.
- Perez-Orive, J., O. Mazor, G. C. Turner, S. Cassenaer, R. I. Wilson, and G. Laurent, 2002, Science **297**, 359.
- Persi, E., D. Horn, V. Volman, R. Segev, and E. Ben-Jacob, 2004, Neural Comput. **16**, 2577.
- Pikovsky, A., M. Rosenblum, and J. Kurths, 2001, *Synchronization: A Universal Concept in Nonlinear Sciences* (Cambridge University Press, Cambridge, England).
- Pinto, R., P. Varona, A. Volkovskii, A. Szücs, H. Abarbanel, and M. Rabinovich, 2000, Phys. Rev. E **62**, 2644.
- Poincaré, A., 1905, *Le Valeur de la Science* (Flammarion, Paris).
- Poincaré, H., 1892, *Méthodes Nouvelles de la Mécanique Céleste* (Gauthier-Villars, Paris).
- Postlethwaite, C. M., and J. H. P. Dawes, 2005, Nonlinearity **18**, 1477.
- Pouget, A., P. Dayan, and R. Zemel, 2000, Nat. Rev. Neurosci. **1**, 125.
- Prinz, A., L. F. Abbott, and E. Marder, 2004a, Trends Neurosci. **27**, 218.
- Prinz, A. A., D. Bucher, and E. Marder, 2004b, Nat. Neurosci. **7**, 1345.
- Rabinovich, M., A. Ezersky, and P. Weidman, 2000, *The Dynamics of Patterns* (World Scientific, Singapore).
- Rabinovich, M., R. Huerta, and P. Varona, 2006, Phys. Rev. Lett. **96**, 014101.
- Rabinovich, M., A. Volkovskii, P. Lecanda, R. Huerta, H. D. I. Abarbanel, and G. Laurent, 2001, Phys. Rev. Lett. **87**, 068102.
- Rabinovich, M. I., and H. D. I. Abarbanel, 1998, Neuroscience **87**, 5.
- Rabinovich, M. I., and R. Huerta, 2006, Phys. Rev. Lett. **97**, 188103.
- Ramirez, J., A. Tryba, and F. Pena, 2004, Curr. Opin. Neurobiol. **6**, 665.
- Reinagel, P., and R. C. Reid, 2002, J. Neurosci. **22**, 6837.
- Reyes, A. D., 2003, Nat. Neurosci. **6**, 593.
- Riesenhuber, M., and T. Poggio, 1999, Neuron **24**, 87.

- Rinzel, J., D. Terman, X. Wang, and B. Ermentrout, 1998, *Science* **279**, 1351.
- Robinson, H., and N. Kawai, 1993, *J. Neurosci. Methods* **49**, 157.
- Rodriguez, E., N. George, J. Lachaux, J. Martinerie, B. Renault, and F. Varela, 1999, *Nature (London)* **397**, 430.
- Rosenblatt, F., 1962, *Principles of Neurodynamics: Perceptions and the Theory of Brain Mechanisms* (Spartan Books, New York).
- Roskies, A., 1999, *Neuron* **24**, 7.
- Rowe, D., 2002, *Behav. Brain Sci.* **24**, 5.
- Roweis, S., and L. Saul, 2000, *Science* **290**, 2323.
- Rubin, J. E., and D. Terman, 2004, *J. Comput. Neurosci.* **16**, 211.
- Rulkov, N. F., 2002, *Phys. Rev. E* **65**, 041922.
- Saari, G., 1995, *Basic Geometry of Voting* (Springer-Verlag, Berlin).
- Sanchez-Vives, M., and D. McCormick, 2000, *Nat. Neurosci.* **3**, 1027.
- Schutter E. D., 2002, *Curr. Biol.* **12**, R363.
- Schweighofer, N., K. Doya, H. Fukai, J. V. Chiron, T. Furukawa, and M. Kawato, 2004, *Proc. Natl. Acad. Sci. U.S.A.* **101**, 4655.
- Scott, A., 2004, Ed., *Encyclopedia of Nonlinear Science* (Routledge, New York).
- Segundo, J. P., and D. H. Perkel, 1969, *UCLA Forum Med. Sci.* **11**, 349.
- Segundo, J. P., G. Sugihara, P. Dixon, M. Stiber, and L. F. Bersier, 1998, *Neuroscience* **87**, 741.
- Seliger, P., L. S. Tsimring, and M. I. Rabinovich, 2003, *Phys. Rev. E* **67**, 011905.
- Silverston, A., 2005, *Cell Mol. Neurobiol.* **25**, 223.
- Silverston, A., M. Rabinovich, H. Abarbanel, R. Elson, A. Szücs, R. Pinto, R. Huerta, and P. Varona, 2000, *J. Physiol. (Paris)* **94**, 357.
- Senseman, D. M., and K. A. Robbins, 1999, *J. Neurosci.* **19**, RC3 1.
- Seung, H., D. Lee, B. Reis, and D. Tank, 2000, *J. Comput. Neurosci.* **9**, 171.
- Seung, H. S., 1998, in *Advances in Neural Information Processing Systems*, edited by M. I. Jordan, M. J. Kearns, and S. A. Solla (MIT, Cambridge, MA), Vol. 10.
- Seung, H. S., and H. Sompolinsky, 1993, *Proc. Natl. Acad. Sci. U.S.A.* **90**, 10749.
- Shadlen, M. N., and W. T. Newsome, 1998, *J. Neurosci.* **18**, 3870.
- Sharp, A., M. O'Neil, L. Abbott, and E. Marder, 1993, *Trends Neurosci.* **16**, 389.
- Shepherd, G., 1998, *The Synaptic Organization of the Brain* (Oxford University Press, New York).
- Sherman, A., and J. Rinzel, 1992, *Proc. Natl. Acad. Sci. U.S.A.* **89**, 2471.
- Shilnikov, A., and G. Cymbalyuk, 2005, *Phys. Rev. Lett.* **94**, 048101.
- Shu, Y., A. Hasenstaub, and D. McCormick, 2003, *Nature (London)* **423**, 288.
- Silberberg, G., S. Grillner, F. LeBeau, R. Maex, and H. Markram, 2005, *Trends Neurosci.* **28**, 541.
- Simmers A. J., and M. Moulins, 1988, *J. Neurophysiol.* **59**, 740.
- Singer, W., 1999, *Neuron* **24**, 49.
- Singer, W., 2001, *Ann. N.Y. Acad. Sci.* **929**, 123.
- Singer, W., and C. M. Gray, 1995, *Annu. Rev. Neurosci.* **18**, 555.
- Sjöström, P. J., G. G. Turrigiano, and S. B. Nelson, 2001, *Neuron* **32**, 1149.
- Softky, W. R., 1995, *Curr. Opin. Neurobiol.* **5**, 239.
- Solis, M., and D. Perkel, 2005, *J. Neurosci.* **25**, 2811.
- Sompolinsky, H., and I. Kanter, 1986, *Phys. Rev. Lett.* **57**, 2861.
- Sompolinsky, H., H. Yoon, K. Kang, and M. Shamir, 2001, *Phys. Rev. E* **64**, 051904.
- Soto-Trevino, C., P. Rabbah, E. Marder, and F. Nadim, 2005, *J. Neurophysiol.* **94**, 590.
- Soto-Trevino, C., K. A. Thoroughman, E. Marder, and L. E. Abbott, 2001, *Nat. Neurosci.* **4**, 297.
- Stein, S. G., S. Grillner, A. I. Selverston, and G. S. Douglas, 1997, Eds., *Neurons, Networks, and Motor Behavior* (MIT, Cambridge, MA).
- Stent, G. S., and W. O. Friesen, 1977, *Biol. Cybern.* **28**, 27.
- Stone, E., and D. Armbruster, 1999, *Chaos* **9**, 499.
- Stone, E., and P. Holmes, 1990, *SIAM J. Appl. Math.* **50**, 726.
- Stopfer, M., V. Jayaraman, and G. Laurent, 2003, *Neuron* **39**, 991.
- Strogatz, S. H., 2001, *Nonlinear Dynamics and Chaos: With Applications to Physics, Biology, Chemistry and Engineering* (Perseus Books Group, Cambridge, MA).
- Szekely, G., 1965, *Acta Physiol. Acad. Sci. Hung.* **27**, 285.
- Szücs, A., R. D. Pinto, M. I. Rabinovich, H. D. I. Abarbanel, and A. I. Selverston, 2003, *J. Neurophysiol.* **89**, 1363.
- Szücs, A., P. Varona, A. Volkovskii, H. D. I. Abarbanel, M. Rabinovich, and A. Selverston, 2000, *NeuroReport* **11**, 563.
- Szücs, A., A. I. Selverston, M. I. Rabinovich, and H. D. I. Abarbanel, 2004, *Soc. Neurosci Abs.* **420**, 4.
- Tams, G., A. Lorincz, A. Simon, and J. Szabadics, 2003, *Science* **299**, 1902.
- Terman, D., A. Bose, and N. Kopell, 1996, *Proc. Natl. Acad. Sci. U.S.A.* **93**, 15417.
- Thompson, A. M., and J. Deuchars, 1994, *Trends Neurosci.* **17**, 119.
- Tiitinen, H., J. Sinkkonen, K. Reinikainen, K. Alho, J. Lavikainen, and R. Naatanen, 1993, *Nature (London)* **364**, 59.
- Tohya, S., A. Mochizuki, and Y. Iwasa, 2003, *J. Theor. Biol.* **221**, 289.
- Traub, R. D., and R. Miles, 1991, *Ann. N.Y. Acad. Sci.* **627**, 277.
- Tsodyks, M., T. Kenet, A. Grinvald, and A. Arieli, 1999, *Science* **286**, 1943.
- Tsodyks, M., and H. Markram, 1997, *Proc. Natl. Acad. Sci. U.S.A.* **94**, 719.
- Tsuda, I., 1991, *World Futures* **32**, 167.
- Turrigiano, G. G., E. Marder, and L. Abbott, 1996, *J. Neurophysiol.* **75**, 963.
- Vaadia, E., I. Haalman, M. Abeles, H. Bergman, Y. Prut, H. Slovin, and A. Aertsen, 1995, *Nature (London)* **373**, 515.
- van Essen, D. C., 1979, *Annu. Rev. Neurosci.* **2**, 227.
- van Vreeswijk, C., L. F. Abbott, and G. B. Ermentrout, 1994, *J. Comput. Neurosci.* **1**, 313.
- van Vreeswijk, V., and H. Sompolinsky, 1996, *Science* **274**, 1724.
- Varona, P., C. Aguirre, J. J. Torres, M. I. Rabinovich, and H. D. I. Abarbanel, 2002, *Neurocomputing* **44-46**, 685.
- Varona, P., M. I. Rabinovich, A. I. Selverston, and Y. I. Arshavsky, 2002, *Chaos* **12**, 672.
- Varona, P., J. J. Torres, H. D. I. Abarbanel, M. I. Rabinovich, and R. Elson, 2001, *Biol. Cybern.* **84**, 91.
- Varona, P., J. J. Torres, R. Huerta, H. D. I. Abarbanel, and M. I. Rabinovich, 2001, *Neural Networks* **14**, 865.

- Venaille, A., P. Varona, and M. I. Rabinovich, 2005, Phys. Rev. E **71**, 061909.
- Vogel, E. K., and M. G. Machizawa, 2004, Nature (London) **428**, 748.
- Vogels, T., K. Rajan, and L. Abbott, 2005, Annu. Rev. Neurosci. **28**, 357.
- Volterra, V., 1931, in *Animal Ecology*, edited by R. N. Chapman (McGraw-Hill, New York), pp. 409–448.
- von der Malsburg, C., 1999, Neuron **24**, 95.
- von der Malsburg, C., and W. Schneider, 1986, Biol. Cybern. **54**, 29.
- Voogd, J., and M. Glickstein, 1998, Trends Neurosci. **21**, 370.
- Wang, X., 2001, Trends Neurosci. **24**, 455.
- Wang, X.-J., and J. Rinzel, 1995, *The Handbook of Brain Theory and Neural Networks* (MIT, Cambridge, MA), p. 686.
- Waugh, F., C. Marcus, and R. Westervelt, 1990, Phys. Rev. Lett. **64**, 1986.
- Wilson, H. R., 1999, *Spikes, Decisions, and Actions* (Oxford University Press, New York).
- Wilson, H. R., and J. D. Cowan, 1973, Kybernetik **13**, 55.
- Wilson, M. A., and B. L. McNaughton, 1993, Science **261**, 1055.
- Wilson, M. A., and B. McNaughton, 1994, Science **265**, 676.
- Wolfe, J., and K. Cave, 1999, Neuron **24**, 11.
- Yuste, R., J. MacLean, J. Smith, and A. Lansner, 2005, Nat. Rev. Neurosci. **6**, 477.
- Zeeman, E., and M. Zeeman, 2002, Nonlinearity **15**, 2019.
- Zhilulin, V. P., and M. I. Rabinovich, 2004, Neurocomputing **58-60**, 373.
- Zhilulin, V. P., M. I. Rabinovich, R. Huerta, and H. D. I. Abarbanel, 2003, Phys. Rev. E **67**, 021901.